

Mitochondrial gene transcription and genome copy number in freeze tolerant larvae of the Arctic woolly bear caterpillar, *Gynaephora groenlandica*, and the Goldenrod gall fly, *Eurosta solidaginis*

by

Sarah Anne Barber

B.Sc., University of Victoria, 1997

A Thesis Submitted in Partial Fulfillment of the

Requirements for the Degree of

MASTER OF SCIENCE

In the Department of Biology

We accept this thesis as conforming

to the required standard



Dr. D.B. Levin, Supervisor (Department of Biology)



Dr. L.R. Page, Department Member (Department of Biology)



Dr. R.A. Ring, Department Member (Department of Biology)



Dr. A. Ekramoddoullah, External Examiner (Pacific Forestry Centre)

© Sarah Anne Barber, 2001
University of Victoria

All rights reserved. This thesis may not be reproduced in whole or in part, by photocopy or other means, without the permission of the author.

QL493
B37

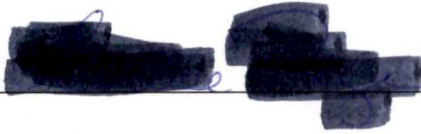
Supervisor: Dr D.B. Levin

ABSTRACT

The Arctic woolly bear caterpillar, *Gynaephora groenlandica*, and Goldenrod gall fly, *Eurosta solidaginis*, are two species of freeze tolerant insects. Both use a system of cryoprotectants and reduced metabolism characteristic of diapause to enhance cold hardiness. Mitochondrial degradation was previously suggested as an adaptive response to cold in *Gynaephora*, and postulated to occur in *Eurosta*. Molecular analyses were used to examine mitochondrial gene transcription and to analyze changes in mitochondrial copy number during cold hardiness in both species. Epifluorescent microscopy using bisbenzimidazole, a DNA specific chromophore, showed increased maximum mitochondrial density in fat body cells of winter collected *Eurosta* larvae held at 10°C compared to cells from fall collected larvae. Northern analysis using mitochondrial specific probes, cytochrome oxidase and 16S ribosomal RNA, demonstrated increased high molecular weight transcripts in winter collected *Eurosta* larvae, while in *Gynaephora* processed mitochondrial transcripts were more abundant in cold adapted larvae. Northern blot results were consistent with increased RNA stability with cold adaptation in both *Eurosta* and *Gynaephora*, although different mechanisms were suggested. Dot blot analyses indicated that mitochondrial genome copy number was reduced in cold adapted *Gynaephora* larvae, but that there was no decrease in copy number in *Eurosta* cold adapted larvae. Restriction digests of total DNA from *Eurosta*, *Gynaephora*, and *Drosophila* hybridized with mitochondrial probes indicated the presence of mitochondrial derived sequences in nuclear genomes.

Examiners:

Dr. D.B. Levin, Supervisor (Department of Biology)



Dr. L.R. Page, Department Member (Department of Biology)



Dr. R.A. Ring, Department Member (Department of Biology)



Dr. A. Ekramoddoullah, External Examiner (Pacific Forestry Centre)

TABLE OF CONTENTS

ABSTRACT	ii
TABLE OF CONTENTS	iv
LIST OF FIGURES	vi
ACKNOWLEDGMENTS	viii
DEDICATION	ix
1. INTRODUCTION	1
1.1 Insects and Cold	1
1.2 Insect Cold Hardiness	2
1.3 Diapause	7
1.4 Mitochondria and Cold Hardiness	8
1.5 The Arctic woolly bear caterpillar, <i>Gynaephora groenlandica</i>	11
1.6 The goldenrod gall fly, <i>Eurosta solidaginis</i>	12
1.7 Mitochondrial Genes and Genomes	14
1.8 Objectives	18
2. Respirometry	19
2.1 Introduction	19
2.2 Materials and Methods	22
2.3 Results	25
2.4 Discussion	27
3. Maximum Mitochondrial Density	32
3.1 Introduction	32

3.2 Materials and Methods	36
3.3 Results	37
3.4 Discussion	40
4. Northern Blots, Dot blots and Southern blots.....	45
4.1 Introduction	45
4.2 Materials and Methods	47
4.3 Results	57
4.4 Discussion	63
5. Summary and Conclusions	77
REFERENCES	116

LIST OF FIGURES

Figure 1. Simple Respirometer	79
Figure 2. <i>E. solidaginis</i> Average Respiration Rates	80
Figure 3 <i>G. groenlandica</i> Average Respiration Rates	81
Figure 4. <i>E. solidaginis</i> Fat Body Cell, Summer Collected Larvae	82
Figure 5. <i>G. groenlandica</i> Fat Body Cell, Summer Collected Larvae	83
Figure 6. <i>E. solidaginis</i> Fat Body Mitochondria, Fall Collected Larvae	84
Figure 7. <i>E. solidaginis</i> Fat Body Mitochondria, Winter Collected Larvae	85
Figure 8. <i>E. solidaginis</i> Mean Maximum Mitochondrial Density Graph	86
Figure 9. COI PCR Product	87
Figure 10. COI Multiple Sequence Alignment	88
Figure 11. 16S PCR Product	89
Figure 12. <i>tam</i> PCR Product	90
Figure 13. <i>E. solidaginis</i> COI Northern Blot	91
Figure 14. <i>G. groenlandica</i> COI Northern Blot	92
Figure 15. <i>E. solidaginis</i> and <i>G. groenlandica</i> 16S Northern Blot	93
Figure 16. Maximum Hybridization Intensity Graph, <i>E. solidaginis</i> COI, 1.5 kb	94
Figure 17. Maximum Hybridization Intensity Graph, <i>E. solidaginis</i> COI, 2.3 kb	95
Figure 18. Maximum Hybridization Intensity Graph, <i>E. solidaginis</i> COI, 2.8 kb	96
Figure 19. Maximum Hybridization Intensity Graph, <i>E. solidaginis</i> 16S, 1.15 kb	97
Figure 20. Maximum Hybridization Intensity Graph, <i>E. solidaginis</i> 16S, 1.3 kb	98
Figure 21. Maximum Hybridization Intensity Graph, <i>G. groenlandica</i> COI	99

Figure 22. Maximum Hybridization Intensity Graph, <i>G. groenlandica</i> 16S	100
Figure 23. <i>E. solidaginis</i> and <i>G. groenlandica</i> COI Dot Blot	101
Figure 24. <i>E. solidaginis</i> and <i>G. groenlandica</i> 16S Dot Blot	102
Figure 25. Maximum Hybridization Intensity Graph, <i>E. solidaginis</i> COI Dot Blot	103
Figure 26. Maximum Hybridization Intensity Graph, <i>E. solidaginis</i> 16S Dot Blot	104
Figure 27. Maximum Hybridization Intensity Graph, <i>G. groenlandica</i> COI Dot Blot	105
Figure 28. Maximum Hybridization Intensity Graph, <i>G. groenlandica</i> 16S Dot Blot .	106
Figure 29. <i>E. solidaginis</i> Summary Data, Fall Collected Larvae	107
Figure 30. <i>E. solidaginis</i> Summary Data, Winter Collected Larvae	108
Figure 31. <i>Drosophila melanogaster</i> Restriction Digest	109
Figure 32. <i>E. solidaginis</i> COI Southern Blot	110
Figure 33. <i>E. solidaginis</i> 16S Southern Blot	111
Figure 34. <i>G. groenlandica</i> COI Southern Blot	112
Figure 35. <i>G. groenlandica</i> 16S Southern Blot	113
Figure 36. <i>D. melanogaster</i> COI Southern Blot	114
Figure 37. <i>D. melanogaster</i> 16S Southern Blot	115

ACKNOWLEDGMENTS

I gratefully acknowledge the guidance and support given to me by my supervisor, Dr. David Levin, and committee members Dr. L. Page and Dr. R. Ring. I am also grateful for the participation of Dr. Hugh Danks at the Canada Museum of Nature, and NSERC Industrial Partners Drs. Olga Kukal and Tom Allen at Atlantic Low Temperature Systems, Ltd. Funding for this work was provided by an NSERC Industrial Grant with Atlantic Low Temperature Systems and held by Dr. Levin, and also by the Ray Hadfield Memorial Fellowship (2000), the Edythe Hembroff-Schleicher Scholarship (2000) and the University of Victoria Graduate Teaching and Research Fellowship. I am thankful for assistance from Levin lab members (Dr. Giovana de Amorim, Beatrice Whittome, Jianhe Huang, Mandy Miller, and Dave Harrison), Hawryshyn lab members (Steve Dann and Ted Allison), the Koop sequencing lab, Dr. Moyra Brackley, Eleanore Floyd, and Pauline Tymchuck and the many other departmental members who have helped me with this project. I owe my Mother Donna Trueit, Giovana de Amorim, Steve Dann and Mike Wilson special thanks for their advice in writing this thesis.

DEDICATION

This work is dedicated to John, my Grandmother Helen Trueit, and in memory of my Grandfather, Charles Trueit, who would have been proud.

CHAPTER 1: INTRODUCTION

Insects and Cold

Imagine an icy Ontario winter or Ellesmere Island tundra in February. In Ontario, temperature extremes may differ by more than 30°C in a day [1], while in the Arctic temperatures stay below freezing for months and annual precipitation may be as low as only 100 mm [2]. Arthropods have carved out niches and thrive in these harsh conditions through adaptations that enable them to survive extreme temperature fluctuations, severe cold and desiccation. Insects, in particular, have developed physiological adaptations that confer resistance to cold and desiccation and, in numerous cases, enable an insect to survive freezing.

Insects have developed different behavioral and physiological responses to cold. From a behavioral perspective insects may respond to impending cold temperatures by migrating to more favorable sites, as exemplified by the monarch butterfly, or by implementing strategies to withstand cold [3]. Such behavioral strategies can include utilizing a hibernaculum, a protective structure used for overwintering, or selecting sheltered microhabitats that are less exposed to the elements [3].

Physiological responses to cold are complex and varied, and in insects may include diapause and cold hardiness. Diapause is a developmental pathway characterized by reduced metabolism. It is generally implemented to withstand unfavorable environmental conditions and coordinate timing of development when

more promising conditions resume [4-7]. Cold hardiness, the ability to withstand low temperatures, consists of two broad categories: organisms may be freeze tolerant, in which some degree of extracellular ice formation is endured, or freeze intolerant, in which any ice formation is avoided [3, 8-18]. Both freeze tolerant and freeze intolerant (freeze susceptible) insects produce specific biological compounds to maintain the desired state.

In response to environmental cues that signal the onset of colder conditions, insects may accumulate a variety of protective molecules [17]. Polyhydroxy alcohols (polyols), called cryoprotectants (or antifreezes) confer the ability to supercool by maintaining extra- and intracellular water in a liquid state at temperatures below the normal crystallization temperature [17]. Similarly, antifreeze proteins lower the supercooling point to avoid freezing [17]. Conversely, protein molecules called ice nucleating agents, provide a nucleus for the formation of ice crystals and inhibit ice recrystallization. Use of cryoprotectants, antifreeze proteins, and ice nucleating agents varies among insect species, and within a species use may vary with season and environmental conditions [17].

Insect Cold Hardiness

The subject of insect cold hardiness has been reviewed on many occasions [3, 8-18] and various aspects of the phenomenon have been defined. Cold hardiness in insects can be viewed as the ability of an insect to withstand freezing temperatures through a cold acclimation phase. Cold acclimation leads either to (or both) freeze

resistance in the form of supercooling, or to freeze tolerance [8, 14]. Cold hardy insects are often classified into two groups: those that maintain homeostasis at low temperatures (freeze avoiding), and those that minimize cellular damage caused by freezing (freeze tolerant) [11]. However, this dichotomous classification is overly simplistic and misleading because some insects are freeze tolerant in certain developmental stages and not others, or the same developmental stage may be freeze avoiding to a certain temperature threshold below which the insect is freeze tolerant [3, 19]. Furthermore, laboratory criteria used to determine whether an insect is freeze tolerant or freeze susceptible, such as cooling rate and thawing rate, may not accurately predict the cold hardiness of an insect in nature [18].

The biochemical challenges of dealing with freezing temperatures are summarized as follows: Extracellular ice formation must be regulated through ice nucleating agents or antifreeze proteins, membranes and proteins must be stabilized during water loss, and cells must be able to tolerate ischemia (reduced blood flow) [13]. Cellular damage from freezing can result from a variety of processes. As water is drawn out of cells they experience concentrations of solutes that are too high, either within the cell or in unfrozen extracellular water [10, 17]. Cells may undergo mechanical injury as extracellular ice expands [20], or as ice is recrystallized preferentially forming larger ice crystals [17]. Cells may also be injured when extracellular ice thaws, causing an osmotic imbalance that draws water rapidly back into cells [10]. In addition, intracellular ion concentrations can disrupt cellular metabolic function, and the ischemia caused by extracellular ice may lead to cytotoxic effects [10]. Finally, cold temperatures may cause denaturation of proteins,

alter specificity of enzymes leading to metabolic imbalances [11, 21], or cause fusion of membranes [22, 23].

At a physiological level, the problems faced by a freeze tolerant or freeze intolerant insect relate to the properties of water, both in ice formation and osmotic compensation [10, 13, 21, 24]. Insects have an advantage over other cold hardy animals in that their haemolymph does not mediate gas exchange [25]. Therefore, viscosity of insect body fluids may be increased by cryoprotectants to the extent that other haemolymph circulatory functions (such as excretion and hormone transport) are still possible [25]. High haemolymph viscosity in insects does not compromise transport of oxygen and carbon dioxide to and from tissues.

Whether an insect species or individual is freeze tolerant or freeze intolerant is generally dictated by a series of life cycle trade-offs that may also include habitat selection, dormancy, and food reserves [15]. It may be advantageous for an insect to freeze and invest energy in repairing freeze damage, rather than maintain a supercooled state throughout a season [26]. Freeze tolerant insects utilize carbohydrates more effectively [9], and extensive supercooling increases the chance that spontaneous nucleation may occur, as well as increasing water loss [9, 27]. Conversely, maintaining the ability to supercool may be advantageous in environments where cold is not severe and prolonged [26]. Regardless of whether an organism is freeze tolerant or freeze susceptible, preventing rapid crystallization of extracellular water poses a physiological challenge addressed by compounds like cryoprotectants.

Cryoprotectants are usually low molecular weight alcohols, such as glycerol, that lower the supercooling point of cells and tissues [15, 28]. Supercooling is defined as "a system that remains unfrozen at temperatures below its melting point...and the temperature at which spontaneous freezing occurs in a supercooled system is termed the supercooling point" [9]. The supercooling point is analogous to the temperature of crystallization [24]. Cryoprotectants have a variety of functions in a freeze tolerant insect. They decrease the supercooling point of cytoplasm by acting in a colligative manner (that is, their action depends on the number of molecules present) to bind water. This decreases the amount of free water able to participate in ice formation [17]. Additionally, cryoprotectants function in maintaining osmotic balance. As extracellular water is bound into the crystal lattice of ice, the increased solute concentration of the remaining extracellular fluid draws water out of adjacent cells. Cryoprotectants increase solute concentration within cells, thereby preventing lethal cell shrinkage [25]. Cryoprotectants are relatively non-toxic at high concentrations; they are chemically and biochemically inert and therefore do not interact with critical metabolic reactions within the cell [11].

Cryoprotectants function not only in depressing the supercooling point, but they also play a vital role in preventing dehydration [29]. Tropical insects, and some insects experiencing desiccating summer conditions, produce cryoprotectants, thereby reducing the available water for evaporation [29]. Trehalose has been studied extensively in the process of anhydrobiosis (near complete dehydration), and was found to be effective in stabilizing dry lipids and proteins [30]. Furthermore, certain cryoprotectants such as trehalose and the amino acid proline interact with cellular

membranes and proteins in critical ways. Under normal cellular conditions, the polar head groups of a phospholipid bilayer are hydrated, but as a cell loses water, and the head groups are packed closer together, interactions increase between the hydrophobic tails causing formation of gel phase membrane [23, 30]. Rehydration of a gel phase membrane causes transient leaks that can lead to ionic imbalances and cell death [23, 30]. Trehalose, and to a lesser extent proline, interact with the polar head groups of membrane phospholipids in such a way that they are stabilized when water concentrations decrease [23, 30]. Proline also stabilizes protein under low water conditions [30].

In addition to cryoprotectants, antifreeze proteins, also called thermal hysteresis proteins, may figure prominently in cold hardiness. Antifreeze proteins lower the supercooling point of an insect and are commonly used by freeze intolerant insects [17]. The supercooling point of a fluid is lowered as antifreeze proteins bind to the surface of a growing ice crystal and retard further growth [17]. Antifreeze proteins also inhibit recrystallization of ice upon thawing [15].

Conversely, ice nucleating agents (INAs), are molecules that trigger ice crystal formation at high subzero temperatures [15]. Ice nucleating agents usually initiate ice formation at -8°C to -10°C [17], but may trigger ice formation at temperatures as high as -1°C [31]. Ice nucleating agents may be organic or inorganic molecules [31], or they may be microorganisms associated with the insect tissue [24, 32]. Examples of ice nucleating agents include gut bacteria, calcium phosphate spherules (*E. solidaginis*, [33]), proteinaceous molecules and most potently, external ice itself [24]. Ice nucleating agents allow slower rates of ice formation in

extracellular tissues, preventing the osmotic stress and rapid crystallization that would happen at lower temperatures [24].

Cryoprotectants, antifreeze proteins, and ice nucleating agents act in concert to mediate or prevent rapid crystallization of ice in cold hardy insects. One further adaptation that may contribute to insect cold hardiness is diapause.

Diapause

In insects, diapause is a type of dormancy characterized by behavioral and physiological adaptations that take place in advance of adverse environmental conditions such as cold or dry seasons [4-7]. Dormancy in insects is a state of lowered metabolic rate that is controlled by hormones [5, 7] and influenced by environmental cues such as day length, temperature, and food quality [5, 7, 34]. Diapause may occur in every generation (obligatory diapause), or only in response to certain environmental cues (facultative diapause) [4, 5, 7]. Diapause coordinates development with favorable conditions, and synchronizes development within members of a species [4].

Insect diapause is characterized by increased fat reserves and decreased body water at the onset, and reduced metabolic rates throughout [4, 7]. Because the timing of diapause and cold hardiness often overlap, and the accumulation of glycerol, a cryoprotectant, may be associated with diapause, the two processes have been frequently considered part of the same developmental program [5, 6, 35]. Production of cryoprotectants during a state of diapause may extend the ability of an insect to

tolerate cold [35, 36]. However, the occurrence of diapause in some insects that are not cold hardy, and lack of diapause in some insects that are cold hardy, indicates that while diapause and cold hardiness syndromes may occur simultaneously, any link may be coincidental [5, 6]. Recent discussions appear to have reached a tentative consensus: diapause and cold hardiness appear to be linked in some insects, while no such link is evident in other species [36].

In summary, cryoprotectants, ice nucleating agents, and antifreeze proteins regulate ice formation in cold hardy insects. Reduced metabolism during diapause contributes to cold hardiness by lowering energy demands. The role of mitochondrial degradation, if any, in cold hardiness is unknown. Further investigation of the scope and contribution of mitochondrial degradation in freeze tolerant insects is warranted.

Mitochondria and Cold Hardiness

In addition to the aforementioned physiological adaptations to cold, organelle changes in response to cold have been described for some insect species. During pupation, the cells of insects may show degradation of mitochondria in response to either hormonal cues [37-39], or prolonged freezing [37]. The Arctic woolly bear caterpillar, *G. groenlandica*, had a 10,000-fold reduction in the number of mitochondria per cell in response to freezing when fat body and brain tissue cells were examined [37].

Past experiments investigating insect mitochondrial degradation have focused on mitochondrial enzyme analysis and morphological data generated by electron

microscopy or epifluorescence microscopy, but they have not explored the phenomenon of mitochondrial degradation at the deoxyribonucleic acid (DNA) or ribonucleic acid (RNA) level. In the present study, analysis of mitochondrial DNA (mtDNA) copy number and transcription of mtDNA specific genes allowed comparisons between individuals of the same species that had experienced different stages of cold hardiness. Comparison of mtDNA levels provided insight into whether or not mtDNA is present in greater or lesser quantities in response to cold, and whether or not any change in mtDNA copy number is associated with cold hardiness. Analysis of mitochondrial gene transcription allowed similar comparisons to be made using transcription levels as indicators of mitochondrial activity.

The arctic woolly bear caterpillar, *G. groenlandica*, is an excellent model for the study of mitochondrial degradation based on already published data. The present study used molecular methods to confirm or refute mitochondrial degradation in *G. groenlandica*. To investigate whether or not mitochondrial degradation is a more widespread response to cold common in freeze tolerant insects, a second insect species was also chosen for study. The goldenrod gall fly, *Eurosta solidaginis*, provided a comparative model for mitochondrial changes during cold hardiness.

The insect fat body is analogous to the vertebrate liver and is critical to overwintering. It contains enzymes for oxidation and dehydrogenation, is able to synthesize protein, lipid and glycogen from precursor molecules, and is a production site for cryoprotectants such as glucose, sorbitol and trehalose [4, 34]. As the principal site of intermediary metabolism, the insect fat body influences insect

physiology as a whole, whereas energy production within the fat body is determined by mitochondria [40].

Mitochondrial degradation in fat body cells of *G. groenlandica* reportedly reduced the number of mitochondria per cell to less than one (on average), with recovery of a full complement of mitochondria within hours of warming. The ability to degrade and rapidly regenerate mitochondria was suggested as a possible energy conservation mechanism used by freeze tolerant insects during overwintering [37]. The present study uses molecular techniques to analyze mitochondrial copy number and gene expression in two species of freeze tolerant insects to examine the possibility that mitochondrial degradation is an adaptive physiological response to cold in both species.

Mitochondrial degradation *en masse* is neither well documented in nature nor well understood. Aside from previous examples of mitochondrial degradation during pupation and in response to cold in insect cells, little is known about the processes of mitochondrial degradation and associated rapid regeneration. Indeed, mitochondrial degradation in humans is often associated with apoptosis (programmed cell death). Mitochondria trigger apoptosis by releasing cytochrome *c* into the cytosol, activating caspases, the family of proteases associated with apoptosis [41]. Diseases such as Huntington's, Parkinson's, and Alzheimer's diseases, are all associated with upregulation of mitochondrial mediated apoptosis [42], whereas in cancer and autoimmune diseases mitochondrial mediated apoptosis is downregulated [43]. Freeze tolerant insects that undergo mitochondrial degradation and rapid

mitochondrial regeneration provide a unique opportunity to study these processes under naturally-occurring changes in environmental conditions.

The Arctic woolly bear caterpillar, *Gynaephora groenlandica*

The Arctic woolly bear caterpillar, *Gynaephora groenlandica* (Lepidoptera: Lymantriidae) is found in Canada's high Arctic and in Greenland [44]. *G. groenlandica* caterpillars overwinter within two-layered hibernacula on unsheltered sites on the arctic tundra [3, 45]. The larvae are active and feeding for several weeks during the month of June, after which they spin hibernacula [46-48] and enter diapause [49]. Larvae feed predominantly on the willow, *Salix arctica*, and they rely on basking activities to elevate body temperature [44, 50] and enhance digestive enzyme activity [48]. Metabolic energy is stored in the form of glycogen and used in the synthesis of cryoprotectants, predominantly glycerol [51].

Larval development in *G. groenlandica* is prolonged by harsh environmental conditions. Although it was previously thought that each of a total of 6 larval instars (stages) molted every three to four years [48], a more recent study indicates that larvae proceed to the next instar each active season thereby resulting in a 7-year life cycle [52].

Overwintering *G. groenlandica* larvae respond to cold temperatures using several different mechanisms. The formation of a hibernaculum with two layers (a dark inner layer and a light outer layer) facilitates a "greenhouse effect", whereby the larval temperature is raised significantly above the ambient air temperature [50].

Additionally, orientation of the hibernacula maximizes both hours of sunlight and angle of incident radiation [45, 50]. Larvae are freeze tolerant in both winter and summer, and contain the cryoprotectants glucose and trehalose in the haemolymph [37, 51]. Cold acclimated or previously frozen larvae synthesize glycerol as an additional cryoprotectant [37, 51]. *G. groenlandica* larvae are capable of supercooling to -8°C , below which freezing tolerance allows larvae to withstand temperatures that may dip as low as -50°C [53].

The goldenrod gall fly, *Eurosta solidaginis*

The goldenrod gall fly, *Eurosta solidaginis* (Diptera: Tephritidae), is a freeze tolerant insect that inhabits the stems of goldenrod plants (*Solidago* spp.) during larval stages. *E. solidaginis* is widely distributed in North America, reaching from Texas to Ontario and west to Alberta [54]. The female adult fly lays eggs in the growing bud of the goldenrod plant and larvae develop within the stem [54]. The plant forms a round gall in response to the larval inhabitant. Larvae feed on the tissue inside the gall and pass through two larval instars through the summer [54]. The third larval instar, which is the freeze tolerant overwintering stage, enters diapause in the fall [54, 55]. In late spring, third instar larvae form pupae and adult flies emerge from the gall in early summer to mate. The gall formed on the stem of the goldenrod plant is exposed to the elements throughout winter and affords little protection from freezing temperatures [1]. Larvae are subject to extreme temperature fluctuations

throughout a season with diurnal temperature changes within the gall reaching up to 29°C [1].

E. solidaginis larvae demonstrate reduced metabolism in the fall that is indicative of diapause [55-57] and which coincides with the onset of cryoprotectant synthesis [56, 58-61]. *E. solidaginis* third instar larvae utilize several cryoprotectants over the fall and winter, each with different peak times: glycerol levels peak in early autumn, sorbitol levels peak in early winter, and trehalose levels are highest in midwinter [60, 62].

Freeze tolerance in *E. solidaginis* has been well studied (for a review see [54]), and some of the first reports noted intracellular freeze tolerance in fat body cells [63, 64]. These reports were later questioned because of a common belief that animal cells are not able to survive intracellular freezing. However, more recent studies have confirmed that *E. solidaginis* fat body cells do survive intracellular freezing [65, 66]. Third instar larvae are capable of supercooling to about -8 °C [61], although insects may undergo inoculative freezing (freezing induced by direct contact with ice or with ice nucleating agents) at higher temperatures when moisture-containing galls freeze [67]. Inoculative freezing may also result from calcium phosphate spherules contained within the Malpighian tubules (equivalent to the vertebrate kidney) of the larvae [33]. Lethal freezing can occur at temperatures below -25°C to -50°C depending on the geographic area [68, 69].

E. solidaginis metabolism during overwintering has been investigated at cryoprotectant, enzymatic, and oxygen consumption levels [56, 58-61, 70-75]. Based on mitochondrial enzyme analysis, mitochondrial degradation was suggested by

Joanisse and Storey [76], although further experimentation failed to support this hypothesis [77]. To date, however, there have been no direct investigations into the fate of mitochondria during freezing in *Eurosta solidaginis*. *E. solidaginis* third instar larvae, therefore, provide a comparative model of mitochondrial changes during freeze tolerance. *E. solidaginis* respiratory rates have been documented in the literature and some mitochondrial enzyme studies have been carried out. Because mitochondrial degradation as an adaptive response to cold has been debated in *E. solidaginis*, further analysis is needed.

Mitochondrial genes and genomes

Mitochondria are membrane bounded organelles present in cells that provide metabolic energy in the form of adenosine triphosphate (ATP). All mitochondria contain their own genomes and in most vertebrates and invertebrates the mitochondrial genome is circular, double stranded, and 15-20 kilobase pairs (kbp) long [78-80]. The genome encodes a characteristic set of proteins, ribosomal RNAs (rRNAs), and transfer RNAs (tRNAs). Mitochondrial genomes are highly reduced, containing few (if any) introns and both strands are coding. The mitochondrial genome is transcribed as a single transcript for each DNA strand, and transcripts are processed within the mitochondrion. All translation takes place within the mitochondrion, using mitochondrial tRNAs and ribosomes [78-80].

One of the best characterized and completely sequenced insect mitochondrial genomes, is that of the fruit fly, *Drosophila melanogaster*. The *Drosophila*

mitochondrial genome is 19.517 kbp long, and contains 22 tRNA genes, 2 rRNA genes including the 12S and 16S rRNAs, and 13 protein coding regions for subunits of cytochrome *c* oxidase (including the COI subunit), ATP synthase, NADH dehydrogenase, and cytochrome *b* proteins [81]. All proteins encoded in the mitochondrial genome are components of the electron transport chain.

The inner mitochondrial membrane contains proteins for the electron transport chain while the mitochondrial matrix contains enzymes for several metabolic pathways, including the citric acid cycle, fatty acid β -oxidation, and amino acid metabolism [78, 79]. Electrons produced by these metabolic processes and from glycolysis in the cytosol are transferred to electron acceptors nicotinamide adenine dinucleotide (NAD⁺), nicotinamide adenine dinucleotide phosphate (NADP), flavin adenine dinucleotide (FAD), or flavin mononucleotide (FMN) [78, 79]. NADH (the reduced form of NAD⁺) shuttles electrons to complex I of the respiratory chain, the NADH dehydrogenase complex [78, 79]. Electrons are carried from complex I to complex II, succinate dehydrogenase, *via* ubiquinone that diffuses through the inner membrane [78, 79]. Electrons pass through complex III, ubiquinone-cytochrome *c* oxidoreductase, and are coupled with proton movement from the matrix to the intermembrane space [78, 79]. Electrons are passed to complex IV, cytochrome oxidase (containing cytochromes *a* and *a*₃), by cytochrome *c*, where they are used to reduce oxygen to water and pump protons into the intermembrane space [78, 79]. Protons pumped into the intermembrane space by complexes III and IV, are moved back into the matrix by ATP synthase, an integral membrane protein that couples proton movement down a gradient with formation of ATP from ADP and P_i [78, 79].

Mitochondrial cytochrome oxidase I, or COI, is one of the subunits of mitochondrial cytochrome *c* oxidase, and is encoded on the heavy (gene rich) strand of the *Drosophila* mitochondrial genome. The COI gene is 1,540 base pairs in *Drosophila*, encoding for 512 amino acid residues [81].

Synthesis of protein from a mRNA strand is catalyzed by ribosomes, large molecular structures formed from protein and ribonucleic acid subunits. Nuclear encoded genes are transcribed in the nucleus, and the mRNA is exported to the cytoplasm where they are translated by ribosomes on the rough endoplasmic reticulum. Messenger RNA produced in mitochondria, however, is translated within the mitochondria and is not exported to the cytoplasm [78, 79]. Genes for the RNA component of the ribosomes are encoded within the mitochondrial genome, while associated proteins are encoded in the nuclear genome and imported into the mitochondria [78, 79]. Mitochondrial ribosomes are comprised of a large and a small subunit corresponding to 30S (containing 16S rRNA and associated proteins) and 50S (containing 23S and 5S rRNA and associated proteins) bacterial ribosomes [78, 79]. Associated ribosomal proteins required for the functional ribosome (encoded by nuclear DNA) are imported from the cytoplasm. The *Drosophila* 16S rRNA gene is 1,324 base pairs long, and both the 12S and 16S rRNA genes are found on the light strand of the mitochondrial genome [81].

COI and 16S mitochondrial genes were chosen for study because together they represent both the heavy and the light strands of the mitochondrial genome. Both COI and 16S sequences are highly conserved and conducive to interspecies hybridization experiments. In addition, because COI is associated with the electron

transport chain, levels of this enzyme may be related directly to metabolic activity. Finally, because of its role in mitochondrial protein synthesis, 16S activity may be related directly to the mitochondrial protein requirements of a cell.

Freeze tolerance in insects is thoroughly documented and two well-studied species are the Arctic woolly bear caterpillar, *G. groenlandica*, and the goldenrod gall fly, *Eurosta solidaginis*. Both *G. groenlandica* and *E. solidaginis* maintain cryoprotectant pools to enable freeze tolerance. While mitochondrial degradation has been reported in *G. groenlandica*, molecular tools have not been used to further substantiate this finding. In *E. solidaginis*, mitochondrial degradation has been hypothesized and debated, but molecular evidence is lacking. Northern and Dot blot analysis of both *G. groenlandica* and *E. solidaginis* larval samples analyzed mitochondrial gene expression and mitochondrial copy number in relation to cold adaptation.

This basic research contributes to our understanding of how mitochondrial changes are associated with cold hardiness, and it has broad applications in several disciplines. Foremost, this research adds to existing knowledge in the field of insect cold hardiness. In addition, as stated previously, mitochondrial degradation is not only associated with apoptosis but also plays a role in human disease. Elucidating the pathways for mitochondrial degradation and regeneration in cold hardy insects may provide new therapeutic approaches to treating human disease. Finally, understanding the mechanisms for mitochondrial degradation is critical for preservation of living materials and can be applied in areas as diverse as food storage and tissue storage.

Objectives

The objective of this study was to evaluate the role of mitochondrial degradation as an adaptation to freeze tolerance in the Arctic woolly bear caterpillar, *G. groenlandica*, and the goldenrod gall fly, *Eurosta solidaginis*. This was accomplished by measuring whole body respiration (Chapter 2) and relating the values obtained to maximum mitochondrial number (Chapter 3), COI and 16S gene expression (Chapter 4), and to mitochondrial genome copy number (Chapter 4).

CHAPTER 2 RESPIROMETRY

Introduction

Aerobic organisms take up oxygen from their surroundings for use in cellular respiration. Under carbohydrate metabolism, for every molecule of oxygen used, a molecule of carbon dioxide is released into the environment. Terrestrial insects, such as *G. groenlandica* and *E. solidaginis*, use a tracheal system for respiratory gas exchange [4, 34]. The tracheal system consists of a series of branching narrow tubules that stretches throughout the insect body [4, 34]. Gas exchange takes place at the site of utilization, the interface between tracheoles and cell [4, 34]. Pore structures called spiracles are found at the tracheal openings and an associated closing mechanism can close the tracheal system to the environment to reduce water loss [4, 34].

Microrespirometers used for this study take advantage of the 1:1 ratio of oxygen used and carbon dioxide evolved in cellular respiration [82]. A microrespirometer consists of a syringe, a capillary tube, and a 10% solution of potassium hydroxide (Figure 1) [82]. The insect of interest is placed into a syringe barrel that has had a capillary tube of known volume glued to the top. The plunger is carefully inserted into the barrel leaving room for the insect. The apparatus is placed upright, to the top of the barrel in a water bath of the desired temperature, and a droplet of 10% potassium hydroxide is added to the top of the capillary tube. Carbon dioxide molecules generated by insect respiration are absorbed by the potassium

hydroxide droplet causing a pressure decrease in the syringe barrel [82]. The decreased pressure in the syringe barrel causes the potassium hydroxide droplet to move downwards. The movement of the droplet is directly proportional to the volume of oxygen consumed, thus the amount of oxygen used per unit time and larval weight can be calculated [82].

Larval respiration has been measured in both *G. groenlandica* and *E. solidaginis* previous to this investigation. *G. groenlandica* respiration was measured under field and laboratory conditions after different acclimation regimes [37, 44, 48, 49]. Respiration rates sharply increased with increasing temperature among larvae acclimated to 5°C and 15°C: when measured at 25°C, highest metabolic rates (290 $\mu\text{l O}_2 \text{ hr}^{-1} \text{ g}^{-1}$) were observed among fed larvae, while lowest rates (60-70 $\mu\text{l O}_2 \text{ hr}^{-1} \text{ g}^{-1}$) were observed among nutritionally starved larvae, larvae that were in hibernacula or low temperature acclimated larvae [48]. Correspondingly, metabolic rates increased in both fed and starved larvae in response to increasing temperature [44, 49]. Larvae acclimated to -15°C similarly showed increased metabolic rates as temperature was increased: larvae brought to 23°C after -15°C acclimation for 75 days respired at 95 $\mu\text{l O}_2 \text{ hr}^{-1} \text{ g}^{-1}$ and larvae brought to 23°C after -15°C acclimation for 6 months respired at 38 $\mu\text{l O}_2 \text{ hr}^{-1} \text{ g}^{-1}$ [37].

Oxygen consumption related directly to acclimation temperature in *G. groenlandica* in all previous respiration studies. Growth and development in the Arctic woolly bear caterpillar depends upon thermoregulation; basking activities increase body temperature and metabolic rates [48, 49]. Therefore increased metabolism at warm temperatures allows greater incorporation of dietary intake [48].

Prolonged low temperature acclimation reduced metabolism, as did the presence of a hibernaculum [48]. Consequently, respiration rates were expected to decrease with increasing cold acclimation.

Respiration measurements have been performed on *Eurosta solidaginis* using microrespirometers and computerized flow through respirometry (a computerized gas analysis system) [55-57]. Larval respiration rates were dependent on temperature acclimation and on seasonal collection dates [55, 56]. Oxygen consumption was found to increase 6 fold between 5°C and 10°C for December collected larvae in Ohio, U.S.A. [57]. Similarly, respiration rates were observed to increase with increasing temperature regardless of collection time [56]. However, change in respiration for a 10°C change in temperature (called the Q_{10} value) was equal in summer and autumn (3.4), but decreased to 2.6 in winter collected samples [56]. A large Q_{10} value corresponds to a large change in respiration associated with increasing temperature, whereas a small Q_{10} value reflects a small change in respiration with increasing temperature. This decreasing metabolic response to temperature changes reflects an adaptive mechanism to cope with the fluctuating thermal environment of the gall [56].

Lowered metabolic rates in *E. solidaginis* larvae have also been correlated with diapause [55]. Diapause induction occurs in autumn when maximum larval weight is achieved and when plant tissue begins to senesce and evening frosts occur [55]. Larvae collected in Pennsylvania, U.S.A. that were acclimated to 15°C and measured at 10°C, had average respiration rates of 223 $\mu\text{l O}_2 \text{ hr}^{-1} \text{ g}^{-1}$ in summer but

only $141 \mu\text{l O}_2 \text{ hr}^{-1} \text{ g}^{-1}$ in autumn and $146 \mu\text{l O}_2 \text{ hr}^{-1} \text{ g}^{-1}$ in winter [56]. Decreased metabolism measured by respirometry was indicative of diapause.

The objective of the respirometry experiments was to use oxygen consumption levels to establish the metabolic rates of larvae from various collection and treatment groups. Metabolic rates indicated the physiological state of the larvae and were used in conjunction with mitochondrial gene transcription and genome copy number to compare larval treatment groups.

Materials and Methods

E. solidaginis larvae were collected in late summer (August 29/30, 2000), fall (October 29/30, 2000) and winter (January 1, 2001). Metabolic rates of summer collected larvae were measured at 15°C (designated 'summer active' larvae) to establish a baseline metabolism in active larvae. Metabolic rates of fall and winter collected larvae were measured at 4°C (designated 'fall 4°C ' and 'winter 4°C ' respectively), 10°C (designated 'fall 10°C ' and 'winter 10°C '), and 15°C (designated 'fall 15°C ' and 'winter 15°C '), to assess changes in respiration, gene transcription, and mitochondrial copy number. *G. groenlandica* larvae were measured at 15°C only, due to the small numbers of larvae available. Larvae were designated as summer active larvae ('summer active'), larvae stored at 4°C and had spun hibernacula but were not frozen ('hibernacula' group), larvae that were frozen 2 weeks at -20°C ('summer frozen' group), and larvae frozen for 5.5 months at -20°C ('winter frozen').

Eurosta solidaginis third instar larvae were collected by Dr. Hugh Danks, Biological Survey of Canada (Terrestrial Arthropods), Canadian Museum of Nature. Insects were collected from two sites located near Ottawa, Ontario: Aylmer, Quebec (45° 26'; 75° 50'), and Gloucester, Ontario (45° 21'; 75° 38'). Larvae contained within gall material were shipped in insulated coolers by overnight courier, and were placed in storage upon arrival. Summer collected larvae were stored at 14°C, fall collected larvae were stored at 4°C, and winter collected larvae were stored at -20°C. Larvae were removed from galls as needed for experiments, and weighed using a Sartorius balance (Sartorius Corporation, Edgewood, New York).

G. groenlandica, larvae were collected by Valerie Bennett and Dr. Olga Kukal, on Ellesmere Island, Nunavut, (78° 53' N; 75° 55' W) in June 2000. Larvae were shipped on ice to Victoria by overnight courier and stored at 4 °C upon arrival.

Respiration measurements

Oxygen consumption of individual larvae was measured using a simple respirometer (Figure 1) [82]. Larvae were placed in the barrel of 3cc syringes to which 100 µl capillary tubes had been attached. Two thermobarometers were set up as controls, and did not contain larvae. A drop of 10% potassium hydroxide (10% KOH) was added to the capillary tube, and the apparatus was placed in a controlled temperature (10 or 15°C) water bath (2219 MULTITEMP II thermostatic circulator, LKB Bromma, Sweden), or 4°C refrigerator. Larvae were equilibrated for one hour at the desired temperature before a four hour measurement interval began. The capillary tubes were marked with waterproof felt pen at the bottom of the 10% KOH

droplet at time zero (T_0). After 4 hours (T_4) the bottom of the 10% KOH droplet was marked on the capillary tube, and the oxygen consumption was calculated using the distance the droplet had moved. Each millimeter the droplet moved in the capillary tube corresponded to a known volume, given by the capacity of the capillary tube, in this case 100 μl . The conversion factor for the capillary tube was calculated by dividing the volume of the tube by the length of the tube from the top to the manufacturer's 100 μl mark. With this information the amount of oxygen consumed could be calculated using the distance traveled by the droplet (plus or minus any correction factor given by the two thermobarometer controls), multiplied by the conversion factor of the capillary tube, divided by the time the experiment was run, divided by the weight of the larvae. The correction factor given by the thermobarometer controls was an average of the two values; a positive number if the control droplets had moved down toward the syringe barrel or a negative value if the droplets had moved up towards the top of the capillary tube. Oxygen consumption = (distance moved (mm) by the 10% KOH droplet - average distance moved by thermobarometer controls) x conversion factor of capillary tube (1.538 $\mu\text{l}/\text{mm}$ for 100 μl capillary tube) x time (hrs)⁻¹ x larval weight (g)⁻¹.

An approximation of the Q_{10} values (change in respiration for a 10°C change in temperature) was determined by dividing the 15°C respiration value by the 4°C value. Statistical analysis of respiration data was completed using raw respiration data and GraphPad InStat (version 3.01) Graphpad Software, Inc. The log value of each *E. solidaginis* respiration data point was entered into GraphPad InStat, to approximate a normal distribution. One-way analysis of variance (ANOVA) tests

were performed, as well as the Tukey-Kramer and Dunnett's multiple comparison tests. A P-value of less than 0.05 was considered significant.

At the conclusion of respiration measurements, larvae were dissected and the fat body tissue collected for further use.

Results

E. solidaginis larval respiration was measured among three collection groups: summer collected larvae, fall collected larvae, and winter collected larvae. Summer collected larvae were measured at 15°C, while fall and winter collected larvae were measured at 4°C, 10°C, and 15°C (Figure 2). Summer respiration rates averaged 383.85 +/- 64.85 $\mu\text{l O}_2 \text{ hr}^{-1} \text{ g}^{-1}$ (n=15) when measured at 15°C. Average respiration rates for fall collected larvae were 33.04 +/- 5.61 $\mu\text{l O}_2 \text{ hr}^{-1} \text{ g}^{-1}$ (n= 8) at 4°C, 96.36 +/- 24.32 $\mu\text{l O}_2 \text{ hr}^{-1} \text{ g}^{-1}$ (n=8) at 10°C, and 127.53 +/- 28.37 $\mu\text{l O}_2 \text{ hr}^{-1} \text{ g}^{-1}$ (n=6) at 15°C. Average respiration rates for winter collected larvae were 26.71 +/- 3.13 $\mu\text{l O}_2 \text{ hr}^{-1} \text{ g}^{-1}$ (n=9) at 4°C, 80.84 +/- 7.52 $\mu\text{l O}_2 \text{ hr}^{-1} \text{ g}^{-1}$ (n=9) at 10°C, and 154.30 +/- 20.97 $\mu\text{l O}_2 \text{ hr}^{-1} \text{ g}^{-1}$ (n=9) at 15°C. Approximate Q₁₀ values for *E. solidaginis* larval respiration were 3.86 for fall collected larvae, and 5.95 for winter collected larvae.

Nonparametric ANOVA (Kruskal-Wallis) statistical analysis of *E. solidaginis* respiration data showed that variation among column medians was significantly greater than expected by chance (p<0.0001; Kruskal-Wallis statistic KW=57.775). Logarithmic data analyzed using one-way ANOVA and the Tukey-Kramer test showed significant differences (p<0.0001) among column means for all treatment

groups except: Fall 4°C vs. Winter 4°C; Fall 10°C vs. Fall 15°C; Fall 10°C vs. Winter 10°C, and Fall 15°C vs. Winter 15°C.

G. groenlandica respiration rates were measured among four different collection groups, all from the 2000 summer season: summer collected larvae from the active feeding period, larvae that had spun hibernacula and were stored at 4°C, larvae that had not spun hibernacula but had been stored for two weeks at -20°C, and larvae that had been frozen for 5.5 months at -20°C (Figure 3). All respiration measurements taken of *G. groenlandica* larvae were conducted at 15°C, over an interval of 4 hours, with a temperature equilibration of 1 hour. Average respiration for active summer collected larvae was 218.29 +/- 78.16 $\mu\text{l O}_2 \text{ hr}^{-1} \text{ g}^{-1}$ (n=7). Larvae that had spun hibernacula had an average respiration of 115.05 +/- 65.07 $\mu\text{l O}_2 \text{ hr}^{-1} \text{ g}^{-1}$ (n=3), and larvae that had been frozen for two weeks had an average respiration rate of 168.40 +/- 6.97 $\mu\text{l O}_2 \text{ hr}^{-1} \text{ g}^{-1}$ (n=3). Larvae that had been frozen for 5.5 months had an average respiration of 72.80 +/- 47.56 $\mu\text{l O}_2 \text{ hr}^{-1} \text{ g}^{-1}$ (n=3).

G. groenlandica respiration data were tested using nonparametric ANOVA, and both the Kruskal-Wallis test and the Tukey-Kramer tests. Statistical analysis revealed that there were too few values to assess whether or not data were derived from a normal population, and consequently whether to use parametric or nonparametric analysis. Dunnett's multiple comparison test of means found a significant difference between summer active larvae respiration and winter frozen for 5.5 months ($p < 0.05$). Similarly, the parametric Tukey-Kramer test found that mean respiration values were significantly different for summer active larvae and winter larvae frozen for 5.5 months.

Nonparametric ANOVA (Kruskal-Wallis test) of *G. groenlandica* respiration data showed that variation among column medians was not significantly greater than expected by chance ($p < 0.0632$; Kruskal-Wallis statistic $KW = 7.290$). Dunnett multiple comparisons failed to find significant differences between active summer larvae respiration and respiration data from the hibernacula group and the summer collected larvae frozen for 2 weeks ($p > 0.05$). A significant difference was found, however, between median respiration values from summer collected larvae and larvae frozen for 5.5 months.

Discussion

Oxygen consumption provided a measure of larval metabolic rate. A simple respirometer gives accurate oxygen consumption levels for larvae up to 500 mg [82]. *E. solidaginis* respiration rates as measured by the simple respirometer system described were similar to those reported for field collected larvae from the Northeastern United States [56]. Average respiration rate for summer collected larvae in this study was $383.85 \mu\text{l O}_2 \text{ hr}^{-1} \text{ g}^{-1}$ compared to $\sim 350 \mu\text{l O}_2 \text{ hr}^{-1} \text{ g}^{-1}$ extrapolated from published respiration graphs [56] for summer larvae measured at 15°C . Similarly extrapolated fall 4°C , 10°C and 15°C oxygen consumption values (~ 50 , ~ 100 and $\sim 120 \mu\text{l O}_2 \text{ hr}^{-1} \text{ g}^{-1}$ respectively [56]), were comparable to average rates of 33.04, 96.36, and $127.53 \mu\text{l O}_2 \text{ hr}^{-1} \text{ g}^{-1}$ obtained in this study. Average respiration data calculated for winter collected larvae measured at 4°C and 10°C , 26.79 and $79.42 \mu\text{l O}_2 \text{ hr}^{-1} \text{ g}^{-1}$, were similar to extrapolated data for the same

temperature ranges, ~ 30 and $\sim 75 \mu\text{l O}_2 \text{ hr}^{-1} \text{ g}^{-1}$, respectively [56]. However, average respiration for winter collected larvae at 15°C , $159.44 \mu\text{l O}_2 \text{ hr}^{-1} \text{ g}^{-1}$, was higher than extrapolated published data from Pennsylvania, $\sim 110 \mu\text{l O}_2 \text{ hr}^{-1} \text{ g}^{-1}$ [56], but closer to the extrapolated value for December collected larvae from Ohio ($\sim 140 \mu\text{l O}_2 \text{ hr}^{-1} \text{ g}^{-1}$) provided in another study [57].

As expected, based on previously published results [56, 57], a general trend of increasing respiration rate with increasing temperature was observed for *E. solidaginis* larvae. The approximate Q_{10} value in fall collected larvae was lower than that observed in winter collected larvae. However, small sample sizes for all collection groups, and high variation among individual respiration rates within a treatment group masked the pronounced decrease in winter metabolic rate observed by other researchers [55, 56]. Similarly, the increased Q_{10} value of 5.95 in the winter collected group in this study may be explained by small sample size, individual variations in respiration rates, and the four-hour duration of the experiment. Previous studies that reported Q_{10} values for *E. solidaginis* third instar larvae were based on short 30 minute acclimation and 30 minute measurement periods [56], or an unspecified interval of time [55, 57].

Statistical analysis of *E. solidaginis* respiration data poses a challenge due to the small sample sizes and large variation in rates between individuals from the same treatment group. Analysis of Variance (ANOVA) was used to determine whether or not chosen parameters within a data set were significantly different from each other. The test used for parametric ANOVA is based on whether or not data approximate a normal population, or whether or not the data would form a bell shaped frequency

distribution curve based on infinite sampling [83, 84]. Data that have large variations, extreme outliers, or very small sample sizes may not pass a test for normality [83, 84], as was the case for respiration data in this study. Nonparametric ANOVA, such as the Kruskal-Wallis test, is designed for populations that do not follow a normal distribution, while parametric one-way ANOVA is designed for populations that do follow a normal distribution [83, 84]. The Kruskal-Wallis nonparametric ANOVA compared median values in data sets, while one-way parametric ANOVA compared mean values in data sets [83, 84]. A Tukey-Kramer multiple comparisons post test was used in conjunction with one-way parametric ANOVA to compare all group means.

Data that do not follow a normal distribution can be transformed (the same mathematical algorithm can be performed on each value) in an effort to approximate a normal distribution [83, 84]. The log value of each *E. solidaginis* respiration data point was taken to approximate a normal sample, and the Tukey-Kramer test performed. Statistical analysis of *E. solidaginis* respiration data was performed using raw data with the nonparametric Kruskal-Wallis test, and transformed data with the parametric one-way ANOVA and Tukey-Kramer post test.

The Kruskal-Wallis test found a significant difference ($p < 0.0001$; Kruskal-Wallis statistic $KW = 57.55$), between median values of all *E. solidaginis* respiration and treatment groups. A high Kruskal-Wallis statistic corresponds to a large discrepancy between ranked data in treatment groups. Thus the probability that random sampling would result in a KW statistic as high or higher than 57.55 is less than 0.0001.

One-way ANOVA using log values of *E. solidaginis* average respiration rates found that variation among group means was significantly greater than expected by chance ($p < 0.0001$). The Tukey-Kramer post test found significant differences in the means of most treatment groups. However, there appeared to be no significant differences between fall and winter samples at 4°C, 10°C or, 15°C, and no significant differences between fall samples at 10°C and 15°C. Again, small sample size and large variations between individuals within a group may account for these results.

Decreased metabolic rate and decreased response to temperature changes reflect a state of diapause in *Eurosta solidaginis* [55]. Although differences between fall and winter samples were not significant at all temperatures, a significant difference was found between all samples compared to summer collected larvae measured at 15°C ($p < 0.001$ for all comparisons with summer sample). The drop in metabolic rate in *E. solidaginis* fall collected larvae was consistent with larvae entering diapause.

Results obtained for *G. groenlandica* larvae respiration compared well with previously reported values. Standard *G. groenlandica* respiration was reported to be $\sim 220 \mu\text{l O}_2 \text{ hr}^{-1} \text{ g}^{-1}$, and larvae brought to room temperature after prolonged freezing (6 months) were reported to have a respiration rate of $\sim 84 \mu\text{l O}_2 \text{ hr}^{-1} \text{ g}^{-1}$ [37]. This study recorded average respiration rates of $218.29 \mu\text{l O}_2 \text{ hr}^{-1} \text{ g}^{-1}$, and $72.80 \mu\text{l O}_2 \text{ hr}^{-1} \text{ g}^{-1}$. Similarly, larvae acclimated to 5°C for two months showed respiration rates of approximately $100 \mu\text{l O}_2 \text{ hr}^{-1} \text{ g}^{-1}$ [48]. At 15°C, starved larvae consumed oxygen at a rate of $\sim 120 \mu\text{l O}_2 \text{ hr}^{-1} \text{ g}^{-1}$, while inactive larval metabolic rates approached $175 \mu\text{l O}_2 \text{ hr}^{-1} \text{ g}^{-1}$, and active feeding larval rates were above $200 \mu\text{l O}_2 \text{ hr}^{-1} \text{ g}^{-1}$ [44]. Q_{10} values

were not assessed for *G. groenlandica* larvae due to limited availability of larvae and the high mortality rate among those that were collected which prevented multiple temperature measurements.

The small sample sizes and high variability in individual respiration influenced statistical analysis of *G. groenlandica* larvae respiration rates. Sample sizes were too small to determine whether or not data were derived from a statistically normal population, and thus complicated analysis. Both parametric and nonparametric methods used to test the data agreed that significant differences occurred in median and mean respiration values between the active summer larvae and the winter frozen for 5.5 months group ($p < 0.05$ for both tests).

Respiration data from *E. solidaginis* and *G. groenlandica* larvae were consistent with reported rates of oxygen consumption for both species. A trend of increased respiration with increased temperature was observed in *E. solidaginis*, and a trend of decreased respiration associated with cold adaptation was observed in both *E. solidaginis* and *G. groenlandica*. Given that cold adapted mitochondrial degradation is associated with reduced metabolic rate in *G. groenlandica* [37], reduced oxygen consumption in both species may indicate lower mitochondrial numbers.

CHAPTER 3 MAXIMUM MITOCHONDRIAL DENSITY

Introduction

Insect fat body is a diffuse aggregate of mesoderm-derived cells that serves as a storage organ and the major site of intermediary metabolism [4, 34]. Fat body cells, called trophocytes, are contained within the haemocoel (body cavity), and in young larvae nuclei are round and the cells have few inclusions [4, 34]. As the larvae feed and mature, cells become vacuolated as stores of lipid, glycogen and protein accumulate, causing distortions in the shapes of cells and their nuclei [4, 34]. Metabolic reserves stored in the fat body are primarily used during periods of non-feeding, diapause, and metamorphosis [4, 34].

In the insect fat body, mitochondria are similar to vertebrate liver mitochondria; they are oblong and $\sim 1 \mu\text{m}$ in size as opposed to the much larger, elongated flight muscle mitochondria [40]. Mitochondria have a double membrane system: the outer membrane is permeable to most small molecules, whereas the inner membrane is impermeable to most small molecules and is folded to form cristae that project into the matrix [79, 80]. Metabolic reactions in the cytosol (such as glycolysis) and those in the matrix (such as fatty acid β -oxidation), accumulate reduced electron acceptors that in turn donate electrons to the electron transport chain found in the inner mitochondrial membrane [79, 80]. Electrons are passed down a gradient of electron acceptor complexes, where they are coupled with the movement of hydrogen ions across the inner membrane and into the intermembrane space [79,

80]. The gradient formed by pumping hydrogen ions into the intermembrane space is coupled to ATP synthesis: hydrogen ion movement down the gradient into the matrix is coupled to the formation of ATP through the ATP synthase enzyme [79, 80].

Mitochondria contain their own genome that may be present in multiple copies within each mitochondrion [78, 79]. The mitochondrial genomes of many organisms have been sequenced, and in higher vertebrates a characteristic set of proteins, ribosomal RNA (rRNA), and transfer RNA (tRNA) are encoded [78, 79]. Polypeptides encoded in the mitochondrial genome are components of the electron transport chain and mitochondrial rRNAs and tRNAs function in mitochondrial protein synthesis [78, 79]. Like bacterial genomes, mitochondrial DNA forms a closed circular double-stranded molecule, and in animals has a high proportion of coding sequences [78, 79]. In most animals, transcription of mitochondrial DNA proceeds from one of two promoter regions [78, 79]. One promoter is contained on the heavy strand, which is characterized by a high GC content and contains most mitochondrial genes. The light strand has a high AT content, contains few genes, and is under the transcriptional control of a second promoter. RNA transcription proceeds in opposite directions from each promoter creating one long transcript from each strand [78, 79]. In this respect, each strand of the mitochondrial genome resembles a bacterial operon, with many genes transcribed from a single promoter.

Full length mitochondrial mRNA transcripts are processed by clipping individual mRNAs, tRNAs and rRNAs from a complete strand transcript [78, 79]. A 3' polyadenylation (poly(A)) sequence is added to the mRNA and bases are modified [78, 79]. RNA editing, or changes in information at the mRNA level, may include

modification of a base which changes a protein, or addition or removal of nucleotides [78]. RNA editing in animals occurs in the tRNA for methionine, in which one modified tRNA transcript is used for methionine, or one for formylmethionine, the initiator tRNA in protein synthesis [78, 79]. Other examples of RNA editing also found in fungi, plants and protists include addition or removal of one or more uridines at specific sites, and conversions of cytosine to uridine [78, 79]. Thus transcript length may be different from gene length as a result of mRNA splicing and processing.

Ribosomes encoded for in mitochondria have large 16S and small 12S subunits. This is in contrast to bacterial rRNA in which the 16S rRNA is a component of the small ribosomal subunit [78, 79]. In invertebrates, all of the tRNAs required for mitochondrial protein synthesis are encoded within the mitochondrial genome, and protein synthesis takes place on ribosomes within the mitochondrial matrix [78, 79].

The AT rich mitochondrial genome can be studied using chemicals that bind nucleic acids. The epifluorescent dye bisbenzimidazole, also known as DAPI (4', 6-diamidino-2-phenylindole dichloride) is advantageous for studying mitochondrial DNA in cells. Bisbenzimidazole has a high affinity for mitochondrial AT rich DNA [85], binding preferentially to the minor groove of the DNA double helix [86]. Bisbenzimidazole has a maximum excitation wavelength of 340 nm and a maximum emission wavelength of 448 nm [86]. Bisbenzimidazole stained DNA (nuclear or mitochondrial) emits bright blue light when placed under ultraviolet light. DAPI has

been successfully used by other researchers to view mitochondria within cells [37, 85].

Epifluorescent microscopy of *E. solidaginis* and *G. groenlandica* fat body cells stained with bisbenzimidazole allowed direct observation of mitochondria within cells. The technique provided qualitative and quantitative evidence for changes in mitochondria. Previous to this investigation, DAPI was used to detect loss of mitochondria in fat body and brain tissue of the Arctic woolly bear caterpillar, *G. groenlandica* [37]. Tissues stained with DAPI were viewed by epifluorescence microscopy and the ratio of mitochondria per nucleus was counted. The ratios dropped from greater than 100:1 in both brain and fat body in 15°C acclimated larvae, to 0.04:1 in brain tissue and <0.01:1 in fat body tissue from larvae acclimated to -15°C. This represented a 10,000 fold decrease in the number of mitochondria per cell [37].

The objective of epifluorescent microscopy experiments was to quantify the number of mitochondria per unit area in fat body cells dissected from larvae from various collection and treatment groups. The average number of mitochondria per unit area was used to establish whether or not mitochondrial number changed with treatment group. Mitochondrial number was also compared with respiration data, mitochondrial gene expression data, and mitochondrial genome copy number data.

Materials and methods

Fat body cells dissected from larvae were treated with 0.1% sodium borohydride (to reduce autofluorescence [87]) for 30 minutes on ice, prior to fixing in methanol. Cells were rinsed with phosphate buffered saline (PBS) pH 7.4, fixed in ice cold methanol for 10 minutes, and rinsed twice with PBS. Cells were stained in 2ng/μl bisbenzimidide (Sigma-Aldrich) for 10 minutes on ice, rinsed twice with PBS, and mounted on slides with glycerol:PBS (1:1). Slides were sealed with clear nail polish and stored in the dark.

Cells were viewed using a Zeiss Axioskop 2 epifluorescent microscope and images were acquired by a QIMAGING Microimager II camera (Burnaby, British Columbia) and analyzed using Northern Eclipse 5.0 Image Analysis software (Empix Imaging Inc.). A 10 x ocular lens and 40 x and 63 x /1.5 oil immersion objective lenses were utilized. 16 bit black and white captured images were stored on compact disc. Images were opened, converted to 8 bit format, inverted in Adobe Photoshop5.0 (Adobe Systems Incorporated), and imported into Northern Eclipse for analysis.

E. solidaginis cells were examined in areas where mitochondria were abundant and one image per cell was acquired. A 25 μm by 25 μm grid was overlaid on winter cell images, and the grid section that represented the maximum number of mitochondria visible was counted. To compensate for larger cell diameter in fall collected larvae a 27 μm by 27 μm grid was used. The size increase of the grid was based on the ratio of the 25 μm grid and the average winter cell diameter of 385 μm, and the average cell diameter of 418 μm in fall collected larvae. All fluorescing

objects between 0.5 and 1.0 μm within the plane of focus were counted as mitochondria. Thus maximum mitochondrial density was equal to the maximum number of mitochondria per 25 μm or 27 μm squared area in a digital image, given by all fluorescing objects between 0.5 and 1.0 μm . Mitochondria that fell upon gridlines were excluded from counts. *G. groenlandica* mitochondrial counts were calculated for the number of visible mitochondria per cell.

The maximum number of mitochondria (maximum mitochondrial density) per 25 μm (winter cells) or 27 μm (fall cells) square area, was entered into GraphPad InStat version 3.02 (GraphPad Software, Inc.). Data from all individuals within a treatment group were pooled and statistical analysis compared median and mean values using parametric and nonparametric methods.

Results

Fat body cells from summer collected *E. solidaginis* larvae did not have distinct visible mitochondria, (Figure 4). Cells were small and the nucleus occupied the majority of intracellular space. Mitochondria were not distinctly visible in the cytoplasm and the proximity and brightness of the nucleus had a flooding effect. Similarly, mitochondria in *G. groenlandica* cells were difficult to count because cells were very small, averaging approximately 40 μm (n=50) in diameter, with the nucleus occupying the majority of the cell (Figure 5).

Fat body cells from fall collected *E. solidaginis* larvae were on average 418 μm in diameter (n=68). Cells contained many small lipid filled vacuoles, and dense

cytoplasm (Figure 6). Fat body cells from winter collected larvae were smaller, averaging 385 μm ($n=65$). In contrast to fall cells, winter cells had large lipid vacuoles, dispersed cytoplasm, and evenly distributed mitochondria (Figure 7).

Counts of maximum mitochondrial density for each *E. solidaginis* individual were compared within treatment groups. Both parametric and nonparametric analyses were performed when standard deviations were significantly different within a treatment group. Fall collected larvae measured at 4°C had no significant difference in medians or means among the three individuals in the treatment group (One-way ANOVA $P=0.2204$; Nonparametric ANOVA $P=0.6467$). Fall collected larvae measured at 10°C had one individual whose mean maximum mitochondrial density was significantly different from the other two individuals in the treatment group (One-way ANOVA $P<0.05$). Fall collected larvae measured at 15°C had only one individual so no comparisons were required. A t-test (parametric analysis of variance used to compare two groups only) of frozen winter larvae found no significant difference in the mean maximum mitochondrial density ($P=0.1323$). One-way ANOVA found one individual among winter collected larvae measured at 4°C whose mean maximum mitochondrial density was significantly different from the other two individuals ($P=0.0243$). For winter collected larvae measured at 10°C both parametric and nonparametric analysis found that one of the three individuals had mean and median maximum mitochondrial density values that were significantly different from the other two individuals (Parametric ANOVA $P<0.001$; Nonparametric ANOVA $P<0.01$).

Nonparametric ANOVA comparing all individuals from all treatment groups found significant differences in median values between many individuals ($P < 0.0001$). Most notably, one individual from the winter collected group measured at 10°C had median values significantly different from 14 of the 17 other individuals to which it was compared (P-values from less than 0.05 to less than 0.001).

Mitochondrial counts for individuals within a treatment group were pooled for further statistical analysis. Cells from *E. solidaginis* fall collected larvae measured at 4°C had an average maximum mitochondrial density of 27.64 ± 1.86 (N=107 cells; n=3 individuals), 24.42 ± 1.13 (N=125 cells; n=3 individuals) at 10°C , and 26.08 ± 2.31 (N=48 cells; n=1 individual) at 15°C . Cells from winter collected frozen larvae had a maximum mitochondrial density of 26.20 ± 1.37 (N=211 cells; n=2 individuals), 26.74 ± 1.52 (N=150 cells; n=3 individuals) in winter larvae measured at 4°C , 32.51 ± 2.11 (N=126 cells; n=3 individuals) in winter larvae at 10°C , and 24.93 ± 1.37 (N=150 cells; n=3) in winter larvae at 15°C (Figure 8). Statistical analysis using both parametric and nonparametric methods detected a significant difference in the maximum mitochondrial density of winter collected larvae measured at 10°C , when compared to all other collection and treatment groups. Parametric tests detected a significant difference between the mean maximum mitochondrial density values at a P-value of less than 0.001, while nonparametric tests detected differences in median values at a significance level of $P < 0.05$. Nonparametric correlation analysis found no correlation between respiration rate and maximum mitochondrial density (Spearman $r = -0.6000$; $P = 0.2417$).

G. groenlandica counts for number of visible mitochondria per cell were very low, owing to small cell size, and dense cytoplasm. Active summer larvae had an average of 0.087 visible mitochondria per cell (n=150 cells), larvae that had spun hibernacula had 0.97 visible mitochondria per cell (n=50 cells), larvae that had been frozen for 2 weeks had an average of 0.0 visible mitochondria per cell (n=50 cells), and larvae that had been frozen for 5.5 months had 0.14 mitochondria per cell on average (n=50 cells). Statistical analysis of *G. groenlandica* mitochondrial counts was limited because data were not derived from a statistically normal population, and the standard deviation of the summer frozen group equaled zero. Nonparametric ANOVA failed to find a significant difference between median values of treatment groups (p=0.0592).

Discussion

Fat body cells from winter collected *E. solidaginis* third instar larvae exhibited the large, coalesced lipid droplets characteristic of intracellular freezing [63, 65, 66]. Coalescence of lipid droplets in fat body cells increased the clarity and translucence of cytoplasm compared to fat cells from fall collected larvae. Fat body cells from fall collected larvae had dense appearing cytoplasm resulting in part from the many small lipid droplets scattered throughout the cytoplasm, indicating that cells from these larvae had not experienced intracellular freezing.

While epifluorescent microscopy of fat cells from *E. solidaginis* fall and winter larvae was successful, cells from summer collected larvae were small, with

dense cytoplasm and were extremely opaque. Brightly stained nuclei obscured the cytoplasm and reliable counts were not possible. In cells derived from fall and winter collected larvae, maximum number of mitochondria per 25 μm or 27 μm squared area were counted. The thousands of mitochondria per cell were prohibitive to counting all mitochondria within a cell, and cells were so large that they would not fit within the field of view at a magnification conducive to visualizing mitochondria. Hence, the maximum mitochondrial density was counted per unit area as a means for comparison between fall and winter larval groups.

Maximum mitochondrial density in *E. solidaginis* third instar larvae varied among cells from the same individual, and varied significantly between individuals from a treatment group. Large standard deviations in values for one individual required nonparametric ANOVA, which is less robust than parametric analysis of variance. However, both parametric and nonparametric analysis of variance detected significant differences between individuals from treatment groups (fall 10°C, winter 4°C, winter 10°C, and winter 15°C).

Maximum mitochondrial density in winter collected larvae at 10°C was significantly greater than that for all other groups (p values ranging from <0.05 to <0.001), whereas means from all other treatment groups were not significantly different from each other. These data were not consistent with mitochondrial degradation in *E. solidaginis* third instar larvae during cold acclimation and overwintering. Winter collected larvae measured at 10°C had increased maximum mitochondrial density, although at 15°C the same increase was not observed.

The absence of increased maximum mitochondrial density in winter collected larvae measured at 15°C, compared to winter larvae at 10°C, is representative of the physiological state of the larvae. Recent evidence suggests that *E. solidaginis* larvae studied in Ohio were in a refractory stage of diapause, in which larvae were incapable of development even at permissive temperatures, from mid October to mid December [55]. It was further demonstrated that colder temperatures may produce a lag effect, whereby the refractory stage of diapause is extended. These results suggested that larvae collected in the first week of January, in Ontario, were in the refractory stage of diapause, based on the reduced mitochondrial numbers as measured by maximum mitochondrial density. This was supported by the observation that diapause prevents premature adult emergence during unseasonably warm temperatures [55]. At 15°C, unseasonably warm for Ontario in January, premature progression to pupariation was inhibited by the diapause program, and reflected in the failure to increase numbers of mitochondria. While the presence of a diapause program in *E. solidaginis* third instar larvae may prevent increased mitochondrial density at unseasonably high temperatures, increased mitochondrial density was observed at temperatures immediately below this threshold. It is suggested that temperature response for resumption of development after diapause may be variable among individuals within a population, leading to high mitochondrial density at 10°C in some individuals, while mitochondrial density in others remains low. This is supported by the finding that maximum mitochondrial density varies significantly between individuals among treatment groups.

In *E. solidaginis*, mean maximum mitochondrial density was not significantly different for collection and treatment groups with the exception of winter collected larvae at 10°C, which had increased maximum mitochondrial density. In contrast, respiration rates were not significantly increased in the winter collected larvae at 10°C, suggesting that there is not a positive correlation between respiration rate and maximum mitochondrial density. Indeed, no correlation between respiration rate and maximum mitochondrial density was found using nonparametric correlation analysis (Spearman $r = -0.6000$; $P=0.2417$).

While established protocols were followed [37, 85] the techniques employed in this study were not able to replicate previously published reports of mitochondrial degradation in *G. groenlandica* [37]. Mitochondria were not visible in fat body cells from actively feeding and metabolizing summer collected larvae. *G. groenlandica* larval cells were very small in all individuals examined, and the nuclear staining often obscured the cytoplasm. Even under highest magnification, mitochondria were not visible in the majority of cells, and were not visible as depicted in previous experiments [37]. Because mitochondria could not be reliably counted in cells from active larvae, no conclusions could be made given the inefficacy of the technique: nuclear and mitochondrial DNA are indistinguishable. In other words, mitochondria that are directly surrounding the nucleus are not visible since the nucleus is brightly stained in the same color. In a cell such as one derived from a fall collected *E. solidaginis* larva, where cytoplasm is abundant and the cells large, areas of cytoplasm distanced from the nucleus can be consistently examined. In *G. groenlandica*, however, the small cell size and relatively large nucleus are prohibitive to this

approach. This study was not able to reproduce the results obtained in previous studies, where mitochondrial degradation was quantified in *G. groenlandica* using DAPI [37].

Epifluorescent microscopy using the DNA specific chromophore bisbenzimidazole was successful in fat body cells from fall and winter collected *E. solidaginis* larvae but unsuccessful in fat body cells from summer collected larvae, and from *G. groenlandica* larvae. Results suggest that mitochondrial degradation was not present in *E. solidaginis* larvae as part of a response to cold. Comparison of respiration rate and maximum mitochondrial density in fall and winter collected *E. solidaginis* larvae revealed that there was no correlation between the two parameters. In conclusion, there did not appear to be an association between cold acclimation and maximum mitochondrial density in *E. solidaginis*.

CHAPTER 4 NORTHERN BLOTS, DOT BLOTS, AND SOUTHERN BLOTS

Introduction

Alterations in fat body mitochondria have been noted in association with developmental changes. Rapid mitochondrial regeneration was noted during the first 34 hours of adult life in the cockroach, *Blaberus*, leading to a sevenfold increase in the number of mitochondria [40]. Mitochondria in the fat body of the butterfly, *Calpodus ethlius*, degraded shortly before pupation [88], that is, during the transition from larva to pupa [38]. Mitochondrial degradation was also reported in the arctic woolly bear caterpillar larvae, *G. groenlandica*, in association with cold adaptation, and rapid regeneration was observed upon warming of the larvae [37].

Previous studies established that insect fat body mitochondria undergo radical alterations in response to developmental changes and environmental conditions [37, 38, 40, 88]. Although ultrastructural studies have recorded these mitochondrial changes, patterns of mitochondrial gene transcription and the fate of mitochondrial DNA have not been investigated. Mitochondrial degradation in *G. groenlandica* larvae was demonstrated through the use of epifluorescent microscopy using a dye that specifically stained DNA [37]. It was hypothesized in the present study that mitochondrial degradation, as indicated by degradation of mtDNA, would result in decreased mtDNA copy number, detected by Dot blot hybridization and would result in decreased transcription of mitochondrial cytochrome oxidase subunit I and 16S rRNA genes detected by Northern hybridization.

The cytochrome oxidase respiratory complex is complex IV in the electron transport chain. It consists of 13 separate subunits in mammals, although only three subunits are known to have catalytic function [89]. Three of the cytochrome oxidase thirteen subunits (COI, COII and COIII) are encoded in the mitochondrial genome [79]. The 16S ribosomal RNA is also encoded in the mitochondrial genome. The 16S rRNA subunit combines with nuclear encoded proteins to form the large mitochondrial subunit. The large 16S and small 12S rRNA subunits combine with associated proteins to form a functional mitochondrial ribosome [78].

Fat body tissue, as the site of intermediary metabolism, was expected to show high levels of mitochondrial gene expression during periods of active feeding and growth. However, whether or not mitochondrial gene expression changes during periods of low metabolism such as diapause and cold hardiness has not been previously investigated.

Hybridization analysis used several different techniques. Northern blotting involved transfer of RNA from an electrophoresis gel to a solid support membrane, and preserved the size separation achieved by electrophoresis. Southern blotting involved transfer of DNA from an electrophoresis gel to a solid support membrane, and also preserved size separation of molecules. Dot blots similarly involve transfer of DNA fragments to solid support membrane, though DNA was applied directly to the membrane and was not separated on gels prior to blotting.

Restriction digests and Southern blots of *E. solidaginis*, *G. groenlandica* and *Drosophila* were hybridized with COI and 16S mitochondrial genes and with a chromosomal gene derived from *Drosophila*. Mitochondria specific DNA

polymerase γ is encoded by the *tam* (*tam*) gene on *Drosophila* Chromosome 2 [90]. *tam* is the catalytic subunit of the key enzyme involved in mitochondrial DNA replication [91]. The highly conserved *tam* gene was used as a probe to identify genomic DNA in Southern analyses.

The objective of the Northern and dot blot hybridization experiments was to investigate mitochondrial gene transcription and genome copy number in various larval collection and treatment groups. Mitochondrial gene transcription and genome copy number were compared to respiration data and mitochondrial density data among treatment groups to establish whether or not changes occur with cold adaptation. Southern analysis established whether or not mitochondrial sequences were present in the nuclear genomes of *E. solidaginis*, *G. groenlandica*, and *D. melanogaster*.

Materials and Methods

Larval fat body tissue dissected after respiration measurements was used for RNA or DNA extraction and for preparation of DAPI stained tissue mounted on slides. Larvae were dissected in the presence of phosphate buffered saline (PBS) pH 7.4, and fat body tissue was immediately transferred to sterile 1.5 ml tubes for RNA or DNA isolation, or for slide preparation (Chapter 3).

RNA Extraction

Fat body tissue dissected from whole larvae was homogenized in sterile 1.5 ml tubes using disposable pellet pestles (VWR Canlab). TRIzol reagent [400 μ l] (Invitrogen Canada, Burlington, Ontario) was added to each sample and incubated at room temperature for 15 minutes before freezing in liquid nitrogen for storage purposes.

RNA isolation was carried out using TRIzol reagent inside a biological safety cabinet following manufacturer's instructions. RNA was extracted from TRIzol by centrifuging tissue homogenate at 12,000 x g for 10 minutes at 4°C to remove cellular debris. Homogenates were transferred to clean sterile 1.5 ml tubes and 80 μ l of chloroform was added to each sample. Tubes were shaken vigorously for 15 seconds and incubated on the bench top for 3 minutes. Tubes were centrifuged at 12,000 x g for 15 minutes at 4°C to separate the RNA containing aqueous phase. The aqueous phase was transferred to a fresh sterile 1.5 ml tubes and RNA was precipitated with 200 μ l isopropyl alcohol, followed by a 10 minute bench top incubation and centrifugation at 12,000 x g for 10 minutes at 4°C. Isopropanol was decanted and the RNA pellet was briefly washed in 75% ethanol, followed by centrifugation at 7,500 x g for 5 minutes at 4°C. Ethanol supernatant was decanted and RNA pellets were dried briefly by vacuum centrifugation. RNA was resuspended in autoclaved 0.01% diethyl pyrocarbonate (DEPC water) and incubated at 55°C for 10 minutes.

RNA concentrations were determined using a GeneQuant *pro* RNA/DNA calculator (Amersham Pharmacia Biotech, New Jersey, U.S.A.). Individual RNA samples from the same collection and treatment group were pooled to increase

concentrations of RNA. RNA samples were stored at -80°C until required for further experimentation.

DNA Extraction

Larval fat body tissue dissected from whole larvae was homogenized as above, and 470 μl DNA extraction buffer (0.01M Tris-HCl pH 8.0; 0.1M NaCl; 0.4M DTT; 0.05M EDTA pH 8.0; 2% SDS) and 10mg/ml Proteinase K (Sigma-Aldrich) (final concentration of 0.06 mg/ml) were added to inactivate cellular enzymes and break down cellular debris. Samples were incubated in a 55°C circulating water bath (Haake D8, VWR Canlab) overnight. DNA was extracted following a standard phenol/chloroform procedure. An equal volume of equilibrated phenol [500 μl] was added to the tissue/extraction buffer homogenate and mixed by inversion for 5 minutes. Samples were centrifuged at 15,000 x g for 5 minutes and the aqueous phase transferred to a clean sterile 1.5 ml tube. Two more phenol extractions were performed followed by addition of 500 μl chloroform:isoamylalcohol (IAA) (24:1). Samples were mixed by inversion for 3 minutes, centrifuged for 5 minutes, and the aqueous phase was transferred to a clean sterile 1.5 ml tube. An additional chloroform:IAA extraction was carried out, followed by volume restoration to 500 μl with sterile TE buffer (1M Tris-HCl; 0.5M EDTA) pH 7.5 and addition of 50 μl 3M sodium acetate (NaOAc), and 700 μl 95% ice cold ethanol. Samples were frozen at -80°C for 15 minutes, followed by centrifugation at 15,000 x g for 30 minutes. Supernatant was discarded and the DNA pellet was resuspended in 50 μl sterile distilled deionized water, followed by addition of 500 μl ice cold 100% ethanol.

Samples were again frozen at -80°C for 15 minutes, followed by centrifugation at $15,000 \times g$ for 30 minutes. DNA pellets were dried by brief centrifugation under vacuum and resuspended in TE buffer pH 7.5. DNA concentrations were determined using GeneQuant *pro* as above. DNA samples were stored at -80°C until required.

Drosophila melanogaster Oregon isolate total DNA was obtained by homogenizing whole insects (Northwest Scientific Supply, Victoria), and extracting DNA using the phenol/chloroform method previously described.

Northern Blots

RNA samples were analyzed by denaturing gel electrophoresis and Northern blot analysis [92]. Five (5) μg of each RNA sample was mixed with 10 μl of loading buffer (4.8M formaldehyde; 39% formamide; 0.88 X 3-(N-Morpholino) propanesulfonic acid (MOPS) buffer; 0.31 $\mu\text{g}/\mu\text{l}$ ethidium bromide; 1.3 mM EDTA pH 7.5), heated at 70°C for 10 minutes, and loaded onto a 1% denaturing agarose gel (1% agarose; 1 X MOPS buffer; 0.92M formaldehyde). Gels were run at 5 volts/cm in 1 X MOPS buffer, using FisherBiotech Electrophoresis system (Fisher Scientific, Pittsburgh, Pa.).

Gels were photographed and visualized using the Eagle-eye transilluminator system and software (Stratagene, California) and blotted onto Schleicher & Scheull BAS 85 reinforced nitrocellulose membranes following the method of Sambrook et al. [92]. Denaturing agarose gels were soaked in 0.05 N sodium hydroxide (NaOH) for 20 minutes to partially hydrolyze RNA and increase efficiency of transfer. Gels were rinsed in 20 X SSC (3M sodium chloride (NaCl); 0.3M sodium citrate) for 45

minutes, and placed upon the blot apparatus. Membranes were wetted briefly in distilled deionized water, then rinsed in 2 X SSC and placed on top of the gel. Two (2) pieces of Whatman 3MM paper were placed upon the membrane followed by stacked paper towels. RNA was transferred for 18 hours using a 20 X SSC transfer buffer. After blots were disassembled, membranes were soaked briefly in 6 X SSC and dried on Whatman paper. Dried membranes were wrapped in plastic wrap and transilluminated for 5 minutes to crosslink DNA to the membrane. Membranes were stored at 4°C until required.

Dot Blots

DNA to be used in dot blot analysis was treated with a ribonuclease (RNase A, Sigma-Aldrich) at a final concentration of 0.25 µg/µl. Samples were incubated on the benchtop for 1 hour, and DNA was again extracted. Equal volumes of equilibrated phenol and chloroform:IAA (24:1) [250 µl] were added to each sample, and tubes were mixed by inversion for 5 minutes. Tubes were centrifuged 5 minutes at 15,000 x g, followed by removal of the aqueous phase. Chloroform:IAA (24:1) [500 µl] was added, and tubes were mixed by inversion for 3 minutes and centrifuged at 15,000 x g for 3 minutes. Aqueous phases were transferred to fresh sterile 1.5 ml tubes, the aqueous volume was restored to 500 µl with TE buffer (pH 7.5), 50 µl 3M NaOAc was added. To this 95% ice cold ethanol [700 µl] was added and tubes were frozen at -80°C overnight. The following day tubes were thawed at room temperature, and centrifuged for 30 minutes at 15,000 x g. Supernatants were decanted, DNA pellets resuspended in 50 µl sterile distilled deionized water, and 500

μ l ice cold 100% ethanol was added. Tubes were centrifuged at 15,000 x g for 30 minutes, ethanol was decanted and DNA pellets were briefly dried by centrifugation under vacuum. DNA pellets were resuspended in 15 μ l sterile TE buffer (pH 7.5), and concentrations were determined using a GeneQuant *pro* RNA/DNA calculator (Amersham Pharmacia Biotech, New Jersey, U.S.A.).

One hundred and fifty (150) ng of total RNase A treated DNA from each sample group was analyzed by dot blot analysis. DNA was diluted in 100 μ l lysis buffer (0.8M NaOH; 20 mM EDTA), and 95 μ l TE buffer (pH 7.5), and heat denatured at 100°C for 5 minutes, followed by 5 minutes on ice. Samples were blotted onto Hybond-N membranes (Amersham Pharmacia Biotech) using a Biorad BioDot Apparatus. Membranes were rinsed briefly in 2X SSC, and dried on the benchtop before being wrapped in plastic wrap and crosslinked by UV transillumination for 5 minutes. Membranes were stored at 4°C until used.

Southern Blots

Extracted DNA was subject to restriction digest and southern blotting. Two (2) μ g of total DNA was incubated with restriction enzyme, restriction enzyme buffer, and bovine serum albumin (BSA) (if required according to manufacturers' protocol) at 37°C overnight, and heat inactivated at 65°C for 20 minutes. Enzymes used included HindIII (Gibco BRL), and EcoRI, XhoI, SallI, and BamH1 (New England Biolabs). Completed digests were run on 0.8% agarose gels containing 0.25 μ g/ml ethidium bromide, and transferred to Hybond-N membrane (Amersham Pharmacia Biotech) and subject to southern blot analysis following standard procedures [92].

Restriction digest gels were soaked in denaturing solution (0.5M NaCl; 0.5M NaOH) for 45 minutes with gentle agitation. Gels were rinsed briefly in distilled deionized water, followed by 30 minutes in neutralizing solution (0.5M Tris-HCl; 1.5M NaCl; 0.001M Na₂EDTA; pH 7.2). Neutralizing solution was replaced after 15 minutes, and removed 15 minutes following. Gels were placed face down on a blot apparatus and Hybond-N membranes wetted in water followed by 2 X SSC were placed on top. DNA was blotted for 18 hours using 20 X SSC transfer buffer. After blots were disassembled, membranes were soaked briefly in 6 X SSC, and dried on Whatman paper. Dried membranes were wrapped in plastic wrap and transilluminated for 5 minutes to crosslink DNA to the membrane. Membranes were stored at 4°C until required.

Probe Production

COI, 16S, and *tam* probes were produced using PCR generated gene fragments. COI fragments were generated using *E. solidaginis* DNA as template and the primers COI forward 5'-GGAGGATTTGGAAATTGATTAGTTCC-3' and COI reverse 5' CCCGGTAAAATTTAAAATATAAACTTC-3' (Dalton Chemical Laboratories, Ontario). A step up PCR cycle (cycles of 94°C for 30 seconds, annealing temperature for 45 seconds, and elongation at 72°C for 45 seconds; annealing temperatures of 40°C for 5 cycles; 45°C for 5 cycles; and 50°C for 30 cycles) generated an 800 base pair COI band.

16S PCR fragments were generated using primers designed by the Primer3 program (Whitehead Institute for Biomedical Research). *Drosophila melanogaster*

Oregon isolate DNA was used as template for primer design and 16S and *tam* PCR fragment generation. Touchdown PCR (cycles of 94°C for 30 seconds, annealing temperature for 45 seconds, and elongation at 72°C for 45 seconds; annealing temperatures of 65°C for 3 cycles, 60°C for 3 cycles, and 55°C for 25 cycles) and the primers 16S forward 5'-TGAAAAGTTTAAATAAAGAATTCGGCA-3' and 16S reverse 5'-GAAACCAACCTGGCTTACACCG-3' (GibcoBRL), generated a 610 base pair *Drosophila* 16S fragment.

tam fragments were generated using *Drosophila melanogaster* Oregon isolate DNA template and forward primers 5'-CGCAGAAAACGTGCTGAGCAGTG-3', and reverse primers 5'-CTTGCCTTGGGAACTGGGAAACG-3' (Gibco BRL). A touchdown PCR cycle with annealing temperatures of 68°C for 3 cycles, 65°C for 3 cycles, 60°C for 3 cycles, 55°C for 3 cycles, and 55°C for 25 cycles, produced an expected 1,600 base pair band.

Taq or *Pfu* polymerase enzymes were used in 25 µl PCR reactions, containing 1-10 ng template DNA, 0.2 mM each deoxyribonucleic acid (dNTP), 1 µM each oligonucleotide primer, and 10 X *Taq* buffer (200mM Tris-HCl pH 8.4; 500 mM KCl; 50 mM MgCl₂), or 10 X *Pfu* buffer (200mM Tris-HCl pH 8.8; 20 mM MgSO₄; 100 mM KCl; 100 mM (NH₄)₂SO₄; 1% Triton-X-100; 1 mg/ml nuclease-free Bovine Serum Albumin (BSA)). PCR products were confirmed on 1% agarose gels containing 0.25 µg/ml ethidium bromide, and 1 X TBE buffer. DNA bands of interest were excised and gel purified using Millipore ultrafree-DA gel nebulizers, and Millipore Microcon-100 microconcentrators.

The identity of the 16S and COI PCR fragments was confirmed by cloning the gel purified product using the Zero Blunt[®] TOPO[®] PCR cloning kit for sequencing (Invitrogen) following manufacturer's instructions. Four (4) μ l of gel purified PCR product, 0.5 μ l salt solution (1.2M NaCl; 0.006M MgCl₂), and 0.5 μ l pCR[®]4Blunt-TOPO[®] vector (10 ng/ μ l linearized plasmid vector with *Vaccinia* virus Topoisomerase I covalently bound to the 3' ends; 50% glycerol; 50 mM Tris-HCl, pH 7.4; 1 mM EDTA; 2mM DTT; 0.1% Triton X-100; 100 μ g/ml BSA; bromophenol blue colour indicator) were incubated at room temperature for 30 minutes. Reactions were transformed into chemically competent TOP10 cells (Invitrogen) using heat shock method, and incubated in SOC medium (2% Tryptone; 0.5% yeast extract; 10mM NaCl; 2.5mM KCl; 10 mM MgCl₂; 10mM MgSO₄; 20 mM glucose) for 2 hours. One hundred (100) and 150 μ l of each reaction was plated onto LB plates (1% bacto-tryptone; 0.5% bacto yeast extract; 1% NaCl; 1.5% agar; pH 7.5) containing 50 μ g/ml kanamycin, and plates were incubated at 72°C overnight.

To confirm insert size, colonies were picked using a sterile toothpick, and added to 200 μ l sterile distilled deionized water. One tenth of the reaction volume (2.5 μ l) of diluted cells were used as template in a 25 μ l PCR reaction, using *Pfu* enzyme and M13 universal primers. A touchdown PCR cycle was used with annealing temperatures of 68°C for 3 cycles, 64°C for 3 cycles, 60°C for 3 cycles, and 56°C for 25 cycles, followed by 72°C for 7 minutes, and 20°C for 10 minutes.

Overnight cultures of positive insert clones were made using 10 ml of LB media inoculated with positive clone using a sterile toothpick. Five (5) ml of overnight culture was plasmid purified using a QIAprep Miniprep Kit (Qiagen).

Overnight culture was centrifuged to pellet bacterial cells, and resuspended in 250 μ l Buffer P1 to which RNase A had been added. Two hundred and fifty (250) μ l of Qiagen Buffer P2 was added and tubes were mixed gently by inversion to lyse bacterial cells. Three hundred and fifty (350) μ l of Qiagen Buffer N3 was added and tubes mixed gently by inversion to neutralize lysis. Cells were centrifuged at 13,000 x g for 10 minutes, and resulting supernatant was applied to QIAprep columns. Columns were spun for 60 seconds and washed by adding 0.5 ml Qiagen buffer PB, followed by centrifuging 60 seconds at 30,000 x g. Columns were washed twice with 0.4 ml Qiagen PE buffer, centrifuging at 30,000 x g 60 seconds after each application. Columns were placed in clean sterile 1.5 ml tubes, and plasmid DNA eluted by application of 50 μ l 10mM Tris-Cl pH 8.5, followed by centrifugation for 1 minute. Concentrations of resulting plasmid preps was determined by gel electrophoresis, and sent for sequencing.

Plasmid preparations were sequenced at concentrations of 150 ng/ μ l. Dideoxy chain termination was used in conjunction with dideoxynucleotide fluorescent labels, and ABI Prism automated sequencing. Sequences were analyzed using Chromas 2.01 software (Technelysium Pty. Ltd., Queensland, Australia). Nucleotide sequence identity was determined by using BLAST[□] (Basic Local Alignment Search Tool; National Center for Biotechnology Information (NCBI)), and BLAST[□] sequence alignments (<http://www.ncbi.nlm.nih.gov/blast/Blast>).

Gel purified PCR products were used as template in probe production. Labeling reactions used 25-100 ng of heat denatured, gel purified PCR product, and the Random Primers DNA labeling System (GibcoBRL). Two to five (2-5) μ l of α

³²P-dCTP (New England Nuclear; 10 mCi/ml) was added to each labeling reaction, and probes were isolated using Sephadex G-25 Quickspin columns (Boeringer Mannheim Biochemicals) following manufacturer's protocol. Columns were equilibrated by adding 200 µl TE buffer pH7.5 to tops of columns, followed by 10 seconds of centrifugation. A total of 600 µl of TE buffer was washed through columns, before addition of labeling reactions. Column purified labeling reactions were added to membranes prehybridized with 0.2 mg/ml (final concentration) sonicated herring sperm DNA (Promega), and hybridization buffer (5X SSC, 5X Denhart's solution, and 0.5% SDS).

Hybridizations were carried out at 63°C overnight. Membranes were washed twice with 1X SSC, 0.1% SDS, wrapped in plastic wrap, and placed on phosphor-screens (Fugi Imaging Plate; CR ST-VN). Screens were visualized with Molecular Dynamics Laser Scanning Phosphor-imager (Storm), and analyzed using ImageQuant software (Molecular Dynamics). Maximum intensity of hybridized bands was calculated using ImageQuant software, version 5.0 (Molecular Dynamics).

Results

Probes, Clones, and Sequences

An 800 base pair band was selected from several produced by PCR using cytochrome oxidase I primers and *E. solidaginis* DNA template (Figure 9). The 800 base pair band was cloned, sequenced, and identified as a partial sequence of COI. Nucleotide sequence analysis of *E. solidaginis* COI revealed that the sequence shared

87.0% identity over 600 base pairs with the *Drosophila melanogaster* Oregon isolate COI gene (Figure 10). Similarly, the *E. solidaginis* COI partial sequence shared 87.33% identity over 600 base pairs with the Mediterranean fruit fly, *Ceratitis capitata*, COI gene (Figure 10). Protein translation BLAST[□] showed that the *E. solidaginis* COI partial sequence was 86% identical to the *Ceratitis capitata* COI sequence, and shared 87.8% identity with the *Drosophila* COI protein.

A 610 base pair single band was produced using Primer3 (Whitehead Institute for Biomedical Research) designed 16S primers and *Drosophila melanogaster* Oregon isolate DNA template (Figure 11). The 610 base pair 16S band was cloned and sequenced, and was found to be >99% identical to the Oregon isolate *Drosophila melanogaster* 16S mitochondrial gene sequence.

PCR using *tam* primers and *Drosophila melanogaster* DNA produced a single band product (Figure 12). The single 1,600 base pair band was identified as the *tam* gene fragment based on expected size, and the absence of any other PCR bands.

Northern Blots

COI hybridization of *E. solidaginis* RNA yielded a prominent band at 1,500 bases, and two less prominent bands at 2,370 and 2,880 bases (Figure 13). COI hybridization of *G. groenlandica* RNA yielded two weak bands in all treatment groups corresponding to 1,110 and 1,640 bases (Figure 14). 16S hybridization of *E. solidaginis* RNA yielded a strong band of 1,100-1,200 bases, and a weak band at approximately 1,300 nucleotides (Figure 15). 16S hybridization in *G. groenlandica* displayed a single band at 1,230-1,320 bases (Figure 15).

Maximum intensity of COI hybridization in *E. solidaginis* Northern blots was observed at 1,500 bases, and was identified as the processed mRNA transcript. The 1,500 bp ribonucleotide band derived from active summer larvae was most intense, followed by fall larvae measured at 10°C, winter larvae measured at 15°C, fall larvae measured at 15°C, fall larvae measured at 4°C, winter larvae measured at 4°C, winter larvae measured at 10°C, and finally lowest intensity was observed in frozen winter larvae (Figure 16). Higher molecular weight bands at 2,370 and 2,880 nucleotides increased in intensity in winter groups (Figures 17 and 18). 16S Northern blot hybridization intensity at 1,150 bases was most intense and was identified as the processed 16S transcript. Hybridization intensity was greatest in the active summer larvae, followed by winter larvae at 15°, fall 10°C, winter 10°C, winter frozen, fall 4°C, winter 4°C, and least intense in fall 15°C (see Figure 19). Higher molecular weight 16S band intensity was highest in winter collected larvae (Figure 20).

Maximum intensity of COI hybridization in *G. groenlandica* Northern blots was observed in the 1,600 base band identified as the processed transcript. Hybridization intensity was most intense in the active summer larvae, followed by the summer larvae frozen for 2 weeks, followed by the winter larvae frozen for 5.5 months, and least intense in larvae that had spun hibernacula (Figure 21). 16S northern blot hybridization of the 1,200 nucleotide processed RNA was most intense in larvae that had spun hibernacula, followed by winter larvae frozen for 5.5 months, summer larvae frozen for 2 weeks, and least intense in active summer larvae (Figure 22).

Nonparametric correlation analysis failed to find any correlation between Northern blot hybridization intensities and maximum mitochondrial number in *E. solidaginis* (Spearman r values not considered different than zero, $P > 0.05$), with the exception of 16S processed transcript hybridization intensity (Spearman $r = 0.7857$; $P = 0.0480$). Correlation was also noted between COI and 16S high molecular weight band hybridization intensity (Spearman $r = 0.7381$; $P = 0.0458$).

Dot Blots

Dot blot analysis of *E. solidaginis* and *G. groenlandica* DNA using COI and 16S probes was successful (Figures 23 and 24). *E. solidaginis* dot blots hybridized with COI probes demonstrated maximum intensity in DNA from summer active larvae, followed by winter 10°C, winter 4°C, winter 15°C, fall 15°C, fall 10°C, and least intense in fall 4°C and winter frozen samples (Figure 25). 16S dot blot hybridization was most intense in winter 10°C, followed by winter 4°C, summer active larvae, fall 15°C, winter 15°C, fall 10°C, fall 4°C, and least intense in the winter frozen sample (Figure 26).

Nonparametric correlation analysis failed to find a correlation between dot blot hybridization intensities, and Northern blot hybridization intensities, average respiration rates, or mitochondrial counts (P -values all greater than 0.05).

Dot blot analysis of *G. groenlandica* DNA hybridized with COI probe was most intense in the summer active larvae, followed by summer larvae frozen for 2 weeks, larvae that had spun hibernacula, and least intense in larvae that had been frozen 5.5 months (Figure 27). 16S hybridization was most intense in active summer

larvae DNA, followed by larvae that had spun hibernacula, summer larvae that had been frozen for 2 weeks, and least intense in larvae frozen for 5.5 months (Figure 28).

Average respiration rate, mean maximum mitochondrial density, and hybridization intensities for Northern blot processed transcripts and Dot blots were summarized for *E. solidaginis* (Figures 29 and 30). Resulting graphs illustrated that acclimation temperature had less effect on fall collected larvae in comparison to winter collected larvae.

Southern Blots

Restriction digests and Southern hybridizations of total DNA from *E. solidaginis*, *G. groenlandica*, and *Drosophila* were successful (Figure 31) using all enzymes but BamH1, which appeared degraded. COI and 16S probes were hybridized to membranes with the following results: Uncut *E. solidaginis* DNA yielded bands at >23 and 14.5 kilobase pairs (kbp) when hybridized with COI and 16S probes (Figures 32 and 33). When cut with HindIII, 16S probes detected 6 bands ranging in size from 1.72-9.26 kbp, and COI probe detected 5 bands ranging in size from 2.47-8.46 kbp. When cut with EcoRI, 16S probes detected 2 bands sized 2.54 and 11.1 kbp, while COI probe detected 5 bands ranging in size from 2.47-16.9 kbp. XhoI restriction digests probed with 16S showed 3 bands sized 2.25, 14.9 and >23 kbp, while COI probe showed 2 bands sized 14.5 and >23 kbp. SalI digests probed with 16S and COI revealed 2 bands sized 14.9 kbp and >23 kbp.

Uncut *G. groenlandica* DNA was hybridized with COI and 16S probes yielding bands >23 kbp and 14.9 kbp (see Figures 34 and 35). DNA cut with HindIII

and hybridized with 16S probe yielded one band sized 8.99 kbp, while COI probe detected bands at 14.5 and 8.99 kbp. EcoRI digest hybridized with 16S yielded only one band at 7.73 kbp, while COI probe detected one band at 9.26 kbp. Digestion with XhoI and hybridization with 16S showed two band at 12.98 and 14.9 kbp, and COI hybridization showed 4 bands ranging in size from 10.6-15.4 kbp. SalI digest hybridized with 16S showed two bands sized 14.9 and >23 kbp, while COI digests revealed three bands sized 10.76, 14.9 and >23 kbp.

Uncut *Drosophila* DNA hybridized with 16S and COI probes revealed bands at 14.5 and >23 kbp (see Figures 36 and 37). Digestion of DNA HindIII and hybridization with 16S probe revealed 2 bands sized 12.89 and 10.6 kbp, and COI hybridization gave bands at 4.87, 9.83, and 14.5 kbp. Digestion with EcoRI and hybridization with 16S probe detected bands at 0.787 kbp, while COI detected 5 bands ranging in size from 4.2-14.5 kbp. XhoI digestion and hybridization with 16S probe showed bands at 12.51, 14.5 and 15.4 kbp, while COI probe hybridized to 7 bands sized 2.3-14.1 kbp. SalI digestion and hybridization with 16S probe gave four bands ranging in size from 11.43 to >23 kbp, while COI hybridization detected four bands ranging in size from 2.4 to >23 kbp.

Hybridization of membranes with the *tam* gene (mitochondria specific DNA polymerase γ) from *Drosophila* was successfully used to identify the >23 base pair band in restriction digests. The large band corresponding to >23 kbp was identified as genomic DNA. *E. solidaginis*, *G. groenlandica*, and *Drosophila* restriction digests and Southern blots using mitochondria specific probes yielded results consistent with the presence of nuclear mitochondrial sequences.

Discussion

Previous research on the Arctic woolly bear caterpillar, *G. groenlandica*, suggested that mitochondria are degraded during cold adaptation [37]. Similar suggestions were made for the goldenrod gall fly, *Eurosta solidaginis*, based on mitochondrial enzyme analysis [76]. The activities of three mitochondrial enzymes, citrate synthase, glutamate dehydrogenase and NAD-isocitrate dehydrogenase, all decreased in *E. solidaginis* by over 50% in winter [76]. Further enzyme studies by the same authors, however, did not support this theory of mitochondrial degradation in *E. solidaginis* [77]. Increased β -hydroxybutyrate dehydrogenase, a mitochondrial enzyme involved in fatty acid metabolism, was observed in *E. solidaginis* larvae during overwintering [77]. It was suggested that previous results noting decreases in mitochondrial enzymes during winter may have been affected by enzyme degradation [77]. Furthermore, analysis of mitochondrial oxidation of various substrates by warm and cold acclimated *E. solidaginis* larvae suggested that mitochondria of overwintering larvae must retain function and integrity over a wide range of temperatures [93].

In this study it was hypothesized that a pattern of mitochondrial degradation associated with cold adaptation would lead to decreased mitochondrial gene transcription and decreased mitochondrial DNA copy number. Several experiments were undertaken to determine whether mitochondrial gene transcription or mitochondrial DNA copy number decreased in association with cold adaptation in either *G. groenlandica* or *E. solidaginis* larvae.

Probe Production

Sequence analysis of COI and 16S PCR generated fragments confirmed their identities. The *E. solidaginis* COI partial sequence bearing 87.0 and 87.33 % nucleotide identity with *Drosophila* and *Ceratitis* COI sequences was found to have 87.8 and 86% amino acid identity respectively. Amino acid identity was derived using translation codons generalized for invertebrate mitochondrial genomes. While this provides the best estimation of amino acid identity, many mitochondrial genomes use unique codons which may influence levels of amino acid identity. Because any unique codons used in the *E. solidaginis* mitochondrial genome are not known, exact amino acid identity is uncertain.

Northern Blots

Northern blot analysis detected copies of COI and 16S RNA in all *E. solidaginis* collection and treatment groups. COI hybridization was most intense in the active summer larvae indicating high mRNA copy number. There was decreased hybridization intensity in frozen winter larvae, winter larvae at 4°C, and winter larvae at 10°C. Because the intensity of hybridization was increased in the winter 15°C sample, a trend toward decreasing COI mRNA with cold acclimation was not observed for the winter group as a whole. Increases in higher molecular weight bands, however, were observed in the winter group, especially in the 4°C and 15°C treatment groups.

The intensity of 16S hybridization at 1,150 bases was greatest in the active summer larvae, yet there was no distinct trend toward decreasing hybridization intensity and, therefore, no trend toward decreased mRNA copy number with increasing cold hardiness. As was observed in COI hybridizations, however, hybridization intensity increased in high molecular weight bands from the winter treatment groups.

Both COI and 16S gene transcription in fall collected larvae had decreased processed transcripts at 15°C. However, winter collected larvae at 15°C demonstrated increased processed RNA levels. This may indicate that fall collected larva had decreased response to temperature at the level of mitochondrial RNA processing when compared to winter collected larvae at the same temperatures. In addition, frozen winter larvae may have had increased mitochondrial RNA processing upon warming.

Decreased mitochondrial mRNA processing in fall collected larvae was consistent with a diapause program. Fall collected larvae have high intensity of diapause indicated by failure to pupariate at permissive temperatures [55]. Increased mitochondrial mRNA processing in winter collected larvae may be consistent with the transition from a high intensity phase of diapause to a lower intensity phase in anticipation of resuming development.

Neither COI nor 16S gene expression was correlated with mitochondrial number, and only the processed 16S transcript was correlated with respiration rate in *E. solidaginis*. This may indicate that in *E. solidaginis*, 16S RNA processing was temperature dependent as was respiration. However, small sample size and

nonparametric correlation analysis reduce the power of the finding. Hybridization intensities of high molecular weight transcripts of both COI and 16S mRNA were correlated, indicating that high molecular weight transcripts of each gene were present in a corresponding fashion for each treatment group. There were no other correlations found between hybridization intensity and respiration, or maximum mitochondrial number.

If mitochondrial gene expression was related to maximum mitochondrial density, hybridization intensities would be expected to peak in the winter larvae at 10°C. Hybridization intensities did not increase in the winter larvae at 10°C, and indeed overall fluctuation of hybridization intensities was not consistent with a correlation between COI and 16S gene expression and maximum mitochondrial density.

Increased hybridization of high molecular weight transcripts in winter collected larvae was consistent with the presence of longer mRNA transcripts. Longer transcripts may result from increased transcription of the mitochondrial genome, processing of full length mRNAs, or from RNA editing.

Northern blot analysis of *G. groenlandica* RNA hybridized with 16S produced lowest intensity of hybridization in the active summer larvae, while intensity peaked in larvae that had spun hibernacula. Although intensity decreased slightly in summer larvae frozen for 2 weeks, the intensity of hybridization in larvae frozen for 5.5 months was nearly double the summer value. Similarly, hybridization with COI probe showed slightly decreased intensity of both the 1.6 and 1.0 kb bands in active summer larvae. This pattern of low intensity of hybridization in active summer

samples is in contrast to the trend observed in *E. solidaginis*, in which intensity of hybridization was highest in active summer larvae.

The pattern of low hybridization levels of 16S rRNA genes in *G. groenlandica* summer larvae suggests a high processed RNA turnover rate in actively metabolizing animals. Conversely, the higher intensity of hybridization in larvae that had spun hibernacula and had been frozen suggested that 16S ribosomal RNA transcripts were stabilized under these conditions. COI hybridization intensities supported a theory of mRNA stabilization during cold adaptation, ensuring a steady reserve of transcripts throughout overwintering.

Due to small sample sizes and few treatment groups, correlation analysis could not be completed for *G. groenlandica* data.

RNA Stability

Northern blot analysis of *E. solidaginis* and *G. groenlandica* RNA revealed two opposing patterns of mitochondrial gene expression in response to cold. In *E. solidaginis*, high molecular weight transcripts of COI and 16S genes were increased, while in *G. groenlandica* processed transcripts increased in the absence of high molecular weight transcripts. In *G. groenlandica* processed transcripts were abundant in the absence of high molecular weight bands that would indicate active mitochondrial genome transcription. This was consistent with a theory of processed mRNA stability, while in *E. solidaginis* longer transcripts appeared to be more stable.

RNA stability in organelles has not been well investigated or characterized. However, mRNA stability in oocytes has been known for some time. Messenger

RNA stored in the cytoplasm of oocytes is activated only upon fertilization [94]. This indicates that mechanisms for long term storage of mRNA are in place within cells. Given that the majority of mitochondrial genes have been transferred to the nucleus over evolutionary time, genes controlling mitochondria mRNA stability likely reside in the nucleus [95, 96]. Some of these proteins encoded in the nucleus are believed to interact with 5' and 3' mRNA regions forming secondary structures that protect mRNA from degradation [96]. Polyadenylation of mRNA within the mitochondria may also stabilize mRNA [97]. Although the mechanism is not known, shortening the poly(A) tail on an mRNA generally reduces its half life by targetting to a degradation pathway [97].

RNA degradation within organelles is generally understood to be a rapid process. Mitochondrial RNA half lives generally range from as short as 25 minutes for mRNA to several hours for ribosomal RNA; however, RNA stability is believed to increase as transcription is inhibited [95]. Changes in organelle mRNA stability are believed to contribute to establishing pools of selected mRNAs, and accumulations of stable mRNAs can effect gene transcription [95].

Patterns of Northern hybridizations in *E. solidaginis* and *G. groenlandica* may be representative of two modes of mRNA stability in response to cold: In *E. solidaginis*, high molecular weight RNA in winter collected larvae increased (Figures 18 and 20), consistent with longer mRNA transcripts. Longer transcripts may be more stable due to secondary structures formed, or due to longer poly(A) tails added to mRNA in response to cold. Conversely, *G. groenlandica* Northern blots are consistent with mRNA stability as a result of decreased transcription of the

mitochondrial genome, indicated by the absence of high molecular weight RNA transcripts (Figures 21, and 22) and decreased mitochondrial genome copy number (Figures 27 and 28).

Dot Blots

Dot blot analysis of *E. solidaginis* DNA hybridized with COI probe showed a pattern of high intensity hybridization in active summer larvae, and winter 4°C and 10°C larvae, and least hybridization intensity in fall and frozen winter larval samples. COI hybridization did not reveal a pattern of decreasing intensity of hybridization with cold acclimation in *E. solidaginis*. In accordance with COI hybridization, 16S mitochondrial copy number appeared to increase in winter 4°C and 10°C samples. 16S hybridization was least intense in fall and winter frozen larvae, and highest in summer, and winter samples at 4°C and 10°C. A pattern of decreasing intensity of 16S hybridization with cold adaptation was not observed. Conversely, both COI and 16S hybridizations demonstrated high intensity of hybridization in samples from winter collected larvae measured at 10°C. This peak in hybridization intensity corresponded to a significant rise in maximum mitochondrial density in the same treatment group, suggesting higher mitochondrial copy number and greater mitochondrial density. Decreases in dot blot maximum intensity in fall and winter frozen larvae indicated reduced mitochondrial copy number, and would not be reflected in counts of maximum mitochondrial density since this method identifies whole mitochondria only, and not mitochondrial genome copy number.

Dot blot hybridizations of *E. solidaginis* DNA indicated higher mitochondrial copy number in winter collected larvae measured at 4°C and 10°C, which was reflected in higher maximum mitochondrial density in winter collected larvae measured at 10°C. Dot blot hybridization intensities generally increased with increasing temperature in fall collected larvae, and increased in winter collected larvae with the exception of the 15°C group. However, statistical analysis failed to find a correlation between dot blot hybridization intensity and respiration rate, or mitochondrial copy number. Indeed, no correlation could be found between Dot blot hybridization intensity, and Northern blot hybridization intensity.

Dot blot analysis of *G. groenlandica* DNA with 16S probe showed a trend toward decreasing intensity of hybridization, and therefore decreasing mitochondrial copy number, in successive treatment groups. As would be expected if mitochondrial copy number were decreasing, the intensity of hybridization was least in the larvae frozen 5.5 months. Similarly, COI hybridization was most intense in the active summer larvae and least intense in larvae frozen for 5.5 months. Both of these results are consistent with lower mitochondrial copy number in *G. groenlandica* larvae frozen for 5.5 months when compared to active summer larvae. Decreased hybridization intensity in *G. groenlandica* larvae was consistent with decreased respiration rates.

Mitochondrial degradation in *G. groenlandica* previously described in literature was not associated with a significant decrease in cytochrome *c* protein [37]. The amount of cytochrome *c* in cells as measured by the ratio of cytochrome *c*/DNA did not significantly decrease with decreasing temperature. The authors suggested

that cytochrome *c* was released into the cytosol as mitochondria were degraded. The current study indicated that COI mRNA levels did not decrease with cold adaptation. Previous reports also suggested a greater than 10,000 fold decrease in mitochondrial number in fat body cells from frozen larvae [37]. However, 16S and COI dot blot hybridization intensities indicated 48.98% and 53.81% decreases respectively in mitochondrial copy number. This may indicate that although mitochondrial numbers decrease, mtDNA copy number may be high in the remaining mitochondria.

Decreasing mtDNA copy number in *G. groenlandica* larvae frozen for 5.5 months lends support to a theory of mRNA stabilization associated with mitochondrial genome replication and transcription levels. Northern blot intensity of hybridization for processed COI and 16S transcripts increased in samples from frozen larvae, while mitochondrial copy number measured by dot blot hybridization intensity decreased. mRNA stability must be significantly increased during cold adaptation in order to maintain high levels of processed transcript concurrent with mitochondrial genome copy number reduction. In addition, no high molecular weight bands indicative of full length mitochondrial transcripts were observed in *G. groenlandica*. Previous observations have been made that mRNA stability increases significantly after inhibition of transcription [98]. While the mechanism is not understood, decreased transcription as a result of mitochondrial genome degradation may stabilize *G. groenlandica* mRNA.

Restriction Digests and Southern Blots

Restriction digests of total DNA from *E. solidaginis*, *G. groenlandica*, and *Drosophila* and subsequent Southern blots and hybridizations with 16S and COI probes were used to determine whether or not 16S and COI derived sequences were present in nuclear genomes. In uncut total DNA, only the bands corresponding to the mitochondrial genome would be expected to hybridize with 16S and COI probes. Possible bands included a relaxed open circle mitochondrial genome, a linear mitochondrial genome (the result of mechanical shearing), and a supercoiled mitochondrial genome. In uncut DNA from *E. solidaginis*, *G. groenlandica*, and *Drosophila*, two bands hybridized with both 16S and COI probes. The smaller of the two bands, sized 14.5-15 kbp was identified by size as the mitochondrial genome. Subsequent hybridization of λ HindIII ladder confirmed that the larger of the two bands was substantially greater than 23 kbp (the limit of the ladder), and was consistent in size with genomic DNA.

Membranes were hybridized with a chromosomally derived *Drosophila* gene that encodes the mitochondria specific DNA polymerase γ (*tam*), to ensure that the band greater than 23 kbp was chromosomal in origin, and not an open circle form of the mitochondrial genome. *tam* is located on chromosome 2 of the *Drosophila* genome [90], and does not have any regions of homology with the *Drosophila* mitochondrial genome. Specific hybridization of *tam* to the large >23 kbp band confirmed that the band was genomic, and not mitochondrial in origin

Hybridization of 16S and COI probes to *Drosophila*, *E. solidaginis*, and *G. groenlandica* genomic DNA suggested that mitochondrial derived sequences are

present in the nuclear genome of all three species of insects. Restriction digests of *Drosophila* total DNA, and calculations of expected band sizes based on cut sites in the mitochondrial genome further support this theory. For example, the restriction enzyme XhoI has one restriction site in the *Drosophila* mitochondrial genome, and therefore would produce one band when hybridized with a mitochondria specific probe: a linear mitochondrial genome. When hybridized with COI however, *Drosophila* XhoI restriction fragments showed a total of seven bands ranging in size from 2.3-14.1 kb, and disappearance of the putative genomic band. Hybridization of 16S showed three bands, corresponding to 12.5, 14.5, and 15.4 kbp. Similar observations were made for *E. solidaginis* and *G. groenlandica* restriction digests and Southern hybridizations.

Together, the presence of genomic bands in *E. solidaginis*, *G. groenlandica*, and *Drosophila*, and many unpredicted restriction fragments in *Drosophila*, are consistent with nuclear mitochondrial derived sequences. The presence of nuclear sequences derived from mitochondrial genes is not unique to *Drosophila*, *E. solidaginis*, and *G. groenlandica*. Analysis of animal nuclear and mitochondrial genomes has shown that mitochondrial sequences are present in the nucleus of many species. For example, several hundred copies of mitochondrial DNA-like fragments were estimated to be present in the human nucleus including part of the 12S RNA, COI, and two NADH hydrogenase subunits bearing 92.0-92.4% similarity to mitochondrial copies [99]. Additionally, one of the most striking examples of gene transfer was discovered in the domestic cat, *Felis catus*. The domestic cat has an approximately 17 kb mitochondrial genome, of which 7.9 kilobases were duplicated

and transposed to the nuclear genome [100]. The transposed fragment has since been tandemly duplicated 38-76 times [100]. Other animals known to have mitochondrial sequences in the nucleus include rodents, whales, bovids (hollow horned ruminants, for example domestic cattle, sheep, and goats), birds, and invertebrates [101].

Studies of orthopteran (the locusts, *Schistocerca gregaria* and *Italopodisma* spp., and the grasshopper, *Chorthippus parallelus*) mitochondrial sequences revealed that the COI gene is present in the nuclear genome [102]. Multiple copies of COI were localized by *in situ* hybridization to various locations within the nuclear genome, including chromosome centromeres, telomeres, and dispersed throughout the nuclear genome [102]. In addition, 12S rRNA, 16S rRNA, the mitochondrial control region, and various mitochondrial tRNA sequences have also been identified in the nucleus of orthopterans [103, 104].

Moreover, nuclear mitochondrial genes have been described in *Sitobion* aphids. Analysis of total DNA extracted from various aphid populations, and subsequent polymerase chain reaction (PCR) and southern blotting experiments revealed the presence of extra mitochondrial sequences homologous to COI and CO2 [105]. Furthermore, these sequences were present in multiple copies, with differing levels of divergence from the mitochondrial sequence suggesting multiple transfer events [105].

The number of reports citing mitochondrial sequences in the nuclear genomes of many species of plants and animals substantiate the discovery of mitochondrial derived sequences in the nuclear genomes of *Drosophila*, *E. solidaginis* and *G. groenlandica*. Although the mechanism of transfer from mitochondrial genome to

nuclear genome is not known in each instance, several theories have been proposed for the mechanism of intracellular gene transfer [104, 106-108].

Gene transfer may occur when DNA fragments released during organelle breakdown are subsequently taken up by the nucleus and integrated into the host genome. Similarly, release of messenger RNA from organelles, uptake by the nucleus, reverse transcription and integration may result in nuclear copies of mitochondrial genes. Membrane fusion between mitochondria and the nucleus and release of mtDNA followed by recombination events could also lead to mitochondrial gene duplication. Transposition events may also be closely tied to the movement of mtDNA, or to the activation of mitochondrial genes in the nucleus.

The majority of mitochondrial genes transferred to the nucleus are not transcribed owing mainly to selection pressures, absence of proper promoter regions, and different translation codons [108]. For these reasons, it is unlikely that transcription of nuclear 16S or COI-like sequences would complicate Northern analysis. However, 16S and COI probes that hybridized to genomic DNA in Southern blots, would likely also hybridize to genomic DNA in dot blot analysis. This may account for the intensity of hybridization in *G. groenlandica* larvae frozen for 5.5 months. Instead of a complete lack of hybridization that would be expected if mitochondrial numbers drop to less than 0.01 mitochondria per nucleus as previously reported [37], some hybridization was still detected. However, the amount of nuclear DNA present in each of the samples applied to the dot blot membrane should be equal among all treatment groups, since all samples were extracted following the same protocol, and all DNA concentrations were determined using a spectrophotometer.

The differences in hybridization intensities in dot blot analyses using 16S and COI probes reflects overall changes in mitochondrial numbers, and would not be influenced by constant amounts of genomic DNA.

Northern blot analysis of *E. solidaginis* third instar larvae revealed that cold hardy winter larvae have increased high molecular weight mitochondrial transcripts, when compared to active summer larvae. *E. solidaginis* processed mRNA transcript levels were highest in active summer larvae, whereas in *G. groenlandica* larvae processed transcript levels were lowest in active summer larvae. Longer transcripts may lead to increased mRNA stability in *E. solidaginis*, whereas in *G. groenlandica* stability may be related to reduced transcription of the mitochondrial genome, and reduced genome copy number. Dot blot analysis of *G. groenlandica* DNA was consistent with mitochondrial degradation associated with cold adaptation. Conversely, no such trend was evident in *E. solidaginis* larvae. In *E. solidaginis*, *G. groenlandica* and *Drosophila*, restriction and Southern blot analyses detected mitochondria derived sequences in nuclear genomes.

CHAPTER 5 SUMMARY AND CONCLUSIONS

Several conclusions may be drawn from experimental data reported here. Overall, respiration data were consistent with decreased metabolic rates during cold adapted states for both species of insect examined. Northern blots for both *E. solidaginis* and *G. groenlandica* were consistent with a theory of increased stabilization of mRNA during cold adapted states: In *E. solidaginis*, increased transcript length was observed, while in *G. groenlandica* processed mRNA stability increased in the absence of full length transcripts and decreasing mtDNA copy number. Overall reductions of mean mitochondrial copy number and maximum mitochondrial density were not observed in *E. solidaginis* using dot blot analysis and epifluorescent microscopy. Dot blot analysis indicated a reduction in mitochondrial DNA copy number in larvae of *G. groenlandica* that had been frozen for 5.5 months, although the reduction was not consistent with the previously reported 10,000 fold decrease. Restriction digest and Southern analysis revealed the presence of nuclear, mitochondrial derived sequences in *Eurosta solidaginis*, *G. groenlandica*, and *Drosophila melanogaster*.

Results obtained in this study support a theory of mitochondrial degradation in the Arctic woolly bear caterpillar. Further research on *G. groenlandica* mitochondrial degradation may provide clues as to the mechanism of degradation and regeneration of organelles and the genes involved. Although data obtained in this study were not consistent with mitochondrial degradation in *E. solidaginis*, they did illustrate the variability of respiration and maximum mitochondrial density among individuals.

This was suggestive of developmental plasticity among the larvae, in which development of cells and tissue responds to the current environment.

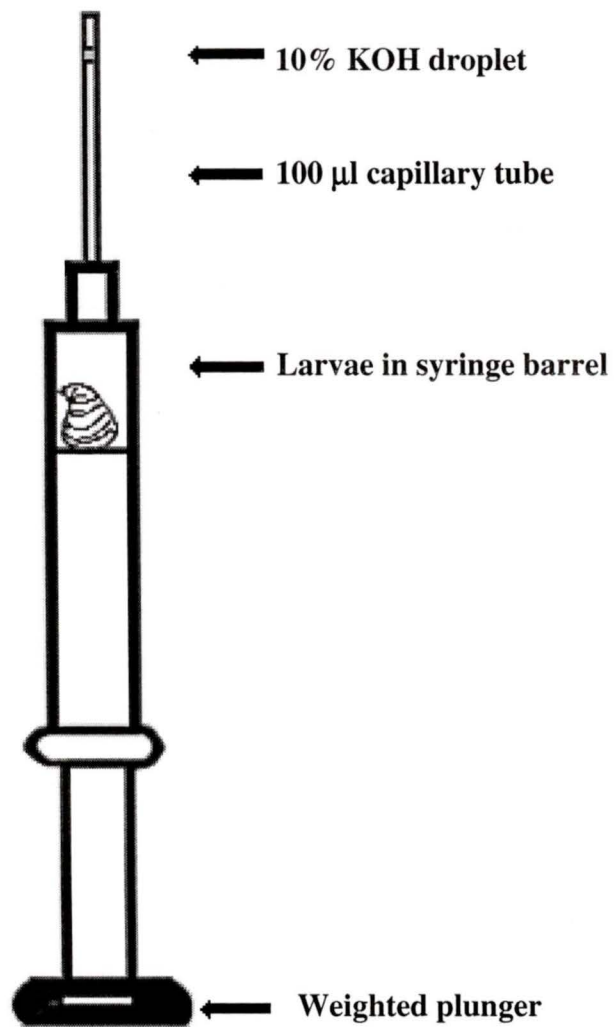


Figure 1. Simple respirometer showing arrangement of syringe barrel, larvae, capillary tube, and 10% potassium hydroxide droplet.

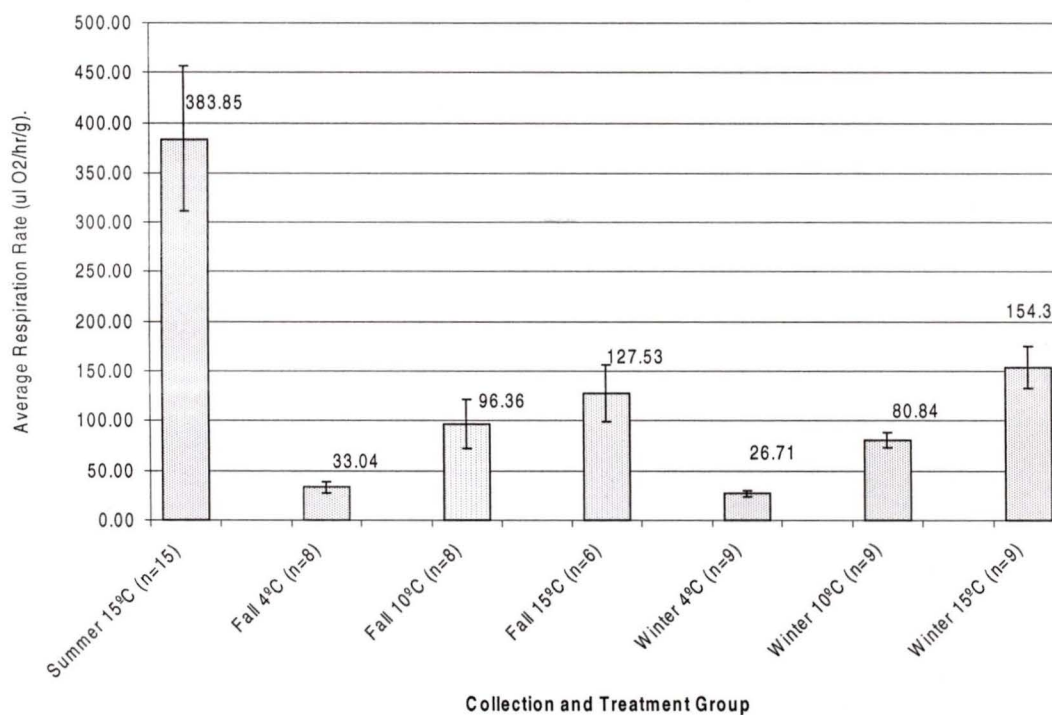


Figure 2. Average respiration rates ($\mu\text{l O}_2 \text{ hr}^{-1} \text{ g}^{-1}$) for *E. solidaginis* third instar larvae collected in Summer, Fall, and Winter; 1 hour equilibration and 4 hour measurement interval at 4°C, 10°C, and 15°C, using a simple respirometer; 95% Confidence interval.

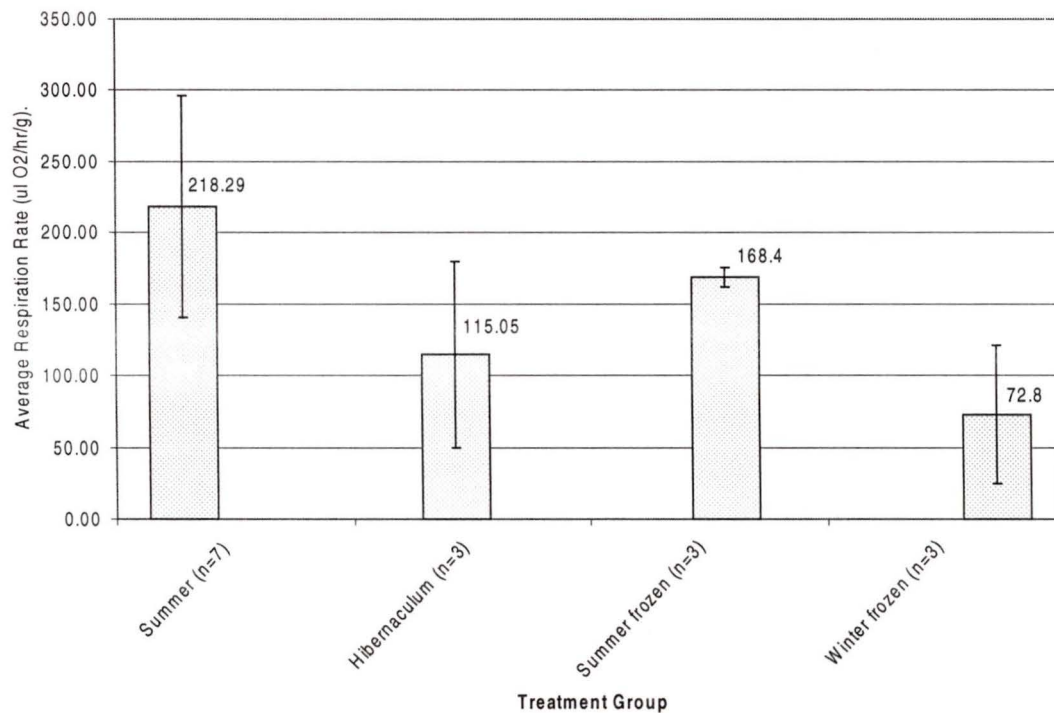


Figure 3. Average respiration rates ($\mu\text{l O}_2 \text{ hr}^{-1} \text{ g}^{-1}$) for *G. groenlandica* larvae; 1 hour equilibration and 4 hour measurement interval at 15°C, using a simple respirometer; 95% Confidence interval.

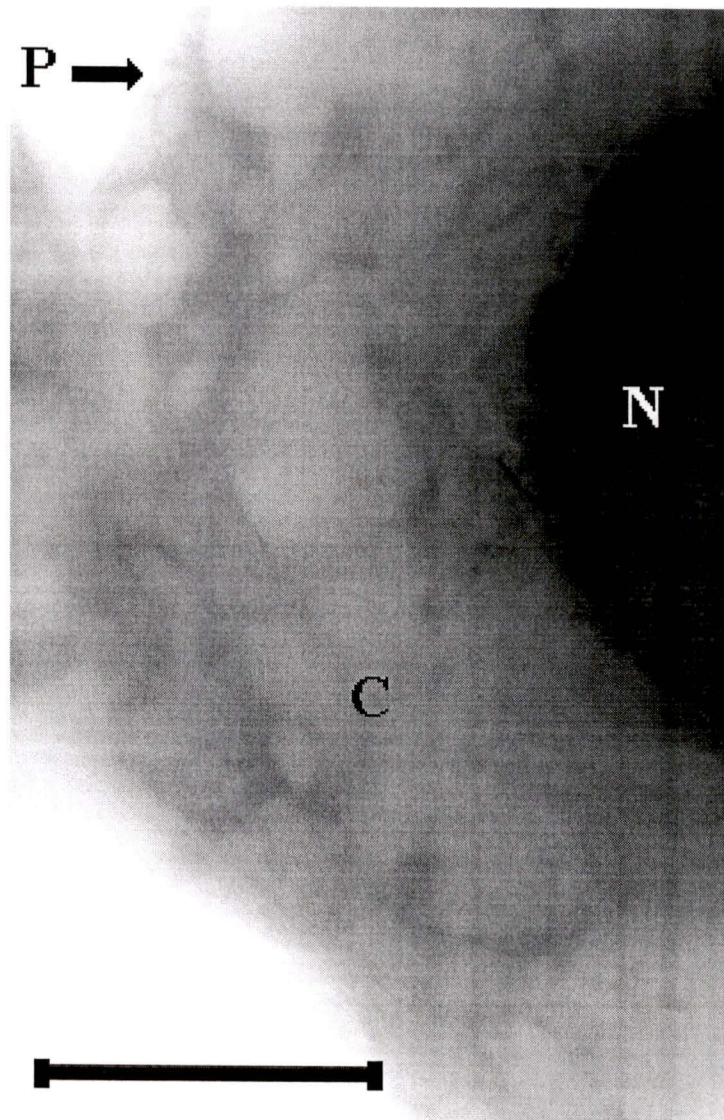


Figure 4. Negative image of a fat body cell from *E. solidaginis* summer collected larvae showing nucleus (N), plasma membrane (P), and cytoplasm (C); 2 ng/ μ l bisbenzimidide. Bar equals 50 μ m.

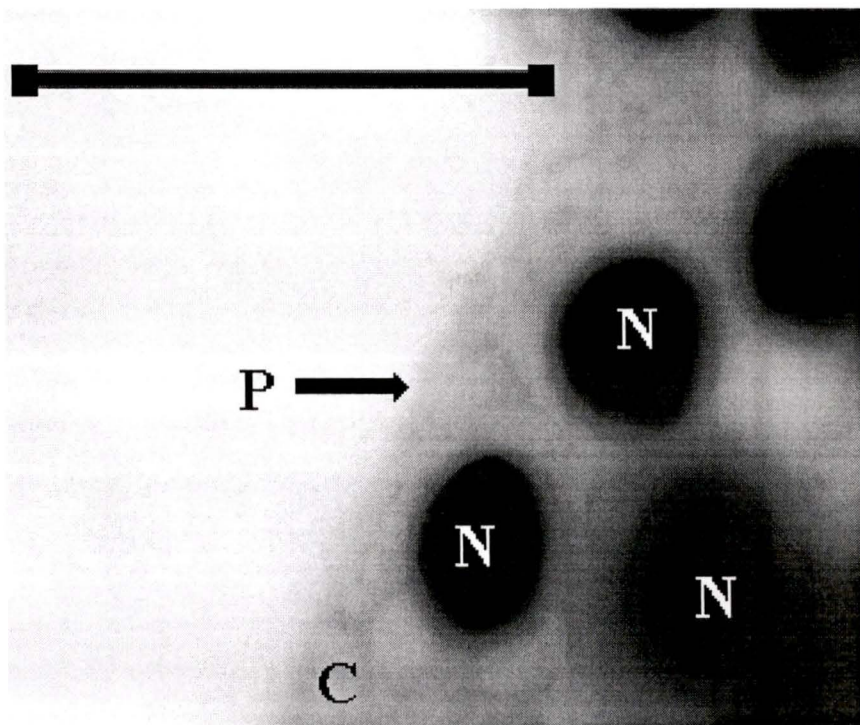


Figure 5. Negative image of fat body cells from *G. groenlandica* summer collected larvae, frozen for 2 weeks at -20°C showing nucleus (N), plasma membrane (P), and cytoplasm (C); $2\text{ ng}/\mu\text{l}$ bisbenzimidide. Bar equals $50\ \mu\text{m}$.

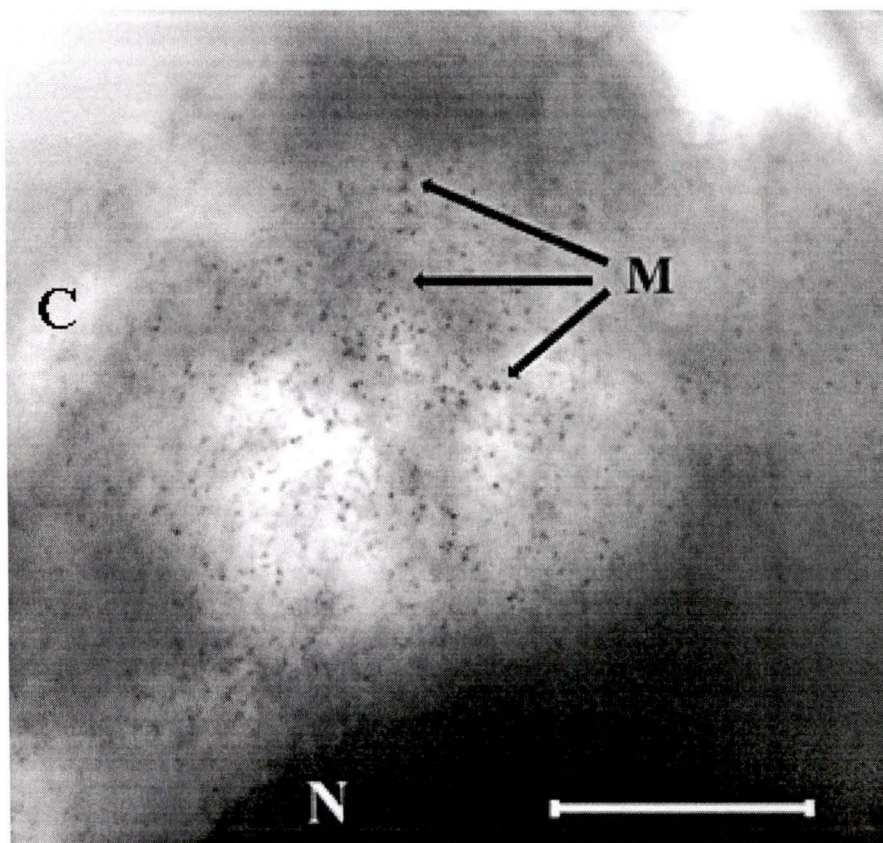


Figure 6. Negative image of a fat body cell from *E. solidaginis* third instar larvae, fall collected and respiration measured at 10°C; showing nucleus (N), mitochondria (M), and dense cytoplasm (C); 2 ng/μl Bisbenzimidazole. Bar equals 50 μm.

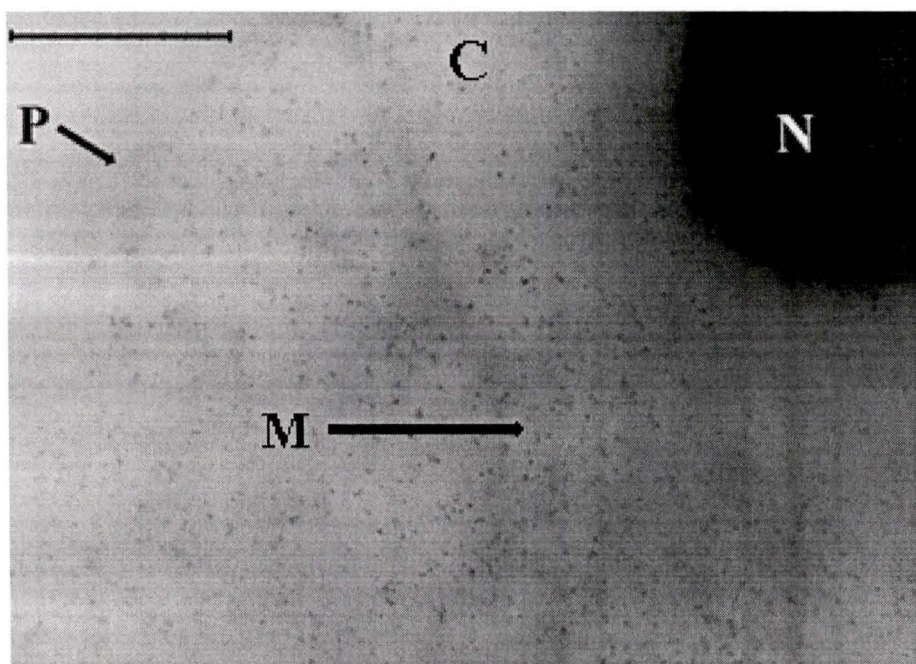


Figure 7. Negative image of a fat body cell from *E. solidaginis* third instar larvae, winter collected and respiration measured at 10°C; showing nucleus (N), plasma membrane (P), and cytoplasm (C) filled with mitochondria (M); 2 ng/ μ l Bisbenzimidide. Bar equals 50 μ m.

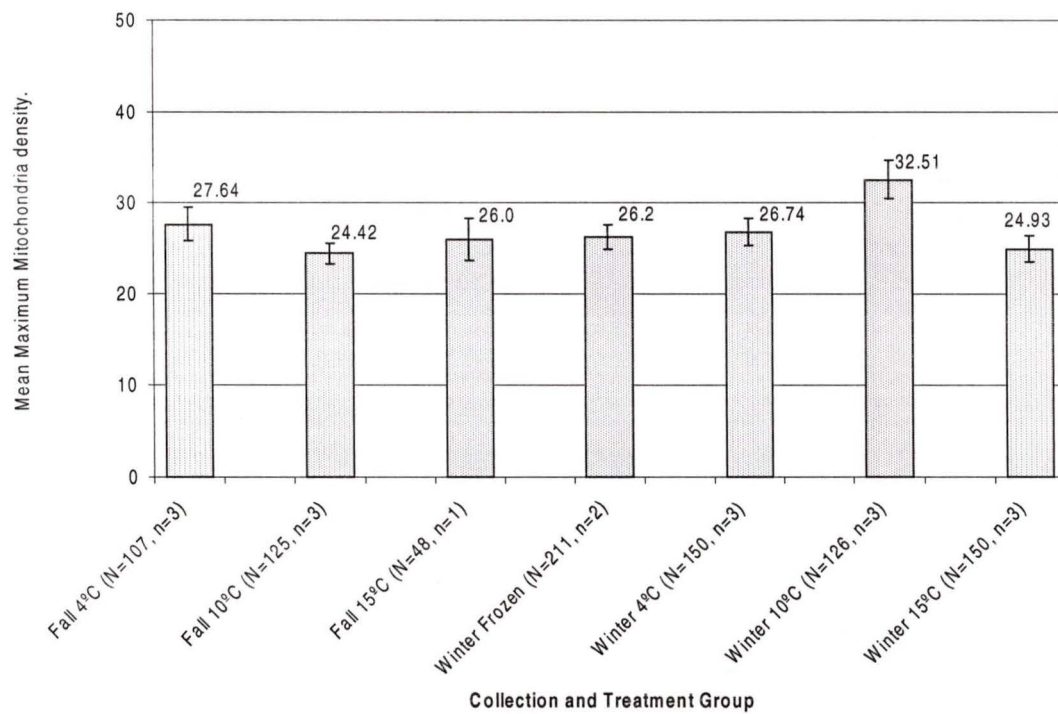


Figure 8. Mean maximum mitochondrial density for *E. solidaginis* third instar fat body cells; larvae collected in fall and winter and respiration measured at 4°C, 10°C, and 15°C; maximum mitochondria per 27 μm squared (fall cells), and 25 μm squared (winter cells).

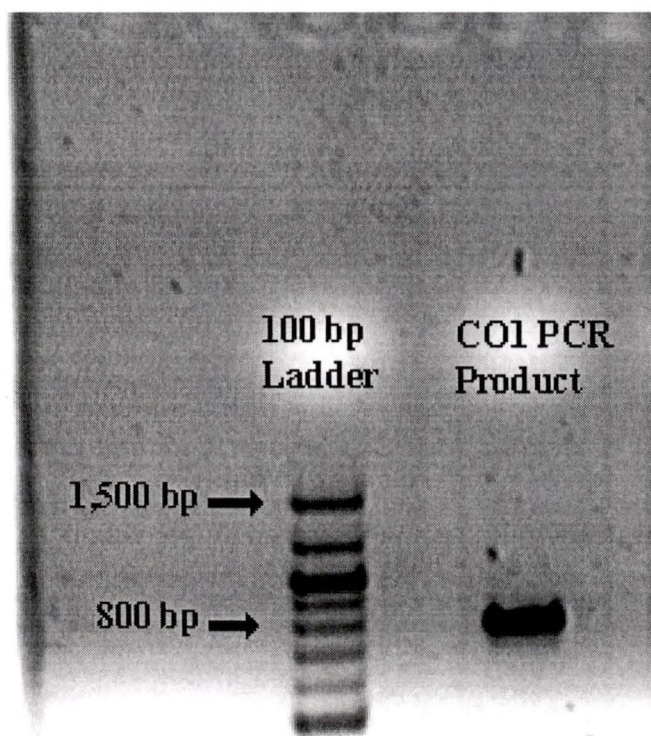


Figure 9. 1% TBE gel showing 800 base pair *E. solidaginis* COI PCR product; 0.25 $\mu\text{g}/\text{ml}$ ethidium bromide.

```

1 Drosophila      ggatttggaattgattagtgaccttaataattaggtgctcct
2 Eurosta        .....t.....a.....c.t..a..a..a
3 Ceratitidis    .....t.....c...a.....

1gatatagcattcccacgaataaataatataagattttgactactacctcctgctctttct
2.....t..t.....t.....t..t.....t.c...a.a
3.....t.....c.....t.....t..t.g..c..at.c...a.a

1ttactattagtaagtagaataagttgaaaatggagctggaacaggatgaactgtttatcca
2...t.....t.....a.....t.....a....c..t
3...t..c.ca.c.c..t...a...c.....t....aa...c..c

1cctttatccgctggaattgctcatgggtggagcttcagttgatttagctatTTTTTctcta
2...c...tt..tg.....a..t...t...c...a.....t
3...c.t..at..act....a...a...a..t...c.....t..

1catttagcagggatttcttcaattttaggagctgtaaattttattacaactgtaattaat
2.....t..a.....t.....g.....c.....a.....
3.....c..a..c.....t.....a.....t.....t.....

1atacgatcaacaggaatttcattagatcgatatacctttatttgtttgatcagtagttatt
2.....t..c.....c..c..a.....g.....c..
3.....t...a...t...a.....a...g....a.at.a

1actgctttattattattattatcaacttccagtactagcaggagctattactatattatta
2....ac..c.tc.....tt.a...tt.....
3.....c.t...c.t.....ct.a...t.....

1acagatcgaaaatttaaatacatcattttttgaccagcggaggaggagatcctatttta
2.....t.....c.....t.....c.....
3....c.....a..t..t.....

1tatcaacatttattttgatttttggtcaccctgaagtttatattttaattttacctgga
2..c.....a..t.....c.....a...
3.....a.....

1tttggataatttctcatattattagacaagaatcaggaaaaaggaaacttttggttct
2.....a.....c....a
3.....a.....a.g.....

1ctaggaataatttatgct
2t.....
3t.....

```

Figure 10. Multiple sequence alignment of (1) *Drosophila melanogaster*, (2) *Eurosta solidaginis*, and, (3) *Ceratitidis capitata* CO1 partial nucleic acid sequence, showing 87% nucleotide identity between *E. solidaginis* and *D. melanogaster*, and, 87.33% nucleotide identity between *E. solidaginis* and *C. capitata*; nucleotides conserved between *E. solidaginis* and *C. capitata* in bold.

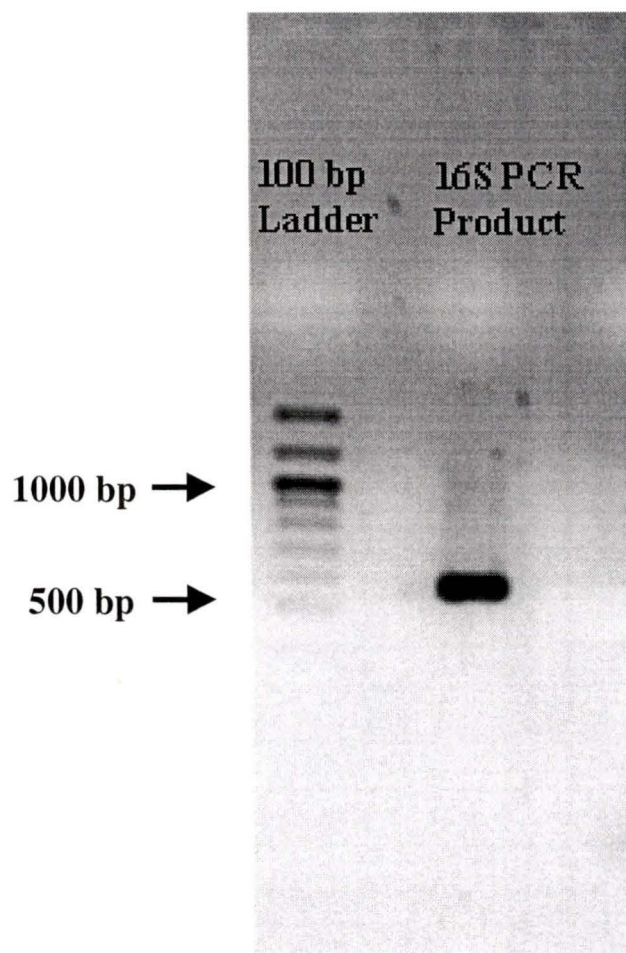


Figure 11. 1% TBE gel showing 610 base pair *Drosophila melanogaster* 16S PCR product; 0.25 $\mu\text{g}/\text{ml}$ ethidium bromide.

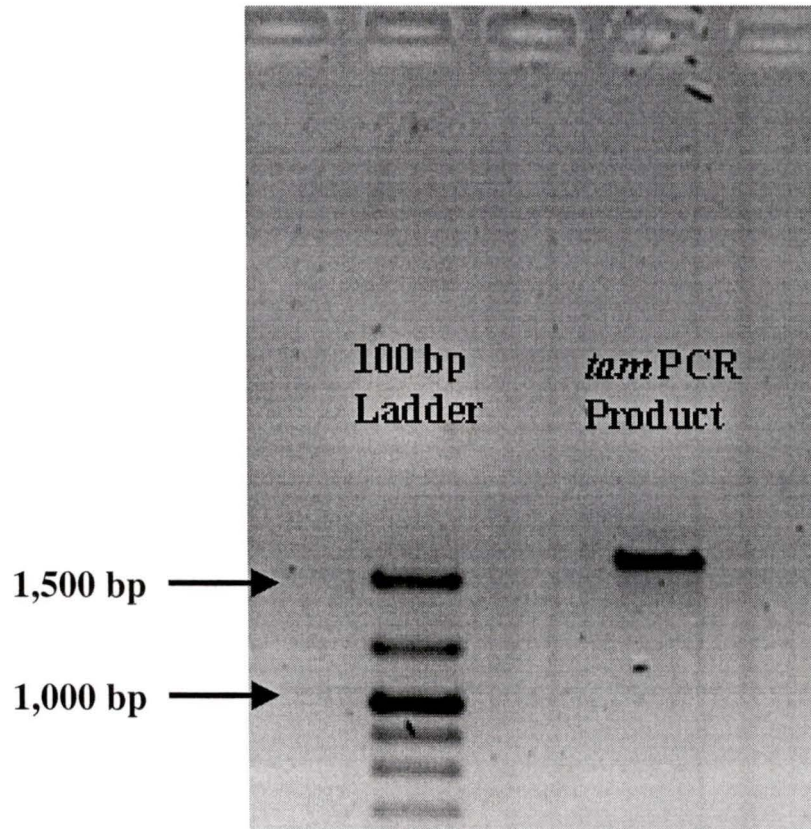


Fig 12. 1% TBE gel showing 1,600 base pair *Drosophila melanogaster tam* PCR product; 0.25 $\mu\text{g/ml}$ ethidium bromide.

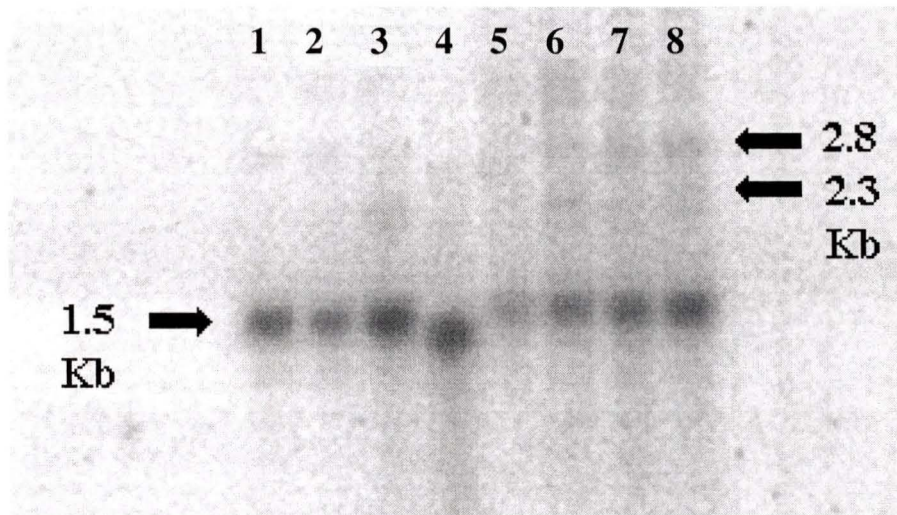


Figure 13. *Eurosta solidaginis* CO1 Northern Blot showing 1.5 kb processed CO1 transcripts, and 2.3 and 2.8 kb transcripts; 5 μ g RNA run on a 1% agarose denaturing gel and transferred to Schleicher & Schuell BAS 85 membranes. (1) summer active; (2) fall 4°C; (3) fall 10°C; (4) fall 15°C; (5) winter frozen; (6) winter 4°C; (7) winter 10°C; (8) winter 15°C.

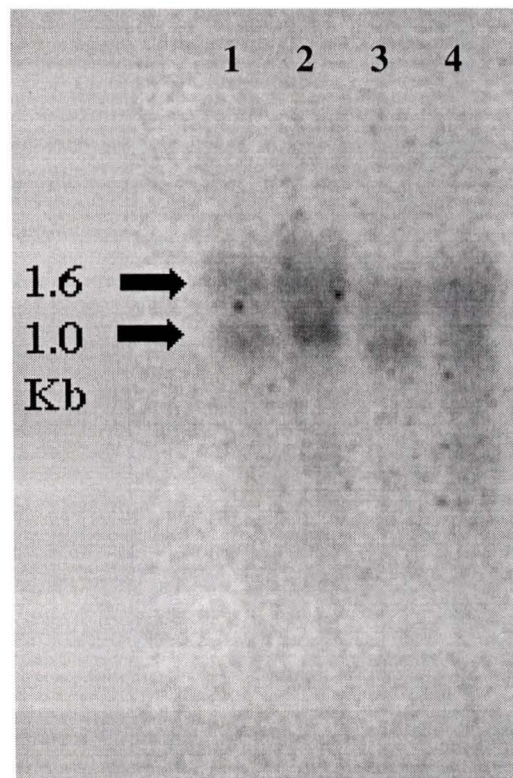


Figure 14. *Gynaephora groenlandica* CO1 Northern Blot showing 1.0 kb processed CO1 transcripts, and 1.6 kb additional bands; 5 μ g RNA run on a 1% agarose denaturing gel and transferred to Schleicher & Schuell BAS 85 membranes. (1) summer active larvae; (2) summer larvae in hibernacula; (3) summer larvae frozen for 2 weeks; (4) summer larvae frozen for 5.5 months.

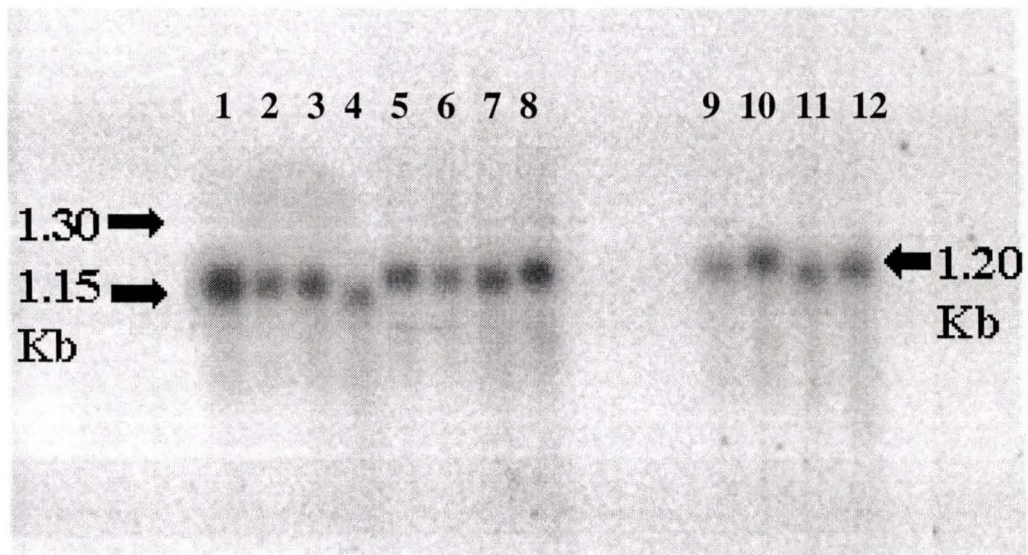


Figure 15. *Eurosta solidaginis* and *Gynaephora groenlandica* 16S Northern Blot showing 1.15 kb processed 16S transcript (*Eurosta*, A-H), and 1.20 Kb processed transcript (*Gynaephora*, I-L); 5 μ g RNA run on a 1% agarose denaturing gel and transferred to Schleicher & Schuell BAS 85 membranes. (1) *Eurosta* summer active; (2) *Eurosta* fall 4°C; (3) *Eurosta* fall 10°C; (4) *Eurosta* fall 15°C; (5) *Eurosta* winter frozen; (6) *Eurosta* winter 4°C; (7) *Eurosta* winter 10°C; (8) *Eurosta* winter 15°C; (9) *Gynaephora* summer active larvae; (10) *Gynaephora* summer larvae in hibernacula; (11) *Gynaephora* summer larvae frozen for 2 weeks; (12) *Gynaephora* summer larvae frozen for 5.5 months.

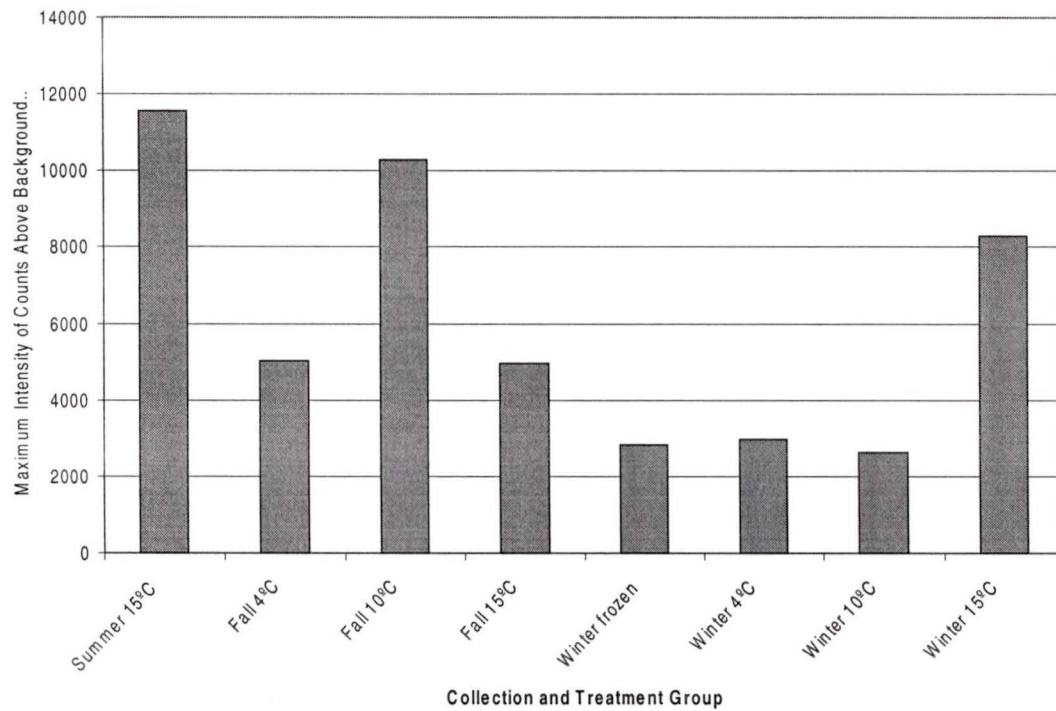


Figure 16. Maximum hybridization intensity graph for *Eurosta solidaginis* third instar larvae CO1 Northern blot, 1.50 Kb processed transcript.

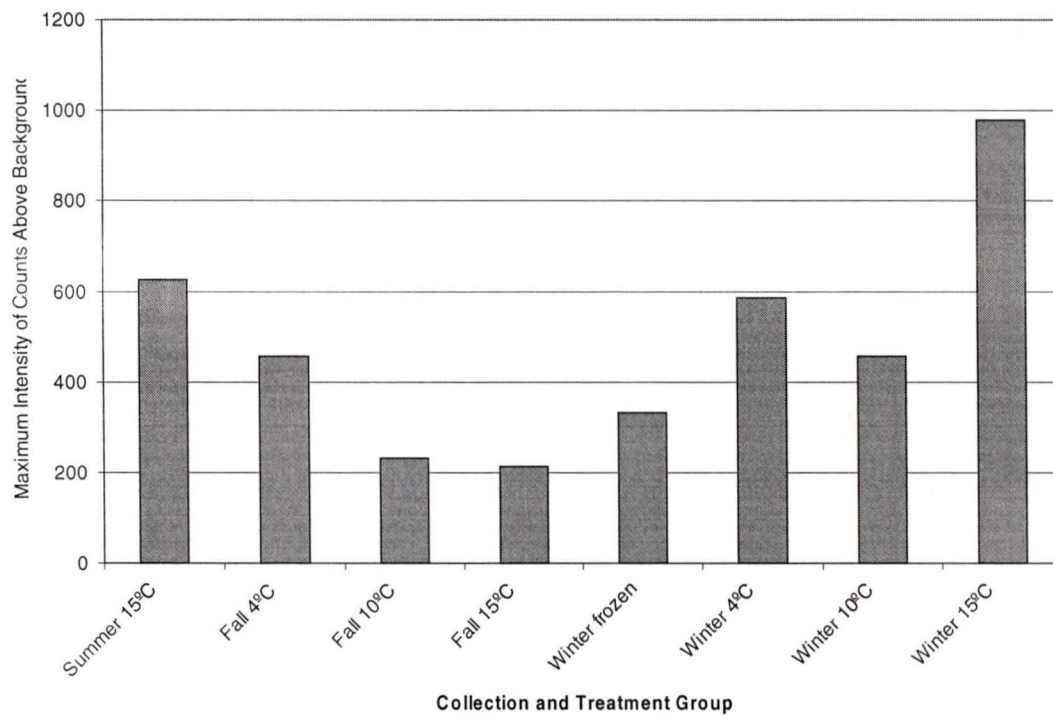


Figure 17. Maximum hybridization intensity graph for *Eurosta solidaginis* third instar larvae CO1 Northern blot, 2.37 Kb transcript.

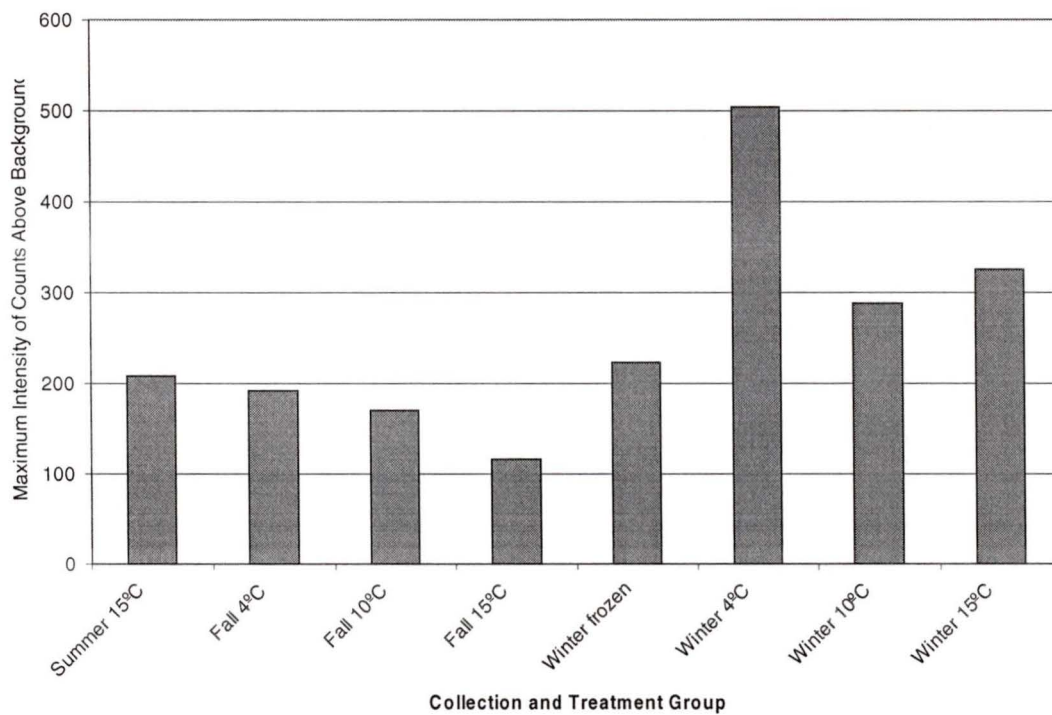


Figure 18. Maximum hybridization intensity graph for *Eurosta solidaginis* third instar larvae CO1 Northern blot, 2.88 Kb transcript.

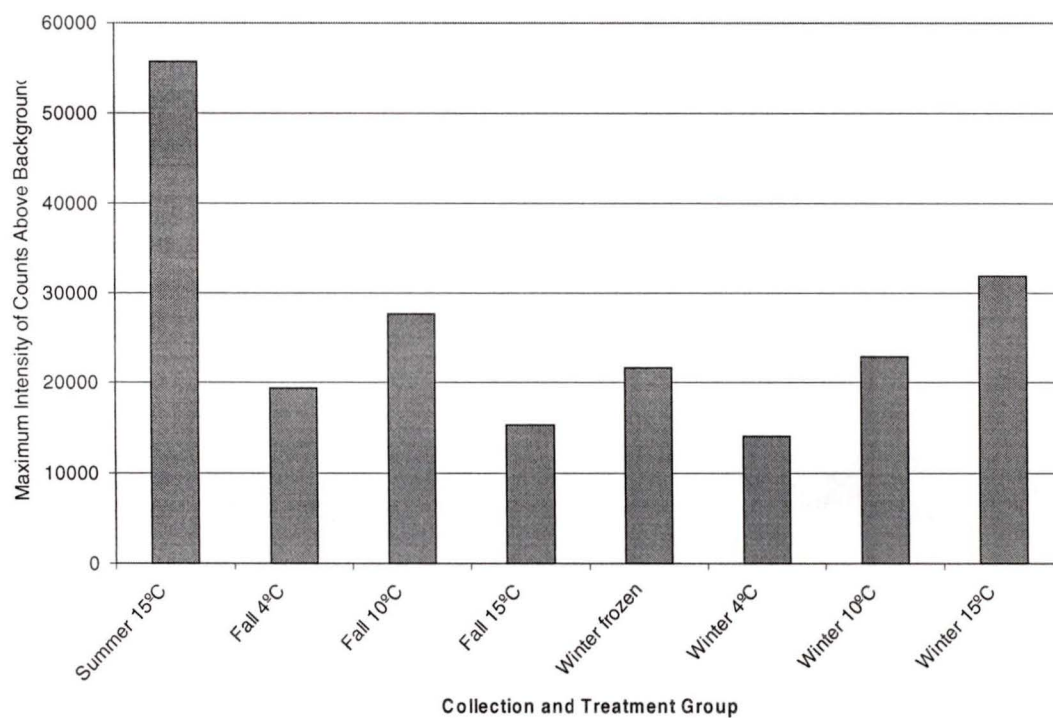


Figure 19. Maximum hybridization intensity graph for *Eurosta solidaginis* third instar larvae 16S Northern blot, 1.15 Kb processed transcript.

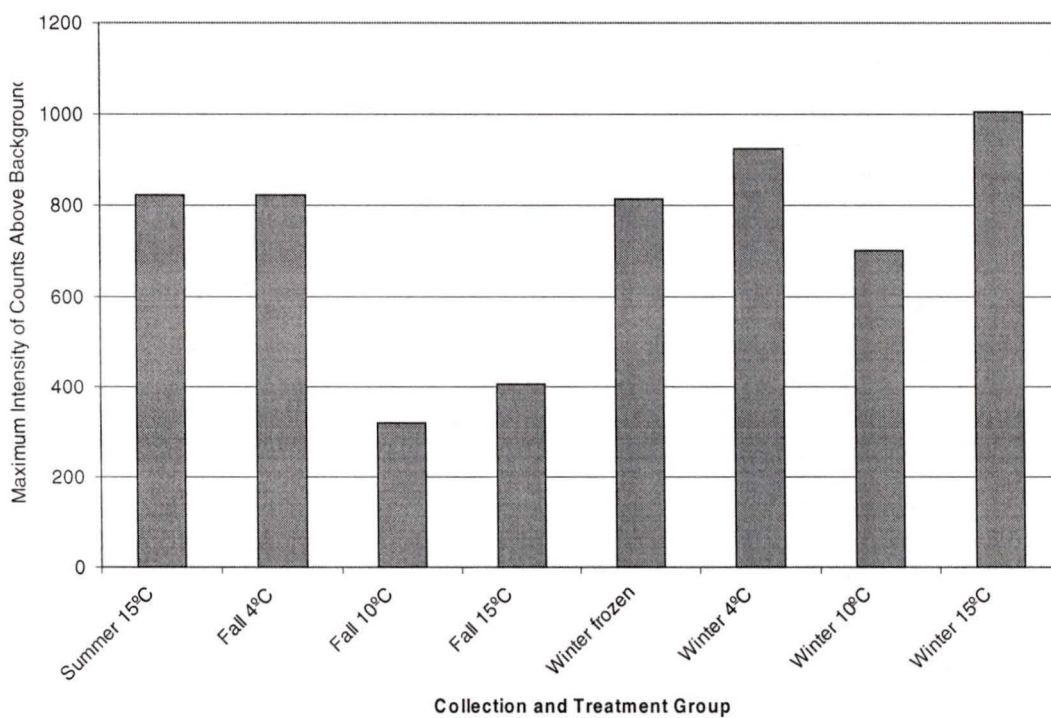


Figure 20. Maximum hybridization intensity graph for *Eurosta solidaginis* third instar larvae 16S Northern blot, 1.30 Kb transcript.

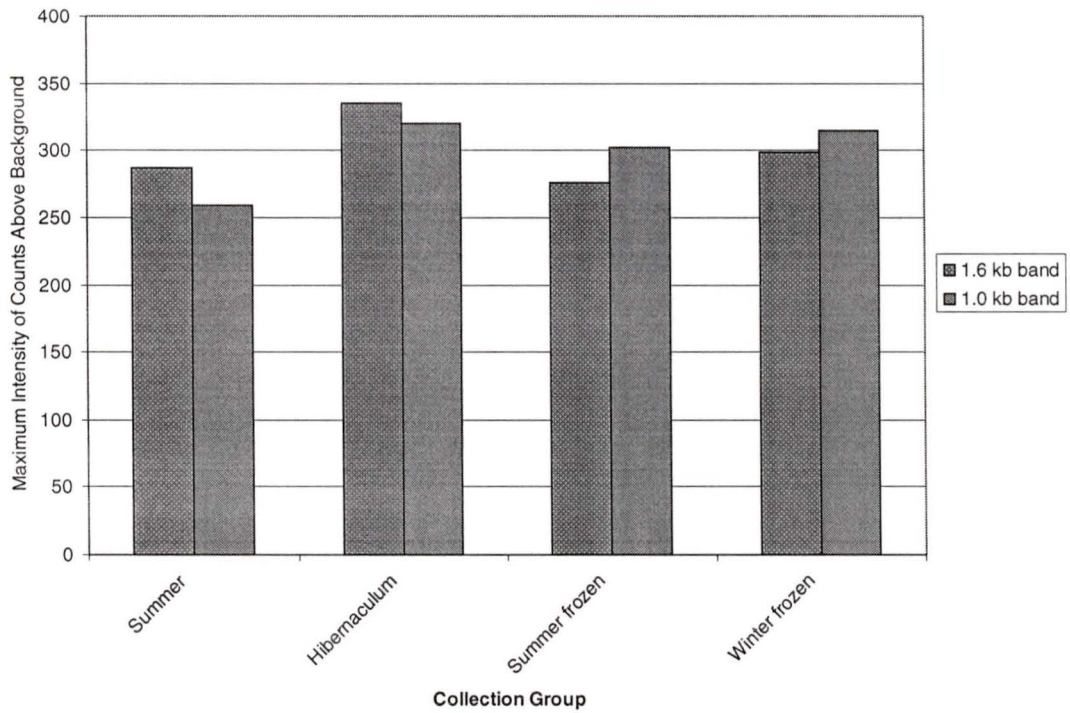


Figure 21. Maximum hybridization intensity graph for *Gynaephora groenlandica* CO1 Northern blot, 1.60 and 1.0 Kb transcripts.

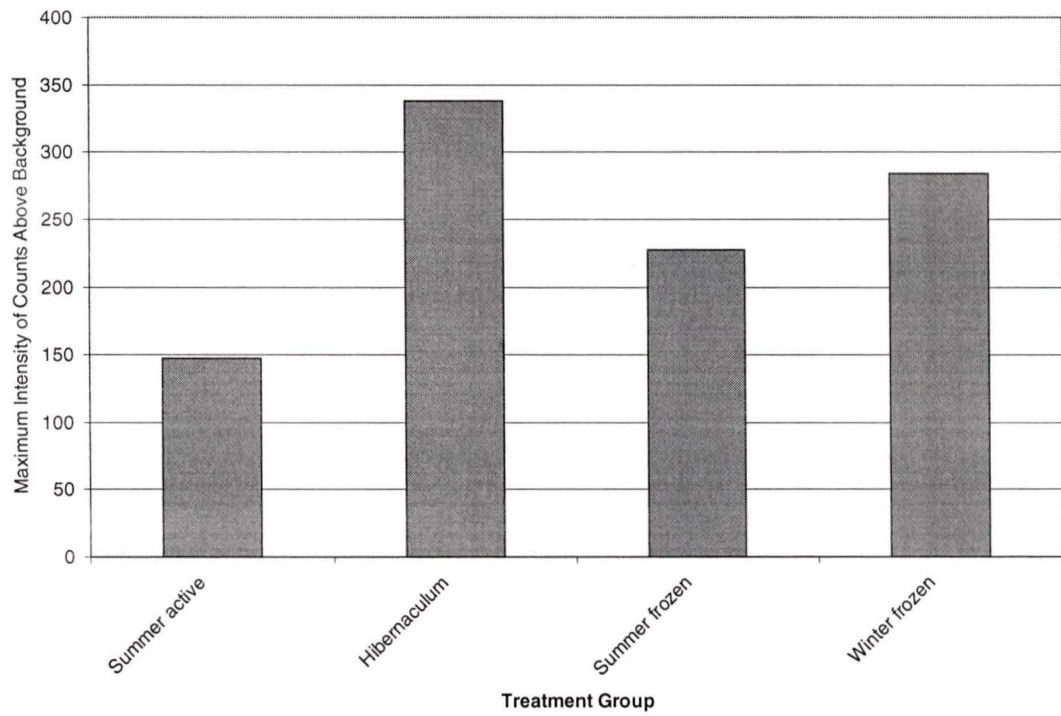


Figure 22. Maximum hybridization intensity graph for *Gynaephora groenlandica* 16S Northern blot, 1.20 Kb processed transcript.

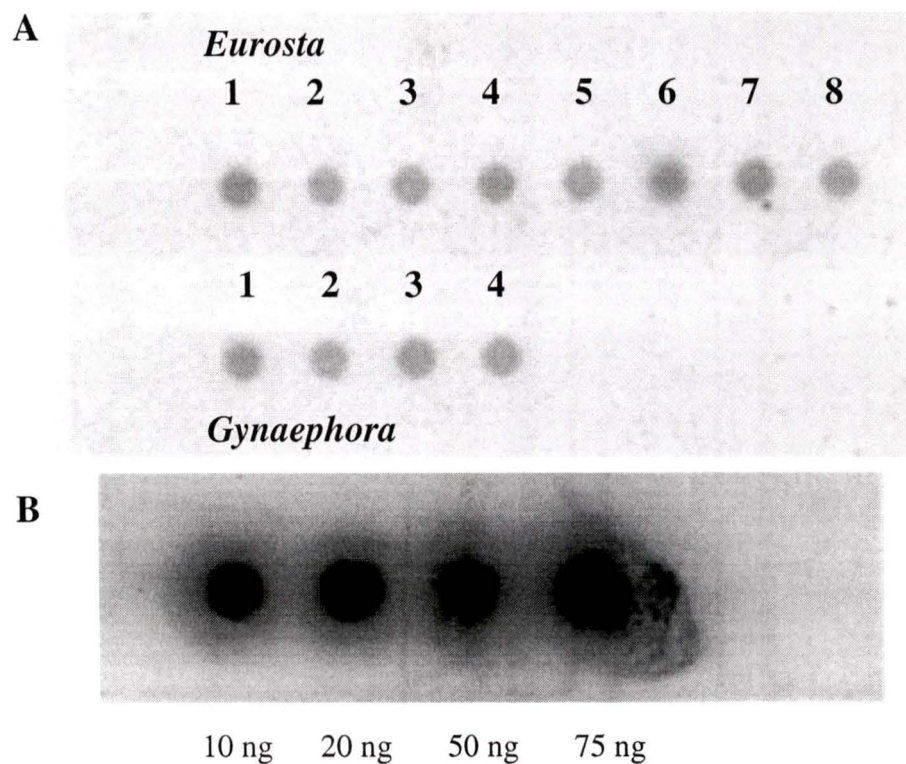


Figure 23. A. Dot blot analysis of *Eurosta solidaginis* third instar larvae DNA and *Gynaephora groenlandica* larvae DNA hybridized with PCR generated CO1 probe; and B. CO1 standard positive control. *Eurosta* series (1) summer active; (2) fall 4°C; (3) fall 10°C; (4) fall 15°C; (5) winter frozen; (6) winter 4°C; (7) winter 10°C; (8) winter 15°C; *Gynaephora* series (1) summer active larvae; (2) summer larvae in hibernacula; (3) summer larvae frozen for 2 weeks; (4) summer larvae frozen for 5.5 months. 150 ng DNA blotted onto Hybond-N membrane.

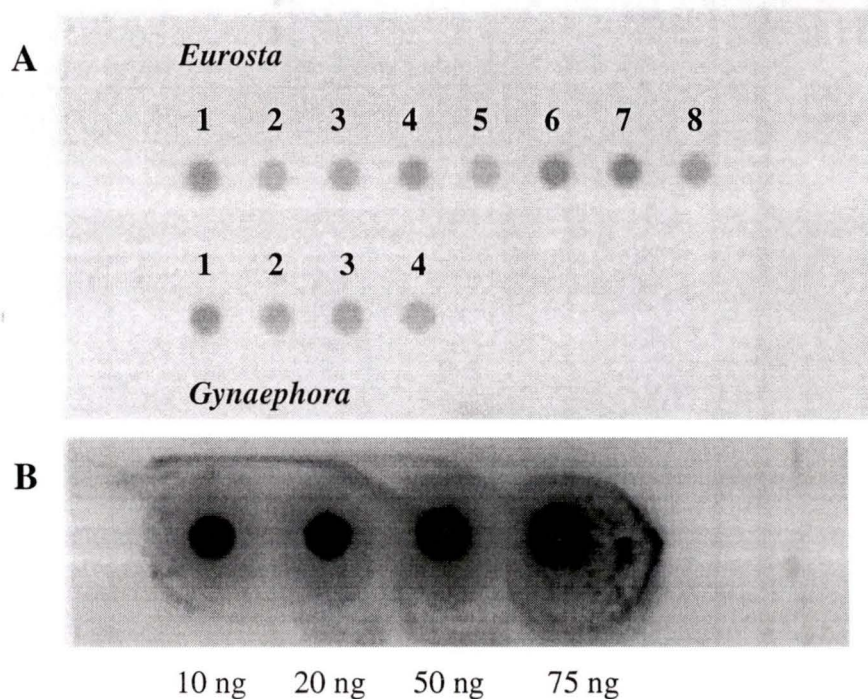


Figure 24. A. Dot blot analysis of *Eurosta solidaginis* third instar larvae DNA and *Gynaephora groenlandica* larvae DNA hybridized with PCR generated 16S probe; and B. 16S standard positive control; *Eurosta* series (1) summer active; (2) fall 4°C; (3) fall 10°C; (4) fall 15°C; (5) winter frozen; (6) winter 4°C; (7) winter 10°C; (8) winter 15°C; *Gynaephora* series (1) summer active larvae; (2) summer larvae in hibernacula; (3) summer larvae frozen for 2 weeks; (4) summer larvae frozen for 5.5 months. 150 ng DNA blotted onto Hybond-N membrane.

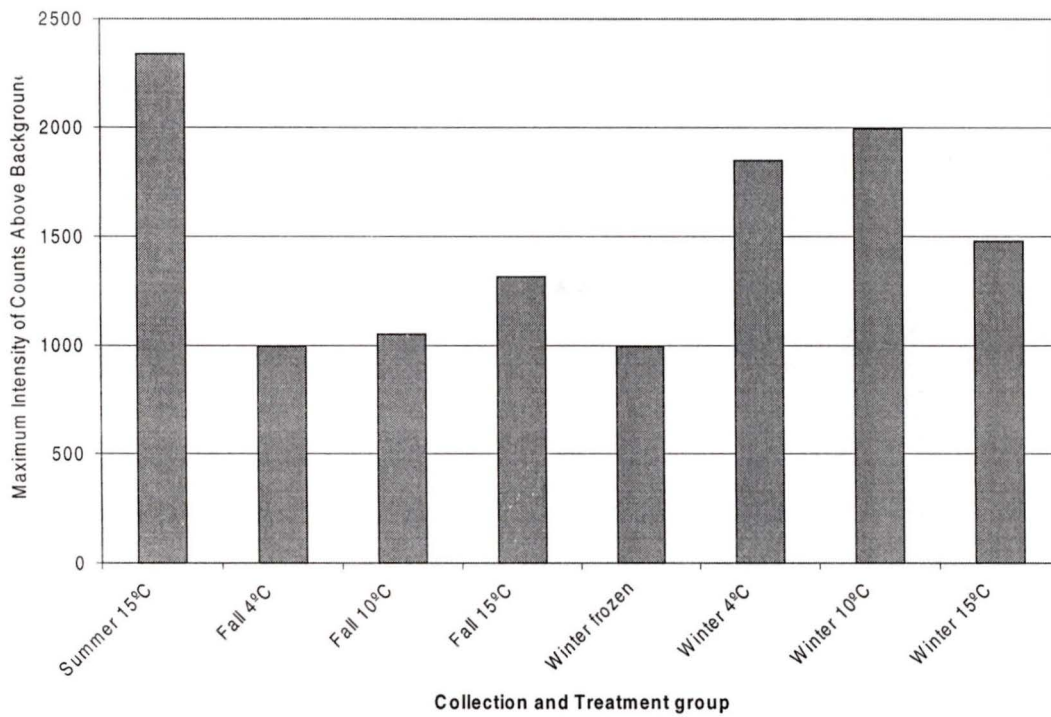


Figure 25. Maximum hybridization intensity graph for *Eurosta solidaginis* third instar larvae CO1 Dot blot.

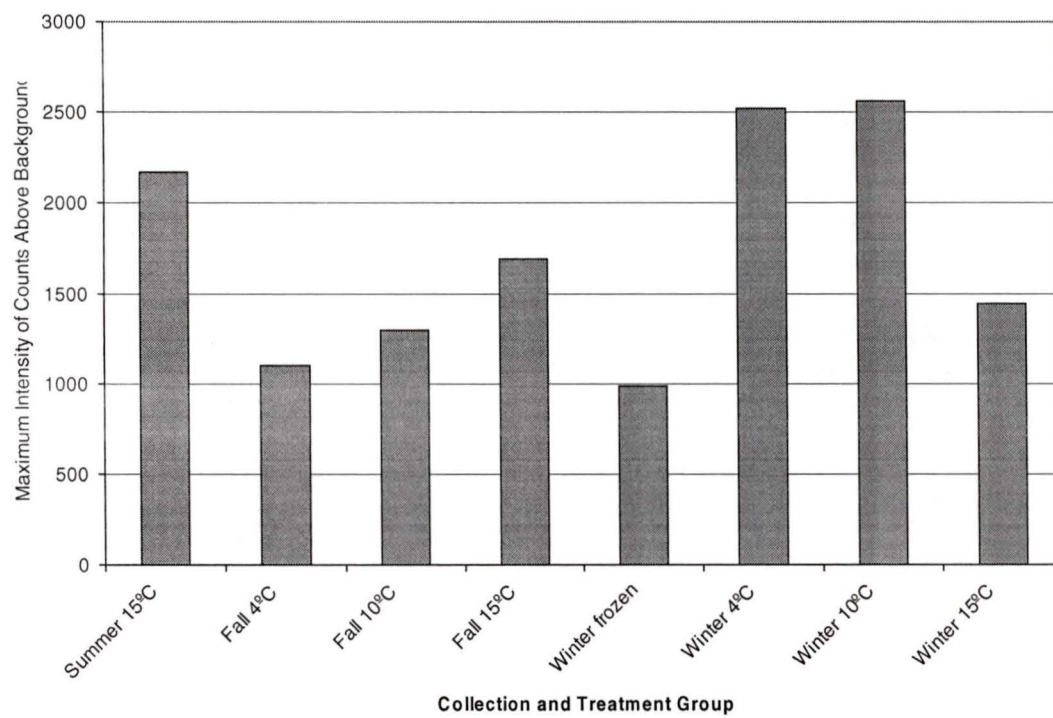


Figure 26. Maximum hybridization intensity graph for *Eurosta solidaginis* third instar larvae 16S Dot blot.

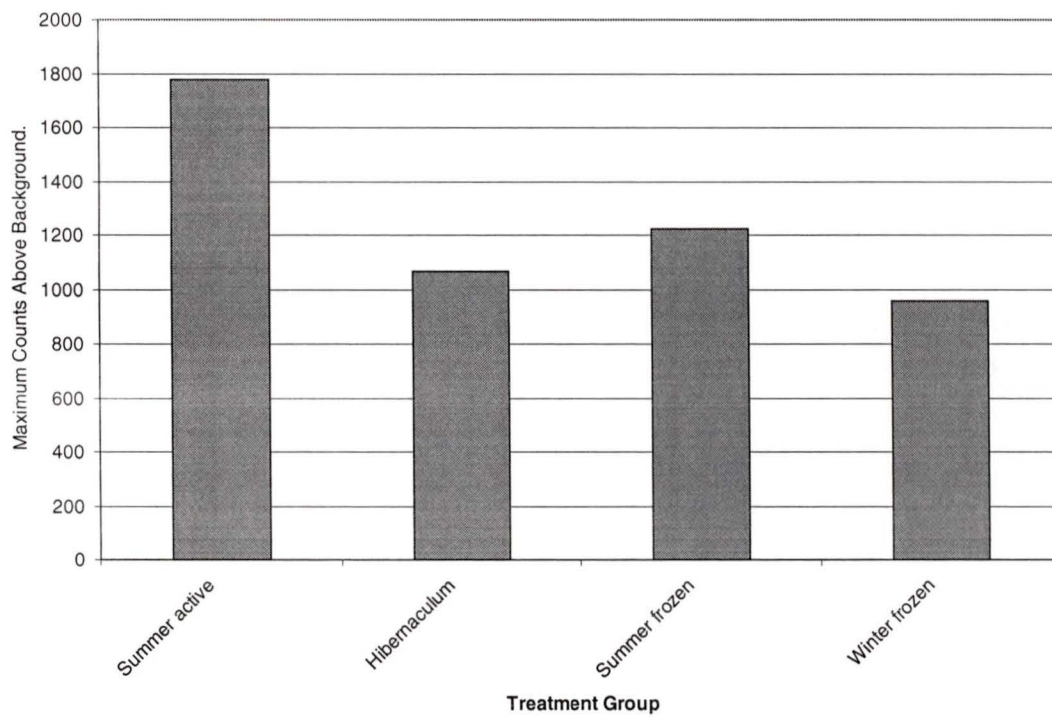


Figure 27. Maximum hybridization intensity graph for *Gynaephora groenlandica* CO1 Dot blot.

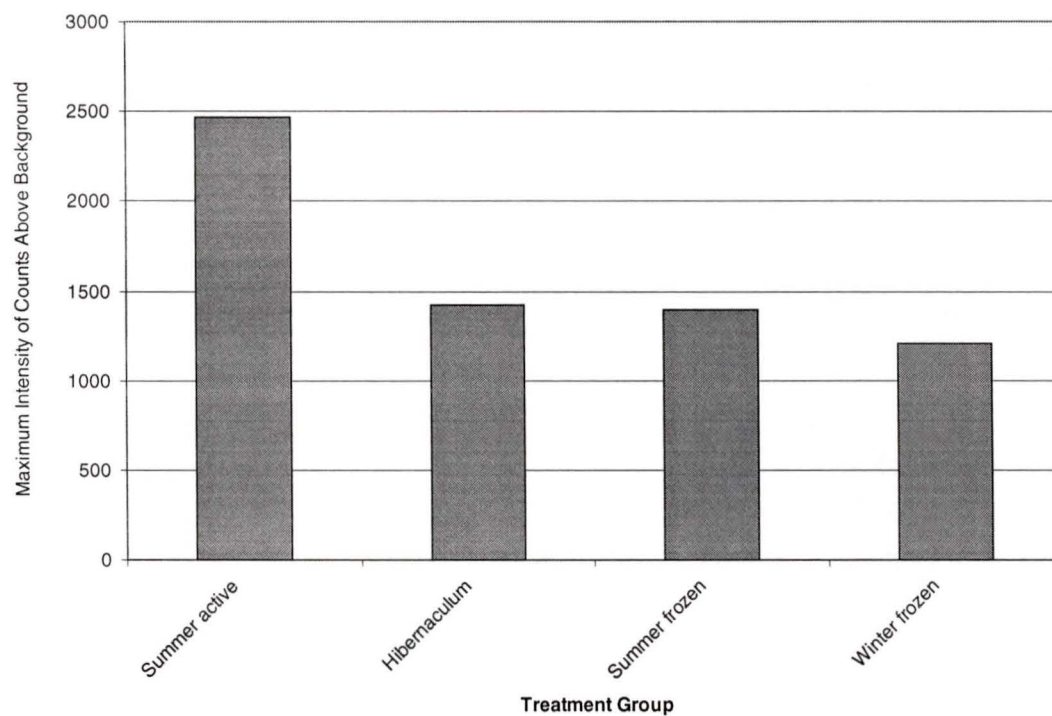


Figure 28. Maximum hybridization intensity graph for *Gynaephora groenlandica* 16S Dot blot.

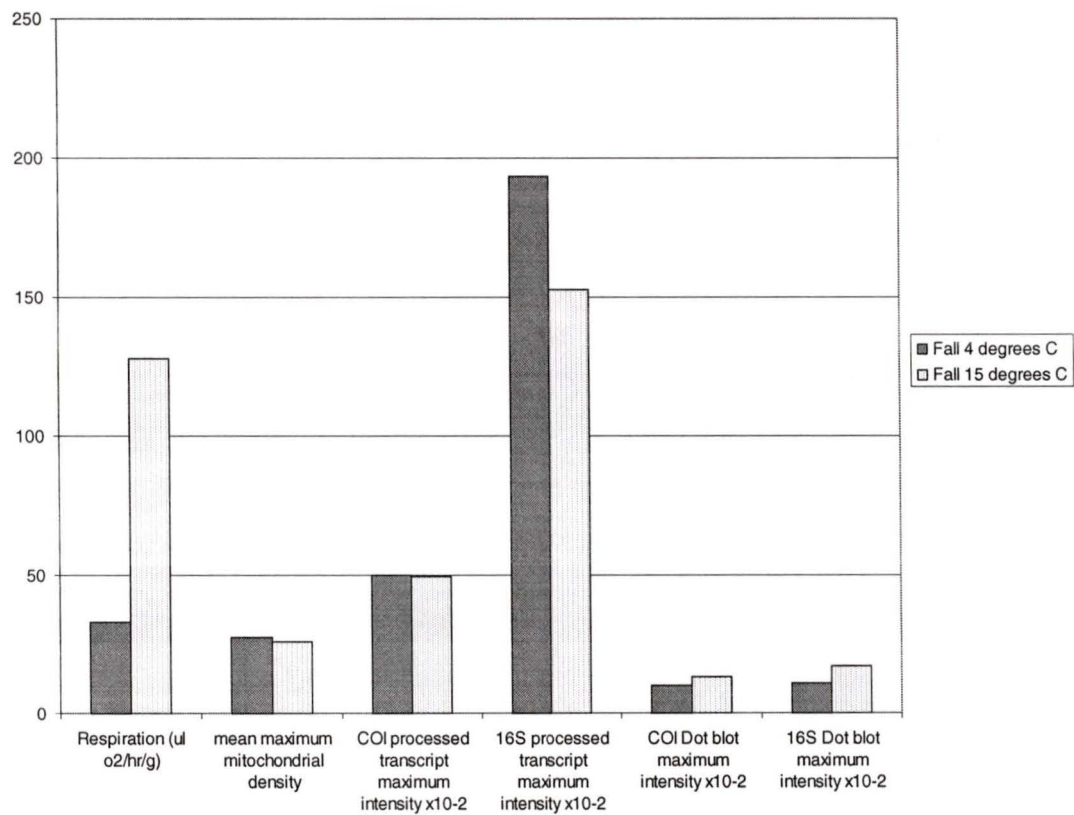


Figure 29. Summary data comparing fall collected *Eurosta* larvae measured at 4°C and 15°C including average respiration rates, mean maximum mitochondrial densities, and hybridization intensities ($\times 10^{-2}$) from Northern blots and Dot blots.

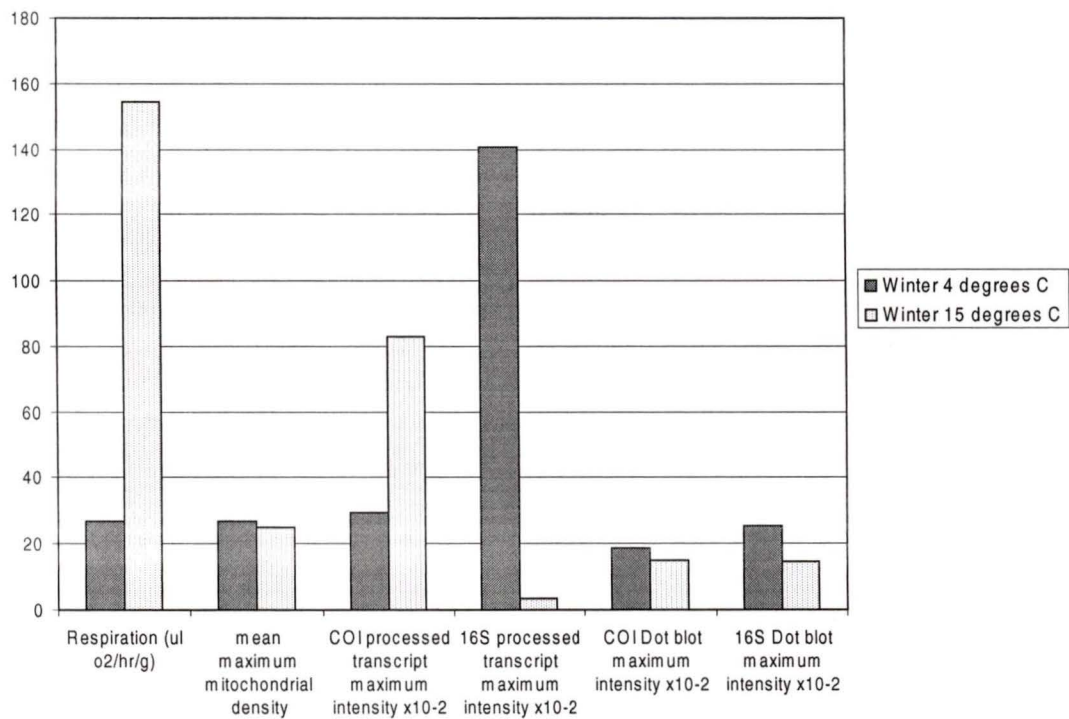


Figure 30. Summary data comparing winter collected *Eurosta* larvae measured at 4°C and 15°C including average respiration rates, mean maximum mitochondrial densities, and hybridization intensities ($\times 10^{-2}$) from Northern blots and Dot blots.

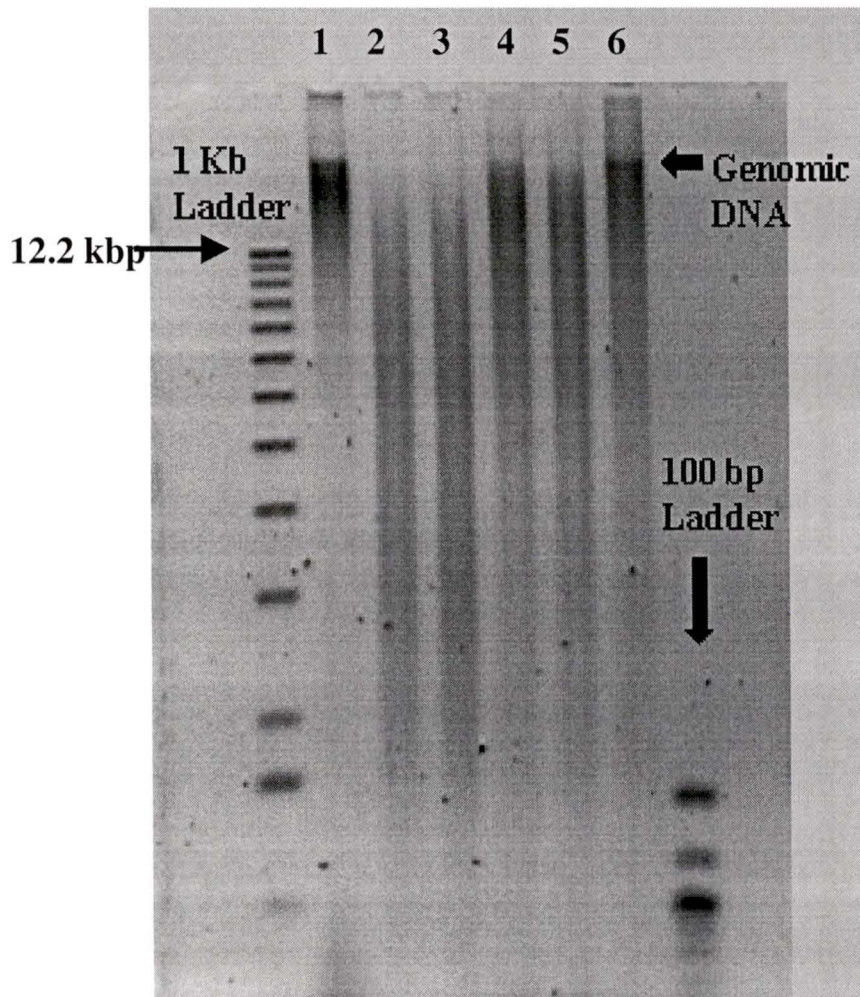


Figure 31. 0.8% agarose gel, *Drosophila melanogaster* restriction digest showing digested DNA and position of undigested genomic bands. (1) uncut DNA; (2) DNA cut with HindIII; (3) DNA cut with EcoRI; (4) DNA cut with XhoI; (5) DNA cut with Sall; (6) DNA cut with BamHI; 0.25 $\mu\text{g}/\text{ml}$ ethidium bromide.

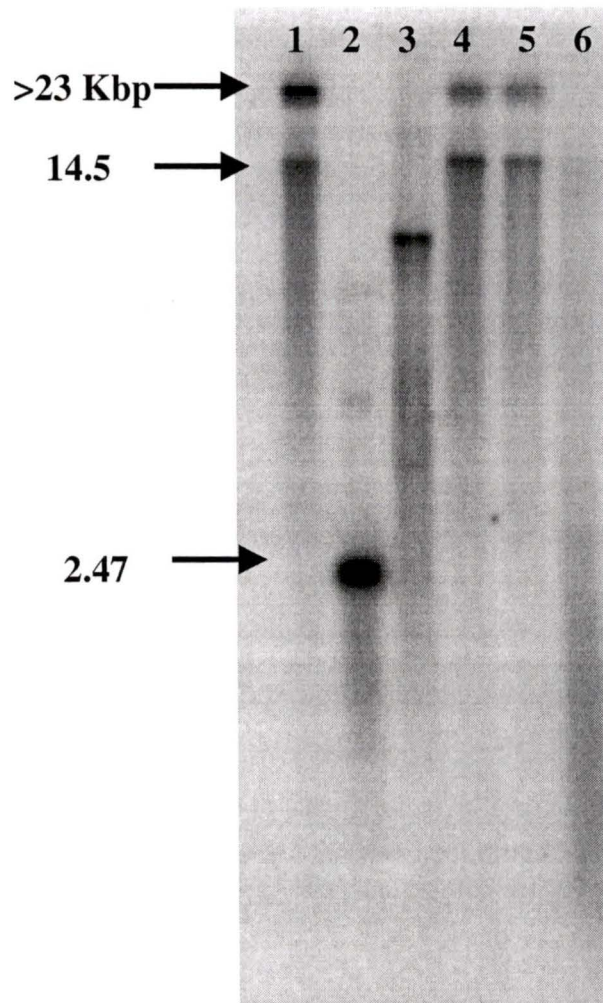


Figure 32. Southern blot analysis of 2 μ g *Eurosta solidaginis* total DNA digested with restriction enzymes; Hybond-N membrane hybridized with CO1 PCR generated probe; (1) uncut DNA; (2) HindIII; (3) EcoRI; (4) XhoI; (5) SalI; (6) BamHI.

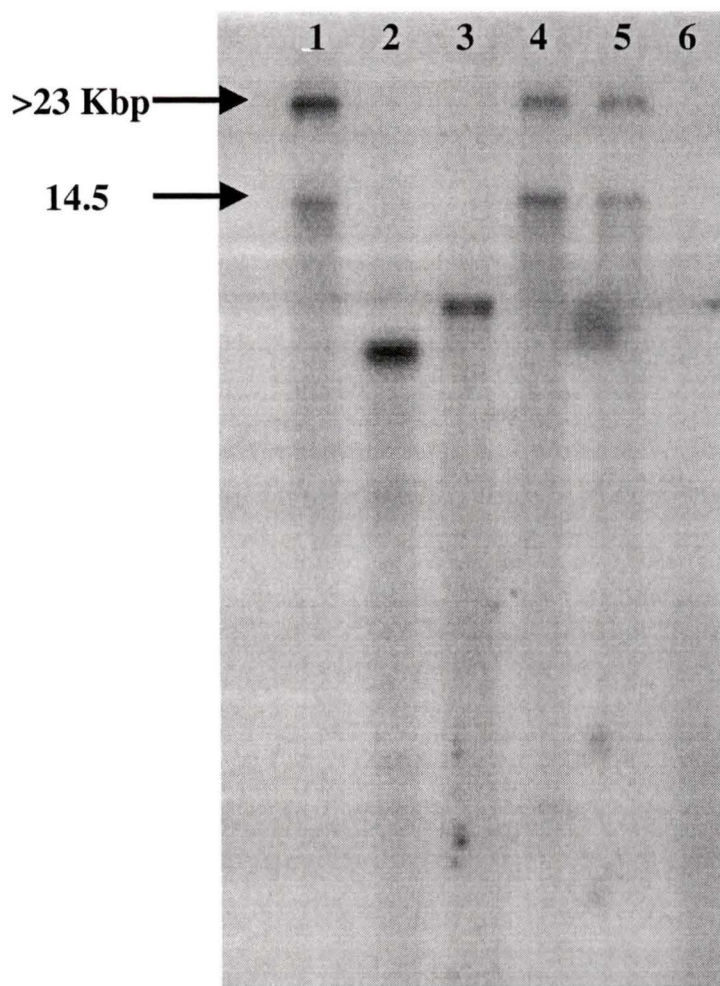


Figure 33. Southern blot analysis of 2 μg *Eurosta solidaginis* total DNA digested with restriction enzymes; Hybond-N membrane hybridized with 16S PCR generated probe; (1) uncut DNA; (2) HindIII; (3) EcoRI; (4) XhoI; (5) SalI; (6) BamHI.

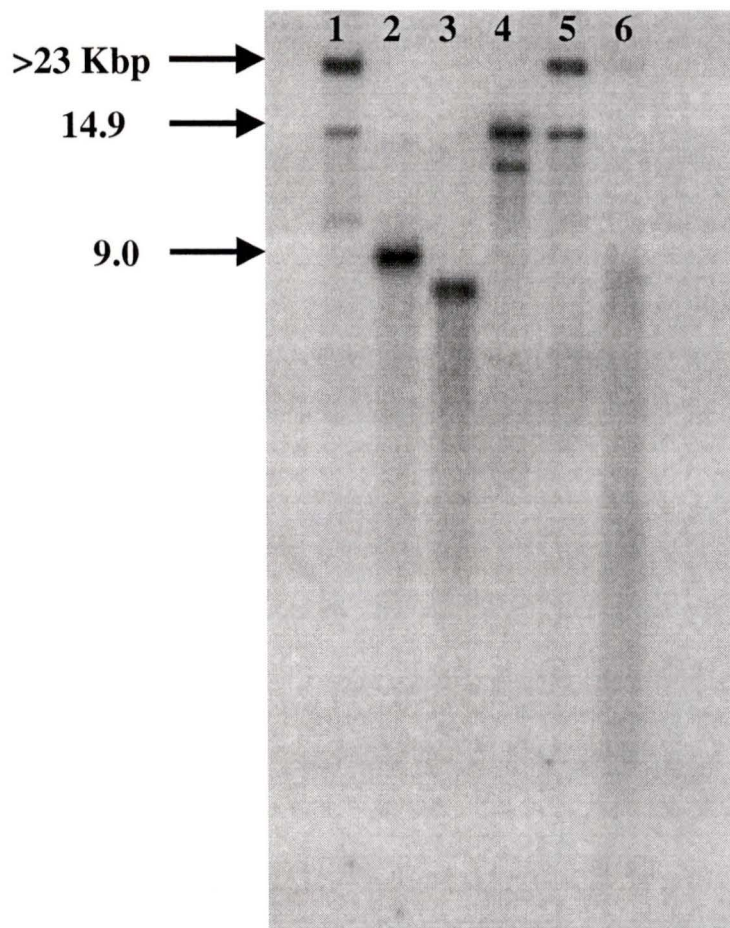


Figure 34. Southern blot analysis of 2 µg *Gynaephora groenlandica* total DNA digested with restriction enzymes; Hybond-N membrane hybridized with CO1 PCR generated probe; (1) uncut DNA; (2) HindIII; (3) EcoRI; (4) XhoI; (5) SalI; (6) BamHI.

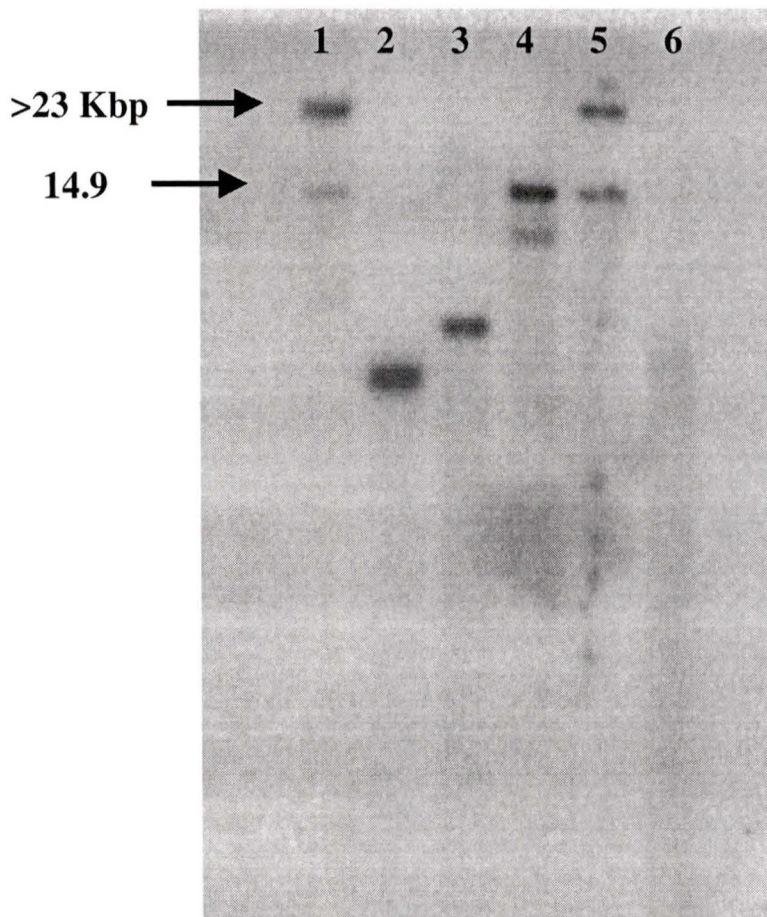


Figure 35. Southern blot analysis of 2 μ g *Gynaephora groenlandica* total DNA digested with restriction enzymes; Hybond-N membrane hybridized with 16S PCR generated probe; (1) uncut DNA; (2) HindIII; (3) EcoRI; (4) XhoI; (5) Sall; (6) BamHI.

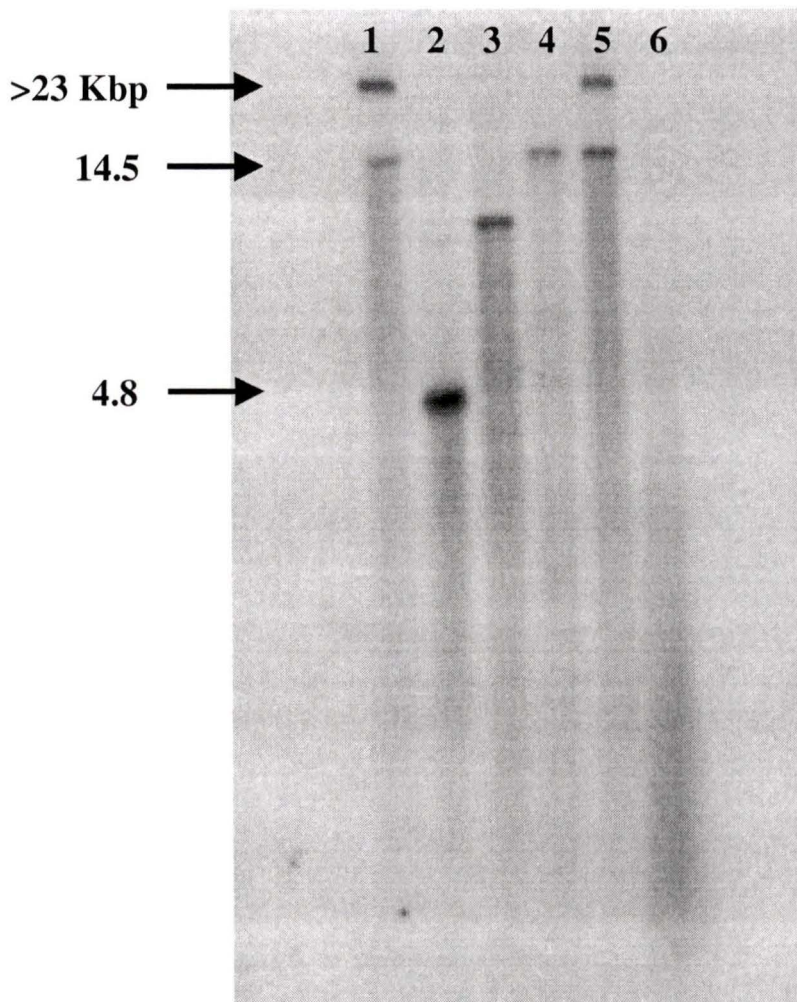


Figure 36. Southern blot analysis of 2 μ g *Drosophila melanogaster* total DNA digested with restriction enzymes; Hybond-N membrane hybridized with CO1 PCR generated probe; (1) uncut DNA; (2) HindIII; (3) EcoRI; (4) XhoI; (5) SalI; (6) BamHI.

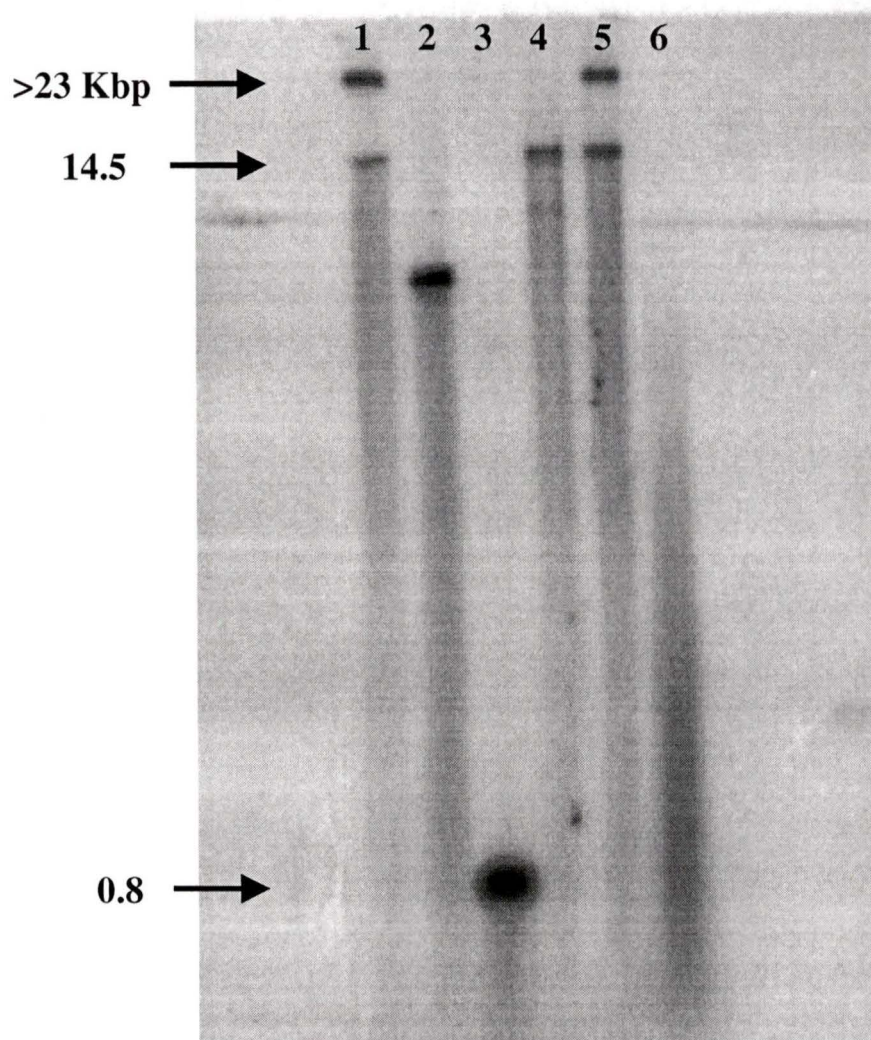


Figure 37. Southern blot analysis of 2 μg *Drosophila melanogaster* total DNA digested with restriction enzymes; Hybond-N membrane hybridized with 16S PCR generated probe; (1) uncut DNA; (2) HindIII; (3) EcoRI; (4) XhoI; (5) SalI; (6) BamHI.

LITERATURE CITED

1. Layne, J.R., *Microclimate Variability and the Eurythermic Nature of Goldenrod Gall Fly (Eurosta solidaginis) Larvae (Diptera, Tephritidae)*. Canadian Journal of Zoology-Revue Canadienne De Zoologie, 1991. **69**(3): p. 614-617.
2. Loken, O., *The Nunavut Handbook*., M. Soublière, Editor. 1999, Michael Roberts Publisher:
3. Lee, R.E., *Insect Cold-Hardiness - to Freeze or Not to Freeze - How insects survive low-temperatures*. Bioscience, 1989. **39**(5): p. 308-313.
4. Chapman, R.F., *The Insects: Structure and Function*. 1976: Elsevier, New York.
5. Denlinger, D.L., *Hormonal control of diapause*, in *Comprehensive Insect Physiology, Biochemistry and Pharmacology*, G.A. Kerkut and L.I. Gilbert, Editors. 1985, Pergamon: p. 353-412. Oxford.
6. Mansingh, A., *Physiological classification of dormancy in insects*. the Canadian Entomologist, 1971. **103**: p. 983-1009.
7. Tauber, M.J., , C.A. Tauber, , and S. Masaki, *Seasonal Adaptations of Insects*. 1986: Oxford University Press, New York.
8. Salt, R.W., *Principles of insect cold hardiness*. Annual Review of Entomology, 1961. **6**: p. 55-74.
9. Zachariassen, K.E., *Physiology of cold tolerance in insects*. Physiological Reviews, 1985. **65**(4): p. 799-832.
10. Storey, K.B. and J.M. Storey, *Natural freezing survival in animals*. Annual Review of Ecology and Systematics, 1996. **27**: p. 365-386.
11. Storey, K.B. and J.M. Storey, *Freeze tolerance in animals*. Physiological Reviews, 1988. **68**(1): p. 27-84.
12. Storey, K.B., *Life in a frozen state: adaptive strategies for natural freeze tolerance in amphibians and reptiles*. American Journal of Physiology, 1990. **258**(3 Pt 2): p. R559-68.
13. Storey, K.B., *Biochemistry of natural freeze tolerance in animals: molecular adaptations and applications to cryopreservation*. Biochemistry and Cell Biology, 1990. **68**(4): p. 687-98.
14. Danks, H.V., *Modes of seasonal adaptations in the insects: I. Winter survival*. Canadian Entomologist, 1978. **110**: p. 1167-1205.

15. Danks, H.V., *The wider integration of studies on insect cold-hardiness*. European Journal of Entomology, 1996. **93**(3): p. 383-403.
16. Loomis, S.H., *Comparative invertebrate cold hardiness*, in *Insects at Low Temperature*, R.E. Lee and D.L. Denlinger, Editors. 1991, Chapman and Hall: p. 301-317. New York.
17. Lee, R.E., *Principles of insect low temperature tolerance*, in *Insects at Low Temperature*, R.E. Lee and D.L. Denlinger, Editors. 1991, Chapman and Hall: p. 17-45. New York.
18. Baust, J.G. and R.R. Rojas, *Insect cold hardiness - facts and fancy*. Journal of Insect Physiology, 1985. **31**(10): p. 755-759.
19. Kukal, O. and J.G. Duman, *Switch in the Overwintering Strategy of 2 Insect Species and Latitudinal Differences in Cold Hardiness*. Canadian Journal of Zoology-Revue Canadienne De Zoologie, 1989. **67**(4): p. 825-827.
20. Mazur, P., *Freezing of Living Cells - Mechanisms and Implications*. American Journal of Physiology, 1984. **247**(3): p. C125-C142.
21. Franks, F., S.F. Mathias, and R.H. Hatley, *Water, temperature and life*. Philosophical Transactions of the Royal Society of London B Biological Sciences, 1990. **326**(1237): p. 517-31; discussion 531-3.
22. Quinn, P.J., *A lipid-phase separation model of low-temperature damage to biological membranes*. Cryobiology, 1985. **22**(2): p. 128-46.
23. Crowe, J.H., J.F. Carpenter, and L.M. Crowe, *The role of vitrification in anhydrobiosis*. Annual Review of Physiology, 1998. **60**: p. 73-103.
24. Lee, R.E. and J.P. Costanzo, *Biological ice nucleation and ice distribution in cold-hardy ectothermic animals*. Annual Review of Physiology, 1998. **60**: p. 55-72.
25. Davenport, J., *Animal Life at Low Temperature*. 1992: Chapman & Hall, London.
26. Leather, S.R., K.F.A. Walters, and J.S. Bale, *The Ecology of Insect Overwintering*. 1993: Cambridge University Press, Cambridge.
27. Ring, R.A., *Insects and their cells*, in *Low Temperature Preservation in Medicine and Biology*, M.J. Ashwood and J.B. Farrant, Editors. 1980, Pitman Medical: p. 187-217. Kent.

28. Costanzo, J.P., R.E. Lee, Jr., A.L. DeVries, T. Wang, and J.R. Layne, Jr., *Survival mechanisms of vertebrate ectotherms at subfreezing temperatures: applications in cryomedicine*. Federation of American Societies for Experimental Biology Journal, 1995. **9**(5): p. 351-8.
29. Ring, R.A. and H.V. Danks, *The role of trehalose in cold-hardiness and desiccation*. Cryo-Letters, 1998. **19**(5): p. 275-282.
30. Crowe, J.H., F.A. Hoekstra, and L.M. Crowe, *Anhydrobiosis*. Annual Review of Physiology, 1992. **54**: p. 579-599.
31. Zachariassen, K.E. and E. Kristiansen, *Ice nucleation and antinucleation in nature*. Cryobiology, 2000. **41**(4): p. 257-79.
32. Steigerwald, K.A., M.R. Lee, R.E. Lee, and J.C. Marshall, *Effect of biological ice nucleators on insect supercooling capacity varies with anatomic site of application*. Journal of Insect Physiology, 1995. **41**(7): p. 603-608.
33. Mugnano, J.A., R.E. Lee, and R.T. Taylor, *Fat body cells and calcium phosphate spherules induce ice nucleation in the freeze-tolerant larvae of the gall fly *Eurosta solidaginis* (Diptera, Tephritidae)*. Journal of Experimental Biology, 1996. **199**(2): p. 465-471.
34. Wigglesworth, V.B., *The Principles of Insect Physiology*. 1972: Chapman Hall, London.
35. Mansingh, A. and B.N. Smallman, *Variation in polyhedric alcohol in relation to diapause and cold-hardiness in the larvae of *Isia isabella**. Journal of Insect Physiology, 1972. **18**: p. 1565-1571.
36. Denlinger, D.L., *Relationship between cold hardiness and diapause*, in *Insects at Low Temperature*, R.E. Lee and D.L. Denlinger, Editors. 1991, Chapman and Hall: p. 174-197. New York.
37. Kukal, O., J.G. Duman, and A.S. Serianni, *Cold-induced mitochondrial degradation and cryoprotectant synthesis in freeze-tolerant arctic caterpillars*. Journal of Comparative Physiology B, 1989. **158**(6): p. 661-71.
38. Locke, M. and J.V. Collins, *the structure and formation of protein granules in the fat body of an insect*. The Journal of Cell Biology, 1965. **26**: p. 857-884.
39. Locke, M. and J.V. Collins, *Protein uptake into multivesicular bodies and storage granules in the fat body of an insect*. The Journal of Cell Biology, 1967. **36**: p. 453-483.

40. Keeley, L.L., *Neuroendocrine regulation of mitochondrial development and function in the insect fat body*, in *Energy Metabolism in Insects*, R.G.H. Downer, Editor. 1981, Plenum Press. New York.
41. Kroemer, G., *Mitochondrial control of apoptosis*, in *Mitochondria and Cell Death*, G.C. Brown, D.G. Nicholls, and C.E. Cooper, Editors. 1999, Portland Press: p. 1-15. London.
42. Beal, M.F., *Mitochondria, NO and neurodegeneration*, in *Mitochondria and Cell Death*, G.C. Brown, D.G. Nicholls, and C.E. Cooper, Editors. 1999, Portland Press: p. 43-54. London.
43. Shi, Y., *A structural view of mitochondria-mediated apoptosis*. *Nature Structural Biology*, 2001. **8**(5): p. 394-401.
44. Kukal, O., B. Heinrich, and J.G. Duman, *Behavioral thermoregulation in the freeze-tolerant Arctic caterpillar, Gynaephora groenlandica*. *Journal of Experimental Biology*, 1988. **138**: p. 181-193.
45. Lyon, B.E. and R.V. Cartar, *Functional significance of the cocoon in two arctic Gynaephora moth species*. *Proceedings of the Royal Society of London Series B-Biological Sciences*, 1996. **263**(1374): p. 1159-1163.
46. Kukal, O. and P.G. Kevan, *The influence of parasitism on the life-history of a high Arctic insect, Gynaephora groenlandica (Wocke) (Lepidoptera, Lymantriidae)*. *Canadian Journal of Zoology-Revue Canadienne De Zoologie*, 1987. **65**(1): p. 156-163.
47. Kukal, O., *Winter mortality and the function of larval hibernacula during the 14-year life-cycle of an Arctic moth, Gynaephora groenlandica*. *Canadian Journal of Zoology-Revue Canadienne De Zoologie*, 1995. **73**(4): p. 657-662.
48. Kukal, O. and T.E. Dawson, *Temperature and food quality influences feeding-behavior, assimilation efficiency and growth-rate of Arctic woolly-bear caterpillars*. *Oecologia*, 1989. **79**(4): p. 526-532.
49. Bennett, V.A., O. Kukal, and R.E. Lee, *Metabolic opportunists: Feeding and temperature influence the rate and pattern of respiration in the high arctic woollybear caterpillar Gynaephora groenlandica (Lymantriidae)*. *Journal of Experimental Biology*, 1999. **202**(1): p. 47-53.
50. Kevan, P.G., T.S. Jensen, and J.D. Shorthouse, *Body temperatures and behavioral thermoregulation of high Arctic woolly-bear caterpillars and pupae (Gynaephora rossii, Lymantriidae, Lepidoptera) and the importance of sunshine*. *Arctic and Alpine Research*, 1982. **14**(2): p. 125-136.

51. Kukal, O., A.S. Serianni, and J.G. Duman, *Glycerol metabolism in a freeze-tolerant arctic insect: an in vivo ¹³C NMR study*. Journal of Comparative Physiology B, 1988. **158**(2): p. 175-83.
52. Morewood, W.D. and R.A. Ring, *Revision of the life history of the High Arctic moth *Gynaephora groenlandica* (Wocke) (Lepidoptera : Lymantriidae)*. Canadian Journal of Zoology-Revue Canadienne De Zoologie, 1998. **76**(7): p. 1371-1381.
53. Danks, H.V., O. Kukal, and R.A. Ring, *Insect cold-hardiness - Insights from the Arctic*. Arctic, 1994. **47**(4): p. 391-404.
54. Baust, J.G. and M. Nishino, *Freezing tolerance in the goldenrod gall fly (*Eurosta solidaginis*)*, in *Insects at Low Temperature*, R.E. Lee and D.L. Denlinger, Editors. 1991, Chapman and Hall: p. 260-275. New York.
55. Irwin, J.T., V.A. Bennett, and R.E. Lee, *Diapause development in frozen larvae of the goldenrod gall fly, *Eurosta solidaginis* Fitch (Diptera : Tephritidae)*. Journal of Comparative Physiology B-Biochemical Systemic and Environmental Physiology, 2001. **171**(3): p. 181-188.
56. Layne, J.R. and C. Ten Eyck, *The effects of temperature and season on the O₂ consumption of third-instar larvae of the goldenrod gall fly (*Eurosta solidaginis*)*. Physiological Entomology, 1996. **21**(1): p. 71-75.
57. Lee, R.E., R.A. Dommel, K.H. Joplin, and D.L. Denlinger, *Cryobiology of the freeze-tolerant gall fly *Eurosta solidaginis* - Overwintering energetics and heat-shock proteins*. Climate Research, 1995. **5**(1): p. 61-67.
58. Joannis, D.R. and K.B. Storey, *Enzyme-activity profiles in an overwintering population of freeze-tolerant larvae of the gall fly, *Eurosta solidaginis**. Journal of Comparative Physiology B-Biochemical Systemic and Environmental Physiology, 1994. **164**(3): p. 247-255.
59. Storey, J.M. and K.B. Storey, *Winter survival of the gall fly larva, *Eurosta solidaginis* - Profiles of fuel reserves and cryoprotectants in a natural population*. Journal of Insect Physiology, 1986. **32**(6): p. 549-556.
60. Baust, J.G. and R.E. Lee, *Environmental triggers to cryoprotectant modulation in separate populations of the gall fly, *Eurosta solidaginis* (Fitch)*. Journal of Insect Physiology, 1982. **28**(5): p. 431-436.
61. Storey, J.M. and K.B. Storey, *Freezing and cellular-metabolism in the gall fly larva, *Eurosta solidaginis**. Journal of Comparative Physiology B-Biochemical Systemic and Environmental Physiology, 1985. **155**(3): p. 333-337.

62. Morrissey, R.E. and J.G. Baust, *The ontogeny of cold tolerance in the gall fly, Eurosta solidaginis*. Journal of Insect Physiology, 1976. **22**: p. 431-437.
63. Salt, R.W., *Survival of frozen fat body cells in an insect*. Nature, 1959. **184**: p. 1426.
64. Salt, R.W., *Intracellular freezing in insects*. Nature, 1962. **193**(4821): p. 1207-1208.
65. Lee, R.E., J.J. McGrath, R.T. Morason, and R.M. Taddeo, *Survival of intracellular freezing, lipid coalescence and osmotic fragility in fat-body cells of the freeze-tolerant gall fly Eurosta solidaginis*. Journal of Insect Physiology, 1993. **39**(5): p. 445-450.
66. Morason, R.T., A.L. Allenspach, and R.E. Lee, *Comparative ultrastructure of fat-body cells of freeze-susceptible and freeze-tolerant Eurosta solidaginis larvae after chemical fixation and high-pressure freezing*. Journal of Insect Physiology, 1994. **40**(2): p. 155-164.
67. Hankison, S.J. and R.E. Lee, *Water content of the gall regulates susceptibility to inoculative freezing in larvae of the goldenrod gall fly, Eurosta solidaginis*. American Zoologist, 2000. **40**(6): p. 1045-1045.
68. Salt, R.W., *Natural occurrence of glycerol in insects and its relation to their ability to survive freezing*. Canadian Entomologist, 1957. **89**: p. 491-494.
69. Baust, J.G. and R.E. Lee, *Divergent mechanisms of frost-hardiness in two populations of the gall fly, Eurosta solidaginis*. Journal of Insect Physiology, 1981. **27**(7): p. 485-490.
70. Rojas, R.R., R.E. Lee, and J.G. Baust, *Relationship of environmental water-content to glycerol accumulation in the freezing tolerant larvae of Eurosta solidaginis (Fitch)*. Cryo-Letters, 1986. **7**(4): p. 234-245.
71. Hamilton, M.D., R.R. Rojas, and J.G. Baust, *Juvenile hormone - Modulation of cryoprotectant synthesis in Eurosta solidaginis by a component of the endocrine system*. Journal of Insect Physiology, 1986. **32**(11): p. 971-979.
72. Storey, K.B. and T.P. Mommsen, *Effects of temperature and freezing on hepatocytes isolated from a freeze-tolerant frog*. American Journal of Physiology, 1994. **266**(5): p. R1477-R1482.
73. Pio, C.J. and J.G. Baust, *Effects of temperature cycling on cryoprotectant profiles in the goldenrod gall fly, Eurosta solidaginis (Fitch)*. Journal of Insect Physiology, 1988. **34**(8): p. 767-771.

74. Joannis, D.R. and K.B. Storey, *Temperature acclimation and seasonal responses by enzymes in cold-hardy gall insects*. Archives of Insect Biochemistry and Physiology, 1995. **28**(4): p. 339-349.
75. Joannis, D.R. and K.B. Storey, *Oxidative stress and antioxidants in stress and recovery of cold-hardy insects*. Insect Biochemistry and Molecular Biology, 1998. **28**(1): p. 23-30.
76. Joannis, D.R. and K.B. Storey, *Mitochondrial enzymes during overwintering in two species of cold-hardy gall insects*. Insect Biochemistry and Molecular Biology, 1994. **24**(2): p. 145-150.
77. Joannis, D.R. and K.B. Storey, *Fatty acid content and enzymes of fatty acid metabolism in overwintering cold-hardy gall insects*. Physiological Zoology, 1996. **69**(5): p. 1079-1095.
78. Lewin, B., *Genes VII*. 2000: Oxford University Press, New York.
79. Lehninger, A.L., D.L. Nelson, and M.M. Cox, *Principles of Biochemistry*. 1993: Worth Publishers, Inc., New York.
80. Alberts, B., D. Bray, J. Lewis, M. Raff, K. Roberts, and J. Watson, *Molecular Biology of the Cell*. Third ed. 1994: Garland Publishing, Inc., New York.
81. Clary, D.O., J.M. Goddard, S.C. Martin, C.M. Fauron, and D.R. Wolstenholme, *Drosophila mitochondrial DNA: a novel gene order*. Nucleic Acids Research, 1982. **10**(21): p. 6619-37.
82. Lee, R.E., *Using microrespirometers to measure O₂ consumption by insects and small invertebrates*. American Biology Teacher, 1995. **57**(5): p. 284-285.
83. Aron, A. and E.N. Aron, *Statistics for Psychology*. 1994: Prentice Hall, Upper Saddle River.
84. Johnson, R.A. and G.K. Bhattacharyya, *Statistics: Principles and Methods*. 1992: John Wiley and Sons, New York.
85. Williamson, D.H. and D.J. Fennell, *The use of fluorescent DNA-binding agent for detecting and separating yeast mitochondrial DNA*. Methods in Molecular and Cellular Biology, 1975. **12**: p. 335-51.
86. Kapuscinski, J., *DAPI: a DNA-specific fluorescent probe*. Biotechnic Histochemistry, 1995. **70**(5): p. 220-33.
87. Haughland, R.P., *Handbook of Fluorescent Probes and Research chemicals*, ed. M.T.Z. Spence. 1996: Molecular Probes, Inc. 268. Eugene, Oregon.

88. Larsen, W.J., *Genesis of mitochondria in insect fat body*. *Journal of Cell Biology*, 1970. **47**: p. 373-383.
89. Lodish, H., A. Berk, S. Zipursky, P. Matsudaira, D. Baltimore, and J. Darnell, *Molecular Cell Biology*. 1999: W. H. Freeman and Company, New York.
90. Ashburner, M., S. Misra, J. Roote, S.E. Lewis, R. Blazej, T. Davis, C. Doyle, R. Galle, R. George, N. Harris, G. Hartzell, D. Harvey, L. Hong, K. Houston, R. Hoskins, G. Johnson, C. Martin, A. Moshrefi, M. Palazzolo, M.G. Reese, A. Spradling, G. Tsang, K. Wan, K. Whitelaw, S. Celniker, and et al., *An exploration of the sequence of a 2.9-Mb region of the genome of Drosophila melanogaster: the Adh region*. *Genetics*, 1999. **153**(1): p. 179-219.
91. Lewis, D.L., C.L. Farr, Y. Wang, A.T. Lagina, 3rd, and L.S. Kaguni, *Catalytic subunit of mitochondrial DNA polymerase from Drosophila embryos. Cloning, bacterial overexpression, and biochemical characterization*. *Journal of Biological Chemistry*, 1996. **271**(38): p. 23389-94.
92. Sambrook, J., E.F. Fritsch, and T. Maniatis, *Molecular Cloning: A Laboratory Manual*, ed. N. Ford, C. Nolan, and M. Ferguson. 1989: Cold Spring Harbor Laboratory Press, New York.
93. Ballantyne, J.S. and K.B. Storey, *Characterization of mitochondria isolated from the freezing-tolerant larvae of the goldenrod gall fly (Eurosta solidaginis) - Substrate preferences, salt effects, and Ph effects on warm-acclimated and cold-acclimated animals*. *Canadian Journal of Zoology-Revue Canadienne De Zoologie*, 1985. **63**(2): p. 373-379.
94. Gilbert, S.F., *Developmental Biology*. Fourth ed. ed. 1994: Sinauer Associates, Inc., Sunderland, Ma.
95. Gruissem, W. and G. Schuster, *Control of mRNA degradation in organelles*, in *Control of Messenger RNA Stability*, J. Belasco and G. Brawerman, Editors. 1993, Academic Press: p. 329-365. San Diego.
96. Higgs, D.C., R.S. Shapiro, K.L. Kindle, and D.B. Stern, *Small cis-acting sequences that specify secondary structures in a chloroplast mRNA are essential for RNA stability and translation*. *Molecular and Cellular Biology*, 1999. **19**(12): p. 8479-8491.
97. Baker, E.J., *Control of poly(A) length*, in *Control of Messenger RNA Stability*, J. Belasco and G. Brawerman, Editors. 1993, Academic Press, Inc.: p. 367-415. San Diego.

98. Attardi, G., P. Cantatore, S. Crews, R. Gelfand, C. Merkel, J. Montoya, and D. Ojala, *A comprehensive view of mitochondrial gene expression in human cells*, in *Mitochondrial Genes*, P. Slonimski, Editor. 1982, Cold Spring Harbor Laboratory: p. 51-71. Cold Spring Harbor.
99. Fukuda, M., S. Wakasugi, T. Tsuzuki, H. Nomiyama, K. Shimda, and T. Miyata, *Mitochondrial DNA-like sequences in the human nuclear genome: Characterization and implications in the evolution of mitochondrial DNA*. *Journal of Molecular Biology*, 1985. **186**(2): p. 257-266.
100. Lopez, J.V., N. Yuhki, R. Masuda, W. Modi, and S.J. O'Brien, *Numt, a recent transfer and tandem amplification of mitochondrial DNA to the nuclear genome of the domestic cat*. *Journal of Molecular Evolution*, 1994. **39**(2): p. 174-90.
101. Zhang, D. and G.M. Hewitt, *Nuclear integrations: Challenges for mitochondrial DNA markers*. *Trends in Ecology and Evolution*, 1996. **11**(6): p. 247-251.
102. Vaughan, H.E., J.S. Heslop-Harrison, and G.M. Hewitt, *The localization of mitochondrial sequences to chromosomal DNA in orthopterans*. *Genome*, 1999. **42**(5): p. 874-880.
103. Gellissen, G., J.Y. Bradfield, B.N. White, and G.R. Wyatt, *Mitochondrial-DNA sequences in the nuclear genome of a locust*. *Nature*, 1983. **301**(5901): p. 631-634.
104. Gellissen, G. and G. Michaelis, *Gene transfer. Mitochondria to nucleus*. *Annals of the New York Academy of Sciences*, 1987. **503**: p. 391-401.
105. Sunnucks, P. and D. Hales, *Numerous transposed sequences of mitochondrial cytochrome oxidase I-II in aphids of the genus Sitobion (Hemiptera: Aphididae)*. *Molecular Biology and Evolution*, 1996. **13**(3): p. 510-524.
106. Obar, R. and J. Green, *Molecular archaeology of the mitochondrial genome*. *Journal of Molecular Evolution*, 1985. **22**(3): p. 243-51.
107. Lang, B.F., M.W. Gray, and G. Burger, *Mitochondrial genome evolution and the origin of eukaryotes*. *Annual Review of Genetics*, 1999. **33**: p. 351-397.
108. Thorsness, P.E. and E.R. Weber, *Escape and migration of nucleic acids between chloroplasts, mitochondria, and the nucleus*. *International Review of Cytology*, 1996. **165**: p. 207-34.

VITA

Surname: Barber

Given Names: Sarah Anne

Place of Birth: Victoria, British Columbia

Educational Institutions Attended:

University of Victoria 1999-2001

University of Victoria 1994-1997

Camosun College 1993-1994

Degrees Awarded:

B.Sc. University of Victoria 1997

Honours and Awards:

Ray Hadfield Memorial Fellowship 2000

Edythe Hembroff-Schleicher Scholarship 2000

Graduate Teaching and Research Fellowship, University of Victoria 2000

Graduate Teaching and Research Fellowship, University of Victoria 1999

Publications:


Abstracts of Temp 2000

UNIVERSITY OF VICTORIA PARTIAL COPYRIGHT LICENCE

I hereby grant the right to lend my thesis to users of the University of Victoria Library, and to make single copies only for such users or in response to a request from the library of any other university, or similar institution, on its behalf or for one of its users. I further agree that permission for extensive copying of this thesis for scholarly purposes may be granted by me or a member of the University designated by me. It is understood that copying or publication of this thesis for financial gain by the University of Victoria shall not be allowed without my written permission.

Title of Thesis:

Mitochondrial gene transcription and genome copy number in freeze tolerant larvae of the Arctic woolly bear caterpillar, *Gynaephora groenlandica*, and Goldenrod gall fly, *Eurosta solidaginis*

Author: 

Sarah Anne Barber

September 4, 2001